Revista Română de Inginerie Civilă

Indexată în bazele de date internationale (BDI)

ProQuest, IET INSPEC, EBSCO, GOOGLE SCHOLAR, CROSSREF, TDNET, DIMENSIONS, DRJI, J-GATE, INDEX COPERNICUS, ULRICH'S, JOURNALSEEK, RESEARCH GATE, SEMANTIC SCHOLAR, ERIHPLUS, WORLDCAT

Volumul 16 (2025), Numărul 1

The threaded displacement piling system

Sistemul de realizare a piloților de îndesare cu spire *1-12*

Lóránd Sata, Sanda Manea

Comparison of green building rating systems and the usage of smart materials using BIM

Comparația sistemelor de evaluare a construcților verzi și utilizarea materialelor inteligente cu BIM *13-25*

N.R Monish Raaj, Vasudevan Ramasamy

Redemption of the lands occupied by the photovoltaic panels in the agricultural circuit

Redarea terenurilor ocupate de panourile fotovoltaice în circuitul agricol *26-35*

Florin-Alexandru Lunga, Bogdan-Darian Toader

Geopolymer concrete as an effective technical variant for reducing CO_2 emissions in the atmosphere during preparing construction materials

Beton geopolimeric ca variantă tehnică eficace pentru reducerea emisiilor de CO_2 în atmosferă în timpul pregătirii materialelor de construcție *36-49*

Lucian Paunescu, Bogdan Valentin Paunescu, Enikö Volceanov, Adrian Ioana

---

Investigating the Instability of a Retaining Wall: Construction Concerns and Design Revisions

Investigarea instabilității unui zid de sprijin: preocupări de construcție și revizuiri de proiectare *50-69*

Houssam Khelalfa, Fethi Boulkhiout, Youcef Kaikea

Ecological fuel obtained by recovery the biomass resulting from the pruning of Paulownia trees and plant residues. Determination of calorific value.

Combustibil ecologic obținut prin utilizarea biomasei rezultate din toaletarea arborilor Paulownia și a resturilor vegetale. Determinarea puterii calorifice. *70-81*

Lukas Ilioni, Ricardo Sbera, Selena Coandă

A look at the large capacity shallow geothermal systems with heat pumps units in terms of optimal control

O privire asupra sistemelor geotermale de mică adâncime de mare capacitate cu unități cu pompe de căldură în ceea ce privește controlul optim *82-90*

Răzvan –Silviu Ștefan, Daniel Cornea

Waste heat energy recovery from an electrostatic painting line
Recuperarea energiei termice reziduale de la o linie de vopsire în câmp electrostatic *91-96*
Diana-Patricia Ţucu, Florian-Tamás Negruţ

Air conditioning system with ice-slurry: theory, simulation and validation
Sistem de aer condiționat cu gheață-slurry: teorie, simulare și validare *97-102*
Emil Iakabos, Florea Chiriac, Anica Ilie, Alina Girip, Madalina Teodora Nichita

Heating systems using heat pump thermal adjustment
Sisteme de încălzire care utilizează reglajul termic al pompei de căldură *103-109*
Florin Iordache, Mugurel Talpiga

Architectural integration of photovoltaic panels on the facades of existing buildings. Case Study
Integrarea arhitecturala a panourilor fotovoltaice pe fatadele cladirilor existente. Studiu de caz *110-118*
Natalia Bărgăoanu, Andreea Zuba

Assessing the impact of air conditioning systems on aerosol dispersion within Intensive Care Units
Evaluarea impactului sistemelor de aer condiționat asupra dispersiei aerosolilor în cadrul Unităților de Terapie Intensivă *119-124*
Cătălin-George Popovici, Emilian-Florin Ţurcanu, Vasilică Ciocan, Nelu-Cristian Chereches, Sebastian-Valeriu Hudișteanu, Ana Diana Ancaș, Marina Verdeș, Marius-Vasile Atanasiu, Larisa Anghel

Geopolymer concrete based on fly ash and slag using recycled aggregate from building demolition
Beton geopolimeric pe bază de cenușă zburătoare și zgură utilizând agregat reciclat din demolarea clădirilor *125-136*
Lucian Paunescu, Enikö Volceanov, Bogdan Valentin Paunescu

MATRIX ROM
3 Politehnicii Street, Bucharest, Romania
Tel. +4021.4113617, +40733882137
e-mail: office@matrixrom.ro
www.matrixrom.ro

EDITORIAL BOARD

Romanian Journal of Civil Engineering is founded, published and funded by publishing house MATRIX ROM
Executive Director: mat. Iancu ILIE

Online edition ISSN 2559-7485
Print edition ISSN 2068-3987; ISSN-L 2068-3987

The threaded displacement piling system

Sistemul de realizare a piloților de îndesare cu spire

Lóránd Sata[1], Sanda Manea[2]

[1]Technical University of Civil Engineering
bd. Lacul Tei nr. 122 - 124, cod 020396, Sector 2, București, Romania
E-mail: sata_lorand@yahoo.com

[2]Technical University of Civil Engineering
bd. Lacul Tei nr. 122 - 124, cod 020396, Sector 2, București, Romania
E-mail: sanda_manea@utcb.ro

DOI: 10.37789/rjce.2025.16.1.1

Abstract.. *Screwsol is one of the recent deep foundation solutions for the "screw" type threaded displacement piling methods. The system is successfully applied in the range 330/500 to 530/700mm not only in Great Britain, France, but also in Central – East Europe, fully covered in by the standard EN 12699:2015 [1]. The paper present by means of more than 250 simple and instrumented loading tests the technological details, the constructional principles and the choosing of dimensions, the application possibilities, the design approaches as well as sustainability evaluation.*

Key words: *displacement piles; screw piles; design approach; sustainability*

Rezumat. *Screwsol este una dintre soluțiile recente de fundare de adâncime prin piloți de îndesare cu spire de tip „șurub". Sistemul este aplicat cu succes în gama de dimensiuni 330/500 până la 530/700 mm nu doar în Marea Britanie, Franța, ci și în Europa Centrală și de Est, fiind pe deplin reglementat de standardul EN 12699:2015 [1]. Lucrarea prezintă, prin intermediul a peste 250 de teste de încărcare simple și instrumentate, detalii tehnologice, principii constructive și modul de alegere a dimensiunilor, domeniile de aplicare, abordările de proiectare, precum și evaluarea sustenabilității.*

Cuvinte cheie: piloți de îndesare, piloți de tip șurub, abordare de proiectare, sustenabilitate

1. Introduction

One of the recent optimal soil displacement drilling solutions is given by the rotary displacement piling system, the Screwsol concept, defined as follows:

Pile in which the pile or pile tube comprises a limited number of helices at its toe, and which is installed under the combined action of a torque and a vertical thrust. By the screwing-in and/or by the screwing-out, the ground is essentially laterally displaced,

The article was received on 19.04.2024, accepted on 24.02.2025 and published on 14.03.2025

and no soil is removed. The technology is covered by the standard ASRO SR EN 12699:2015[1].

The article presents a list of simple and instrumented loading tests for several load types; technological details, design approaches; constructional principles and the choosing of dimensions; application possibilities; the ecological impact analysis and evaluation of the Screwsol rotary displacement piling system [2] [3].

The pile identified by two diameters (core / threads) is applied in the range 330/500 to 530/700mm (Figure 1) [4].

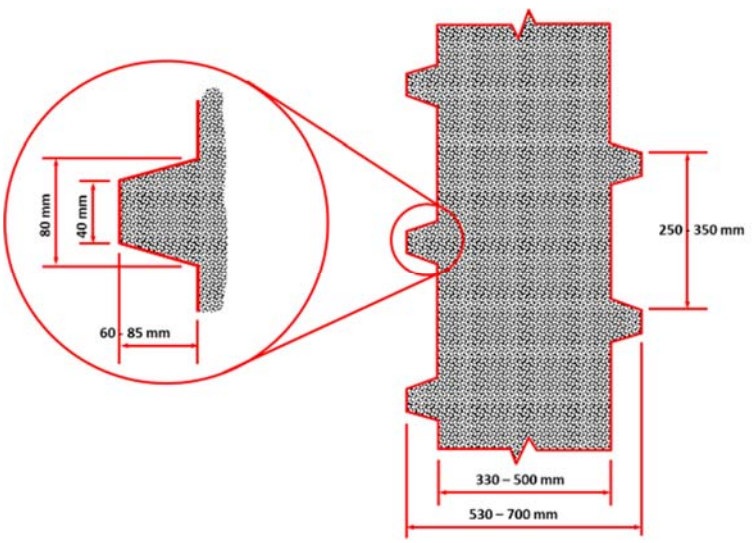

Figure 1. Screwsol pile longitudinal section and thread details.

2. Alizeu wind farm load test / 2013

The tested pile was a Screwsol pile with a diameter of d=330/500 mm (meaning 330 mm cylinder diameter and 500 mm external diameter) and a toe depth of H = 20.95 m from ground level (actual pile length of L = 20.60 m), reinforced on its entire length, to provide support for the strain gages and to protect the pile head from local crushing at high loads. Four reaction piles were used for the load test, executed with the same technology.

The static load test was carried out in equal steps of 125 kN, until failure. Application of a load increment was conditioned by stabilization of settlements for the previous step. Additionally, the pile was equipped with 17 extensometers and during the load test the deformation of the concrete was monitored with a frequency of 1 reading / minute.

Strain gauge measurements were processed in several steps to determine the detailed pile behaviour, and to confirm or contradict the preliminary conclusions based on the classical load test results.

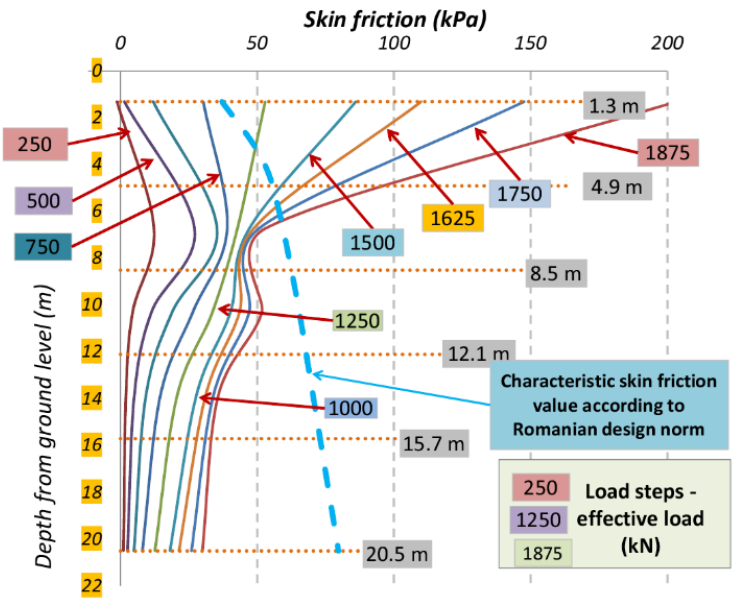

Figure 2. Skin friction diagram.

Pile failure occurred at the 16th load step (2000 kN), most likely by crushing of the pile head due to eccentrical application of the load. This observation is supported by the load-settlement diagrams of the four individual sensors that measured the settlement of the pile, located at the four corners of the pile.

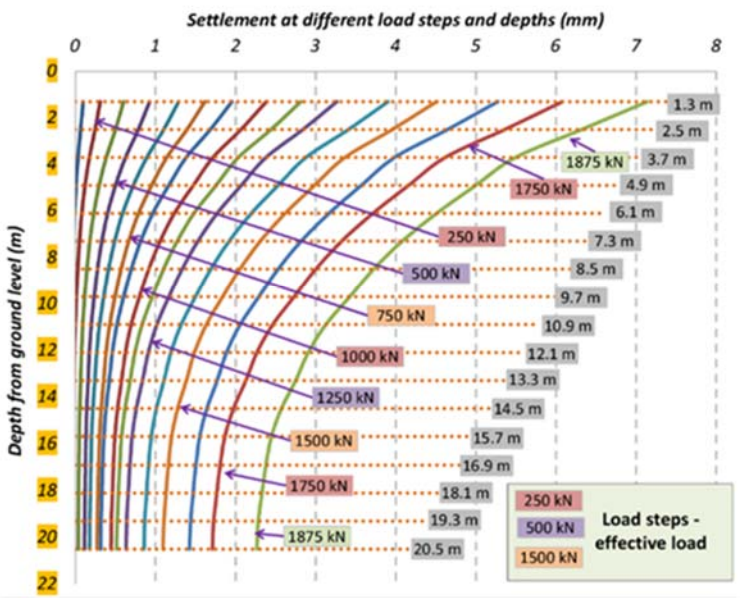

Figure 3. Settlement diagrams.

In case of the Screwsol pile, the most important uncertainty is the choice of the cross-sectional area A (which automatically influences the lateral surface considered in

the calculation of skin friction –Figure 2). Also, the displacement of the soil needs to be taken into consideration when computing pile forces and skin frictions. A third uncertainty is the elastic modulus of the combined concrete-steel pile, which can be safely evaluated for design purposes.

The results presented (Figure 3) consistently reveal the pile's tendency to consume most of the loads in the upper half of its length. In case of efficiently designed non-displacement piles it is expected that most of the loads are transferred through the lower part of the shaft (skin friction) and by tip resistance. Skin frictions in the upper few meters reach values of 200 kPa and more, compared to a maximum of 80 kPa given by the design norm.

However, in this case there are factors that suggest a different behaviour. Due to the presence of the threads, combined with the displacement of the soil, larger shear stresses may develop in the upper part of the shaft. Equally importantly, the soil is homogenous, even at the pile toe level, while in most design scenarios the soil layers towards the pile toe are significantly stiffer.

3. Logistic center Craiova load tests / 2021

The CPT-based design of the foundations was performed according to EC7 [5]:

$$R_{c,k} = \left(R_{b;k} + R_{s;k}\right) = \frac{R_{b;cal}+R_{s;cal}}{\xi} = \frac{R_{c;cal}}{\xi} = Min\{\frac{(R_{c;cal})_{med}}{\xi_3}; \frac{(R_{c;cal})_{min}}{\xi_4}\} \quad (1)$$

Based on the calculations few of the determined pile lengths were the following:
D330/500 – 950kN – L=16.05m
D330/500 – 1100kN – L=17.25m
D430/600 – 1450kN – L=16.55m

Five preliminary, instrumented load tests were executed on area A2. The instrumentation consists of strain gauges and base plates. The strain gauges were placed on the reinforcement cage at a vertical spacing of 1.5 m, with 3 gauges per each level being installed to achieve more precise results (Figure 4) and to confer redundancy in case some gauges would be damaged during pile installation. The base plates were installed on the bottom of the reinforcement cages, practically at pile toe level.

It is noted that all 5 test piles exhibited a load-displacement pattern which is characteristic for friction piles, represented by a considerable quasi-elastic domain until 875 kN to 1625 kN, which represents 17.5 % up to 32.5% of the representative diameter, considered as 50 mm, given that most of the load (and practically all service load) is carried by the shaft. These values are also very close or even exceed the structural capacity of the pile, which can be approximated as A_{int} x $f_{c,d}$ = 0.085 m2 x 16.7 MPa = 1425 kN.

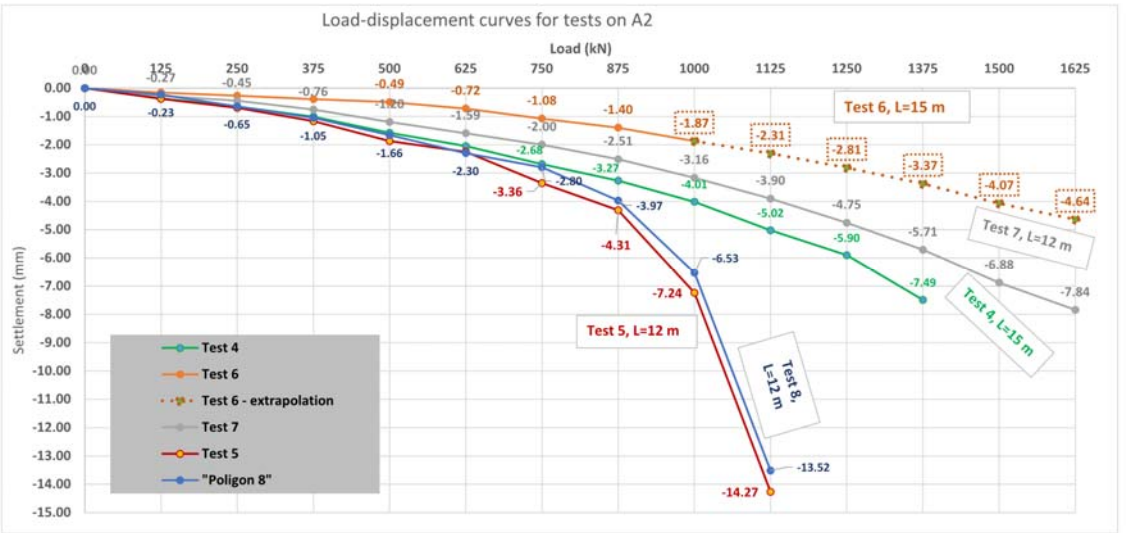

Figure 4. Load-settlement curves for all tests (5 piles).

However, it is noted that all other tests exhibited an extremely favourable pile behaviour. In case of two tests (test 4 and 7) the cracking of the pile head occurred after 1375 to 1625 kN, which are sufficiently large values of ultimate capacity to allow for an efficient pile design after division with partial safety factors. In case of test 6, for which pile head cracking occurred after 1000 kN, an extrapolation was performed, given the large pile length and the extremely small pile displacements (<2 mm) up to this point, to avoid unnecessary overdesign.

The distribution of the skin friction and toe resistance is presented in Figure 5, using a first approach in which the skin friction was calculated while the toe resistance was determined by subtracting the total skin friction from the load step applied during testing.

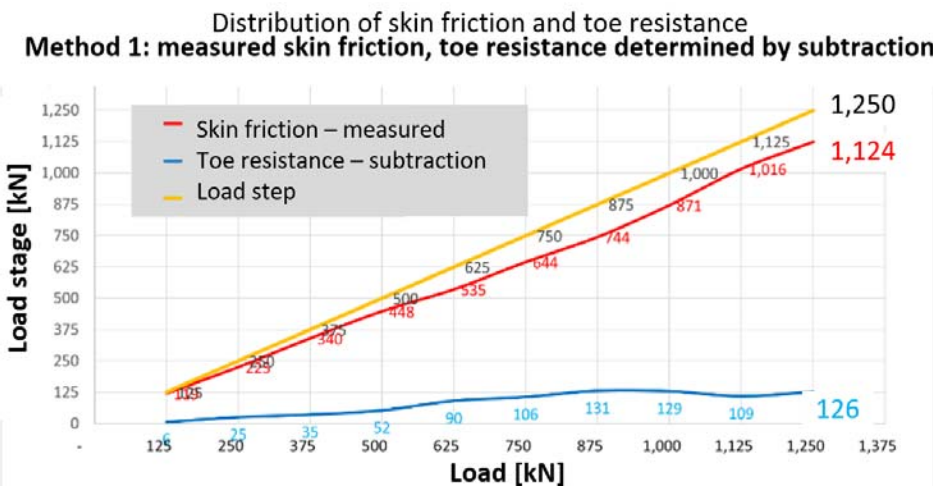

Figure 5. Distribution of skin friction and toe resistance – method 1, test 4.

The diagram shows that the pile shaft carries the largest part of the loads, approximately 90% and practically constant during the load steps.

4. Design approach of Screwsol piles

The Screwsol threaded piling system is recognized for integrating and enhancing the advantages of various piling systems, making it a highly efficient and versatile solution in foundation engineering. The specific benefits of the Screwsol system were highlighting its versatile diameters, relatively low torque requirements, and the use of

Smooth shaft displacement piles and threaded shaft displacement piles are two types of deep foundation elements used to support structures, particularly in challenging soil conditions. The load-bearing capacity of both types primarily relies on end-bearing at the pile tip and skin friction along the pile shaft (Figure 1).

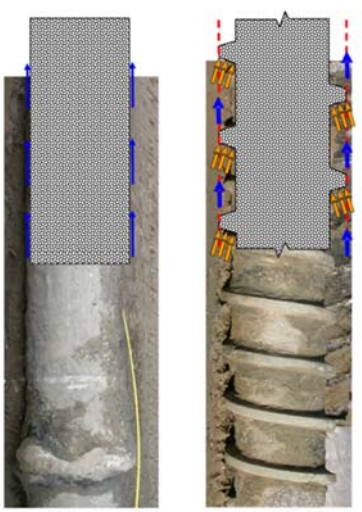

Figure 6. Smooth shaft and threaded shaft soil displacement piles schematic load transfer mechanism

The threaded shaped shaft increases the surface area in contact with the soil, enhancing skin friction resistance. The threaded design provides superior axial resistance, making these piles ideal for tensile load applications, such as wind turbine foundations and transmission towers.

Design based on the prescriptive Method as Outlined in Romanian Norm NP123:2010 [6] and its Updated Version NP123:2022 [7]

This method is based on the guidelines provided in the Romanian Norm NP123:2010 [6], which serves as a prescriptive framework for designing screw piles. Initially, this norm was utilized for the analysis of the first load tests conducted on such piles. The NP123:2010 [6] has since been revised and updated with the release of NP123:2022 [7], which incorporates more recent research findings and technological advancements. This updated version provides enhanced guidelines, reflecting the latest

best practices and improved methodologies for evaluating the load-bearing capacity and performance of soil displacement threaded screw piles.

Using the empirical method for cast-in-place floating bored piles and the assumptions mentioned above, the bearing capacity is determined bellow:

$$R_{c,d} = A_b \times q_b \quad /\gamma_{b2} + U \times \sum (q_s, k_i, l_i)/\gamma_{s2} - G_{pilot}\ (kN) \tag{1}$$

where:

$R_{c,d}$: bearing capacity, design value (kN);
A_b: cross-sectional area at pile toe (m^2);
$q_{b,k}$: toe resistance, characteristic value (kPa);
U: shaft perimeter (m);
$q_{s,ki}$: unitary skin friction (kPa);
l_i: depth of elementary soil layer (<2 m);
$\gamma_{b,2}$, $\gamma_{s,2}$: safety factors for toe and shaft resistance (dimensionless).

The interpretation of the monitoring results of the presented pile tests confirms that the pile geotechnical ultimate capacity exceeds the maximum load value given in the norm. It was also observed that high specific skin friction values were recorded which is significantly different than it is indicated in the design norm NP123-2022 [7]. These results suggest a very good behaviour of threaded piles in loose, medium dense non-cohesive soils as well as in soft, medium consolidated clays and confirm the efficiency of these pile types compared to equivalent bored piles.

The author proposes the already known formulae where the lateral friction is be expressed by the following relationship:

$$q_{s,k,i} \sim \tau_f = (\sigma_i \times tan(\phi_i') + c_i') \times k_{SCR} \tag{2}$$

The author introduced the "k_{SCR}" correlation factor, to establish a relationship between the values set in the design norm and the values of the studied load test results. The author suggests using this correlation factor to enhance the accuracy, reliability, applicability of the calculation, by making it better reflect the real-behavior of the variables in question.

The k_{SCR} correlation factor is considered to be a critical parameter in the design of soil displacement threaded screw piles, influencing the calculation of the pile's load-bearing capacity by accounting for the soil's mechanical properties and its interaction with the pile shaft. The proposed values for the k_{SCR} correlation factor can be summarized as follows:

- Non-Cohesive Soils (Sands and Gravels): k_{SCR} = 0.55 - 0.65

The proposed values for non-cohesive soils reflect the load transfer mechanism predominantly relying on the frictional resistance along the pile shaft and the shear of the interlocked soils with the surrounding compacted soils. The proposed k_{SCR} values within this range ensures that the load-bearing capacity calculations remain conservative, accounting for potential variations in soil density and compaction levels.

This conservative approach helps prevent overestimation of pile performance and enhances the safety and reliability of the foundation system.

- Cohesive Soils (Clays and Silts): k_{SCR} = 0.90 - 1.00

These higher values reflect the load transfer mechanism as the shear resistance of the soil against lateral movement.

By aligning the k_{SCR} values with the inherent properties of different soil types, engineers can ensure that the load-bearing capacity calculations are both accurate and safe, leading to optimized pile designs tailored to specific site conditions.

The partial safety factors $\gamma_{b,2}$, $\gamma_{s,i,2}$, mentioned above are safety factors for toe and shaft resistance and they are dimensionless. They represent technology (pile execution method and concreting technology) and soil related (around the pile shaft and at pile toe) factors, therefore their discussion in relation of the Screwsol cast in situ threaded soil displacement method is rather relevant.

The safety factor for the shaft resistance ($\gamma_{b,2}$), is described as conditioned by the execution technology of the piles versus the soil around the pile shaft. For the Screwsol method the values 1,90 respectively 1,20 is proposed by the author, in cohesive and respectively non-cohesive soils around the piles shaft, for the reasons as follows:

- in cohesive soils, the improvement / the compaction of the soil around the piles shaft is rather limited, while the execution technology (installation steps) is very similar to those of the CFA (continuous flight auger)
- in non-cohesive soils, where the Screwsol method advantages are clearly demonstrated and where the improvement / the compaction of the soil around the pile by the means of the interlocking phenomena provides the best output, the safety factor is proposed with the values given by the norm for the “Driven casing and driven compacted concreting” and the “Vibrated casing and vibrated compacted concrete” technologies

The safety factor for the toe resistance ($\gamma_{s,i,,2}$), is described as conditioned by the concreting technology of the piles versus the soil at the pile toe. For the Screwsol method the values 1,20 respectively 1,20 is proposed by the author, in cohesive and respectively non-cohesive soils at the pile toe, for the reasons as follows:

- in both cohesive and non-cohesive soils, the concreting technology is very similar to those of the CFA (continuous flight auger), the concreting of the pile starting with the slight withdrawal of the drilling tool and simultaneous pumping of the fresh concrete, through the hollow core of the auger, thus injecting and filling of all the cavities and the contact between the pile toe and the surrounding soil is ensured

Design according to the In-Situ Test Results (CPT) Based Method, as Described in Eurocode 2, Annex D [5]

This approach relies on in-situ test results, particularly using Cone Penetration Testing (CPT), as outlined in Eurocode 7-2, Annex D [5]. This method involves conducting field tests to directly measure soil properties such as cone resistance and

sleeve friction. These measurements are then used to determine the bearing capacity and behavior of screw piles under different loading conditions. The CPT-based approach allows for a more site-specific and accurate assessment of pile performance, tailoring the design to the actual soil conditions encountered at the project location.

Eurocode 7-2, Annex D [5], describes the calculation formula for the maximum compressive strength of a pile:

$$F_{max} = F_{max;base} + F_{max;shaft} \quad (3)$$

where:

$$F_{max;base} = A_{base} \times p_{max;base} \quad (4)$$

is the maximum base resistance

and

$$F_{max;shaft} = C_p \int_0^{\Delta L} p_{max;shaft;z} dz \quad (5)$$

is the maximum shaft resistance

where: A_{base} is the cross sectional area of the base, in m2;
C_p is the circumference of the part of the pile shaft in the layer in which the base of the pile is placed, in m;

Maximum base resistance

$$p_{max;base} = 0.5 \times \alpha_p \times \beta \times s \times (\frac{q_{c;I;mean} + q_{c;II;mean}}{2} + q_{c;III;mean} \quad (7)$$

where $p_{max;base}$ is the specific resistance at the base of the pile, while $q_{c;I;mean}$, $q_{c;II;mean}$, $q_{c;III;mean}$, $q_{c;z;a}$ are the CPT cone resistances measured with different methods.

$p_{max;base} \leq 15MPa$

α_p - pile class factor

β - expanded pile toe shape factor (between 0.6 – 1.0)

s - non-circular pile toe shape factor (1.0 for square shape)

At the critical depth the calculated value of qb becomes a minimum.

q_{cm} - mean of the q_c values over the depth from 3D below the base up to the level 1.5D above the pile base

q_{cIm} - mean of the q_{cI} values over the depth from the pile base level to critical depth level.

q_{cIIm} … mean of the lowest q_{cII} values over the depth going upwards from the critical depth to the pile base level, in which progressing upwards a value is only considered if it is lower than the previous one.

q_{cIIIm} … mean of the lowest q_{cIII} values over a depth interval from the pile base level to a level of 8 times the pile base diameter above the pile base. This procedure starts with the lowest q_{cII} value used for the computation of q_{cIIm}.

Maximum shaft friction

$$\mathbf{p_{max;shaft;z} = \alpha_s \times q_{c;z;a}} \quad (8)$$

where: $p_{max;shaft;z}$ is the specific resistance on the lateral surface of the pile,

α_s - shaft friction coefficient

$q_{c;z;a}$ - value of q_c at depth z

Based on the results of the preliminary, later on of the simple, complex and instrumented load tests performed on Screwsol piles and their results correlations with the CPT values, the following values are proposed by the author for the coefficients ∝p and ∝s (Table 1):

Table 1.

α_p and α_s values proposed for Screwsol piles in various soils

Soil type	Soil type	$\propto_p$	$\propto_s$
Non—cohesive	gravel, sandy gravel	0,90	0,005
	gravely sand, coarse sand	0,90	0,007
	medium and fine sand	0,90	0,009
Cohesive	Silt, low plasticity clay	0,80	0,025
	Medium and high plasticity clay	0,80	0,033

The suggested values are consistent with the ranges specified by Eurocode 7 [5] for both driven piles and continuous flight auger (CFA) piles. This alignment supports the claim that Screwsol piles effectively combine the superior bearing capacity characteristics typical of driven piles with the versatile installation techniques associated with bored piles.

The proposed values are derived from extensive correlations established by the author of this thesis through comprehensive analysis and testing conducted over nearly two decades, from 2005 to 2024. This research involved more than 100 different sites, where over 400 load tests and more than 1000 Cone Penetration Test (CPT) measurements were performed.

5. Analysis and evaluation of the CO2 footprint of Screwsol

The use of materials (concrete, steel) is responsible for approximately 95% of total CO2 emissions generated by construction activity.

For the example, it was considered a project with 500 piles with a length of 10.0 m, in two versions: executed with CFA technology and diameter of 600mm, respectively Screwsol technology and diameter 430/600, their bearing capacities being considered to be similar.

The analysis demonstrates that CFA technology with a 600mm diameter results in a significantly larger (30% higher) carbon footprint (Figure 7) compared to Screwsol

technology with a 430/600mm diameter. This difference highlights the importance of selecting appropriate piling methods to minimize the carbon footprint and contribute to broader climate change mitigation and environmental conservation efforts. By opting for Screwsol technology, construction projects can achieve more sustainable outcomes, reducing their overall carbon footprint and contributing to environmental conservation efforts. Moreover, the proper selection of piling method is not just a technical decision but a strategic one that has far-reaching implications for the environment. By prioritizing sustainable and less carbon intensive piling techniques, the geotechnical construction industry can play a pivotal role in reducing greenhouse gas emissions, conserving natural resources, and fostering a more sustainable built environment.

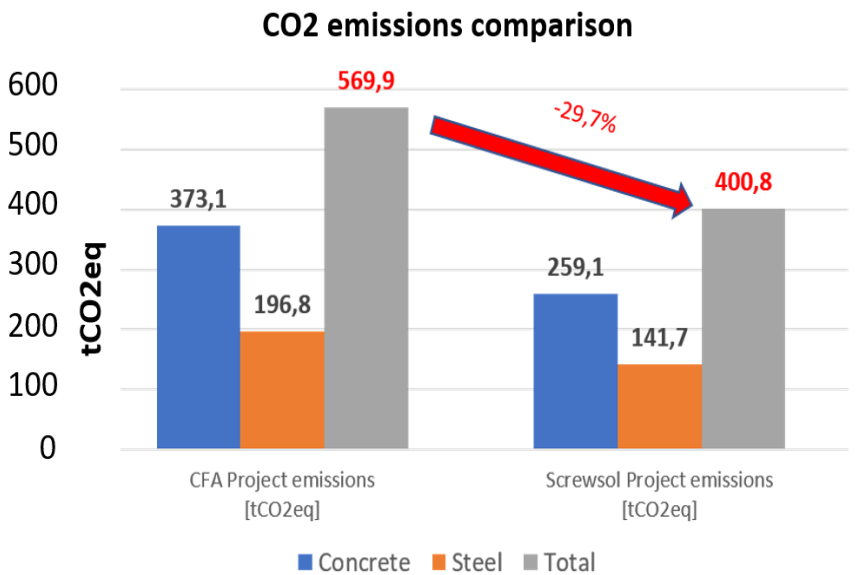

Figure 7. CO2 emissions for CFA and Screwsol.

6. Conclusions

The applicability of Screwsol has been successfully proven both in non-cohesive soils, but also in medium stiff and plastic clay conditions. The execution length of the piles is limited by the characteristics of the in situ soil and the refusal criteria of the soil – drilling torque combination.

The maximum efficiency of the piles is obtained for non-cohesive soil conditions terrain – fine and medium – in loose or medium density. In the case of cohesive soils, the efficiency is high plastic clays. Due to the fact that the dynamic effects produced during execution are reduced through the execution technology, they can also be used to treat soils with liquefaction potential. The presence and level of the groundwater has neither negative influence on the execution technology nor to the efficiency of the piles.

References

[1] ASRO. SR EN 12699:2015, Execution of special geotechnical works - Displacement piles (in Romanian: Execuția lucrărilor geotehnice speciale. Piloți de îndesare).
[2] T. Kaltenbacher, L. Sata, Á. Deli. ”The applications of the Screwsol soil displacement piling solution, Közúti és Mélyépítési Szemle, Budapest, Hungary” (in Hungarian: (A Screwsol talajkiszorításos cölöpözés alkalmazásának lehetőségei), 2008.
[3] L. Sata, ”Small and large diameter soil displacement Screwsol piles in the deep foundation practice”, Proceedings of the 10th Geotechnical Conference (V4), Ráckeve, Hungary, 2005
[4] L. Sata, S. Manea, ”Screwsol – threaded displacement pile”, Revista Construcţiilor, ISSN 1841-1290, Bucharest, Romania. (in Romanian: (Screwsol – Pilot de îndesare înşurubat), 2012.
[5] ASRO. SR EN 1997-2:2007, Eurocode 7: Geotechnical design - Part 2: Ground investigation and testing (in Romanian: Eurocod 7: Proiectarea geotehnică. Partea 2: Investigarea şi încercarea terenului).
[6] NP 123-2010: Regulations on the geotechnical design of pile foundations (in Romanian: Normativ privind proiectarea geotehnică a fundațiilor pe piloți).
[7] NP 123-2022: Regulations on the geotechnical design of pile foundations (in Romanian: Normativ privind proiectarea geotehnică a fundațiilor pe piloți).

Comparison of green building rating systems and the usage of smart materials using BIM

Comparația sistemelor de evaluare a construcților verzi și utilizarea materialelor inteligente cu BIM

N.R Monish Raaj[1], Vasudevan Ramasamy[2]

[1]*Research scholar, Adhiparasakthi Engineering College, Melmaruvathur, Tamil Nadu, India- 603319.*
[2]*Professor/Dean in the department of Civil engineering at Adhiparasakthi engineering college Melmaruvathur, Tamil Nadu, India- 603319.*
*Corresponding author

Email: nrmonishraaj@gmail.com

DOI: 10.37789/rjce.2025.16.1.2

Abstract
The escalating importance of green building practices in tackling environmental challenges necessitates innovative solutions, particularly emphasizing resource conservation, energy efficiency, and occupant well-being. Building Information Modeling (BIM) has emerged as a promising tool to enhance efficiency in construction projects. This sophisticated digital platform enables real-time collaboration and visualization of the construction process. This study aims to explore the potential of BIM in promoting sustainability within smaller-scale building projects. The utilization of Building Information Modeling (BIM) presents a significant opportunity to enhance the design of green buildings. By integrating BIM with building rating systems, architects can ensure that their structures meet the necessary standards for green certification. The study focuses on assessing the impact of Building Information Modeling (BIM) on resource efficiency, energy performance, waste reduction, and cooperative decision-making in small-scale green buildings. Results indicate a positive correlation between BIM adoption and various aspects of sustainability, including early-stage design optimization, energy efficiency analysis, material selection, life cycle assessment, waste reduction, and prefabrication using LEED (Leadership in Energy and Environmental Design), BREEAM **(**Building Research Establishment Environmental Assessment Method)**.** The findings underscore the significance of incorporating BIM into smaller-scale construction projects to promote eco-friendly practices and achieve sustainable outcomes. By leveraging BIM of smart materials, architects and construction professionals can enhance resource efficiency, improve energy performance, reduce waste generation, and facilitate collaborative decision-making throughout the project lifecycle.

Keywords: Building Information Modeling (BIM); LEED (Leadership in Energy and Environmental Design); BREEAM **(**Building Research Establishment Environmental Assessment Method); Green building; Smart Materials;

The article was received on 19.11.2024, accepted on 24.02.2025 and published on 14.03.2025

1.Introduction

In recent years, there has been a heightened global focus on combating climate change and advancing sustainable development, leading to increased efforts to adopt environmentally responsible practices across various industries [1-5]. Recognizing the construction industry's substantial resource consumption and contribution to construction and demolition waste, there has been a notable shift towards promoting more sustainable building techniques within the sector. Green building, which integrates energy efficiency, resource conservation, and occupant well-being, has emerged as a pivotal solution to address environmental concerns[6]. With a primary focus on minimizing the building's impact on the environment, research indicates significant advantages of green buildings compared to conventional structures. Studies suggest that green buildings may achieve remarkable reductions in energy consumption by up to 50%, water consumption by 40%, and carbon emissions by 35% [7]. These statistics underscore the substantial potential of green building practices in mitigating the adverse effects of construction on the natural environment.

Building Information Modeling (BIM) has revolutionized the stages of planning, designing, and construction. BIM is an intelligent digital platform that facilitates real-time collaboration among stakeholders, allowing them to share information and visualize the construction process in three dimensions [7]. This transformation has propelled BIM into an essential technology for enhancing the efficiency of building projects, minimizing construction errors, and enhancing building functionality [8]. As the benefits of Building Information Modeling (BIM) in streamlining construction processes became increasingly evident, researchers and professionals in the field recognized the potential of combining BIM with environmentally friendly building practices [9]. Integrating the data-rich environment of BIM with sustainability analysis has shown promise in facilitating early-stage design decisions that result in energy-efficient designs and ecologically responsible material choices [10]. This synergy between BIM and sustainability analysis offers opportunities to optimize building designs for environmental performance from the outset of the project.

The construction industry's significant impact on global energy, raw material, water, land consumption, and solid waste production has propelled efforts to improve environmental sustainability, given its substantial contributions to these areas: 40% of global energy consumption, 30% of global raw material consumption, 25% of global water consumption, 12% of global land consumption, and 25% of global solid waste production [11]. Sustainable building practices have emerged as a solution to mitigate these environmental impacts [12]. Sustainable buildings aim to reduce water and energy consumption while maintaining occupants' well-being. However, designing sustainable buildings poses challenges due to the need for multidisciplinary design teams to address diverse environmental, social, and economic needs [13]. Building rating systems for sustainable buildings are developed to evaluate the environmental performance of structures [14] and promote sustainability across their planning, construction, and operation phases [15]. A variety of building rating systems have been developed to assess and highlight a building's sustainable performance [16]. These rating tools measure environmental performance, ensuring that optimal sustainable practices are

incorporated into the design, construction, and operation of the building [17]. Building rating systems play a crucial role in guiding decision-making processes for sustainable buildings [18]. To ensure resource efficiency throughout a building's lifecycle, it is imperative to integrate these rating tools into the design process [19]. This integration facilitates the adoption of sustainable design principles from the outset, thereby optimizing the building's overall environmental performance.

This research provides valuable insights into the potential of Building Information Modeling (BIM) to enhance resource efficiency, energy performance, waste reduction, and collaborative decision-making in small construction projects through the analysis of real-world case studies and practical applications. These findings open up new avenues for achieving sustainable outcomes in smart materials construction endeavors. By offering innovative results and evidence-based suggestions, this research aims to equip stakeholders with practical tools to foster a greener and more ecologically responsible built environment, thus contributing to the advancement of sustainable practices in the construction sector. The hypothesis outlined in Figure 1 illustrates the anticipated impact of implementing BIM on sustainability in small construction projects, guiding further investigation into this important area.

- **S1:** Early-stage design optimization is significantly associated with the implementation of Building Information Modeling (BIM) in smart material projects. This hypothesis proposes that the utilization of BIM in smart construction is likely to have a notable positive impact on early-stage design optimization. In essence, BIM is expected to contribute to enhanced design processes and outcomes in smart material projects.
- **S2**: Energy efficiency and performance analysis are significantly correlated with the implementation of BIM in smart material projects. This hypothesis suggests that the integration of BIM in smart material construction projects is anticipated to be closely linked to improved energy efficiency and the capability to conduct more comprehensive performance analysis. It implies that BIM can play a crucial role in augmenting the energy performance of buildings in smart material construction endeavors.
- **S3:** Utilizing Building Information Modeling (BIM) in smart materials projects exhibits a strong correlation with material selection and life cycle assessment. This hypothesis suggests that the adoption of BIM likely enhances material selection procedures and enables comprehensive life cycle assessments in small construction projects. It is anticipated that BIM facilitates making more informed decisions regarding materials and their long-term sustainability.
- **S4:** The application of BIM in smart materials projects is strongly associated with waste reduction and prefabrication. This hypothesis suggests a noticeable reduction in construction waste and an increased utilization of prefabricated components when BIM is implemented in smart materials projects. It indicates that BIM can support the adoption of

environmentally responsible and more efficient building methods, including the use of smart materials.

The hypotheses of the study are as follows:

- S1 or H1: Early-stage design optimization is positively influenced by the implementation of Building Information Modeling (BIM) in small construction projects.
- S2 or H2: Implementation of BIM in small construction projects leads to improved energy efficiency and performance analysis.
- S3 or H3: The utilization of BIM in small construction projects correlates with enhanced material selection procedures and comprehensive life cycle assessment.
- S4 or H4: Integration of BIM in small construction projects is associated with reduced waste generation and increased adoption of prefabrication methods.

These hypotheses serve as the guiding principles for exploring the relationship between BIM implementation and various aspects of sustainability in small-scale construction projects.

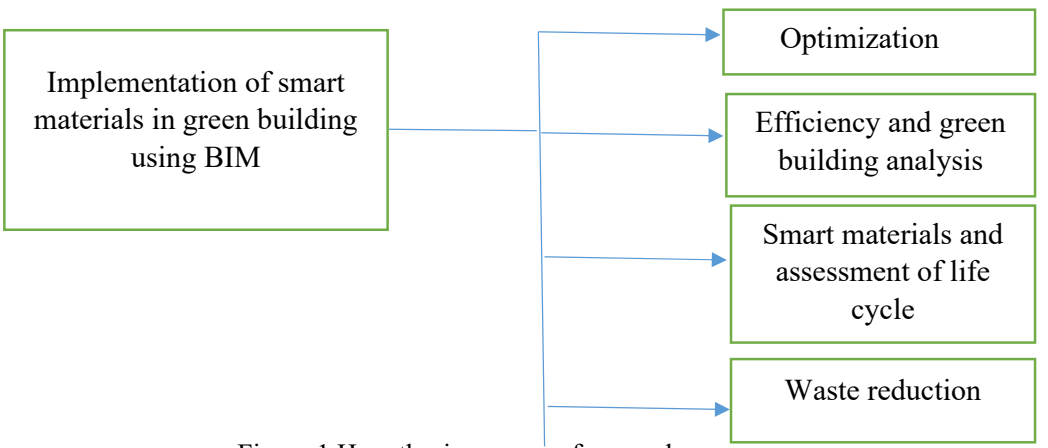

Figure 1 Hypothesis process of research

2. Building Assessment Tools

Building rating systems and assessment tools are commonly utilized to evaluate a building's environmental performance. These include well-known systems such as the Green Building Index (GBI), Green RE, Green Mark, Building Research Establishment Environmental Assessment Method (BREEAM), Leadership in Energy and Environmental Design (LEED), among others. BREEAM, established in the UK in 1990, and LEED, created by the US Green Building Council (USGBC) in 1998, are prominent examples. Additionally, systems like Green Mark (Singapore), GBI, and Green RE (Malaysia) cater to specific regional needs. These rating systems aim to assess a building's sustainability performance by considering factors such as energy efficiency, resource conservation, indoor environmental quality, and overall environmental impact.Building rating tools are systems or frameworks used to evaluate and assess the sustainability and environmental performance of buildings. These tools provide a

standardized method for measuring various aspects of a building's sustainability, including energy efficiency, water usage, materials selection, indoor air quality, and overall environmental impact. Some of the most widely used building rating tools include:

- **Leadership in Energy and Environmental Design (LEED)**: Developed by the U.S. Green Building Council (USGBC), LEED is one of the most recognized green building certification programs globally. It assesses buildings based on criteria such as energy efficiency, water conservation, materials selection, and indoor environmental quality.
- **Building Research Establishment Environmental Assessment Method (BREEAM)**: Originating in the UK, BREEAM evaluates the sustainability performance of buildings across various categories, including energy, water, materials, pollution, and management processes. It provides ratings ranging from Pass to Outstanding based on the overall performance of the building.
- **Green Building Index (GBI)**: GBI is a green rating tool developed specifically for Malaysia. It evaluates buildings based on criteria such as energy efficiency, indoor environmental quality, sustainable site planning, and materials selection

3. Building Information Modelling (BIM)

In recent years, Building Information Modelling (BIM) has emerged as a valuable tool for addressing sustainability challenges. BIM provides a platform for visualizing both the physical and functional aspects of a building, offering a wealth of data, including geometric and semantic information [23]. This data can be integrated into BIM models to propose sustainable measures during the design phase, facilitating more accurate environmental performance analysis and sustainability assessments. Integration with BIM enables collaborative information sharing among stakeholders involved in construction projects. Additionally, BIM is often combined with Life Cycle Assessment (LCA) to enhance a building's sustainability assessment. Automated tools utilizing BIM and LCA can calculate energy consumption and carbon emissions, aiding decision-makers in optimizing building performance. Research has demonstrated that integrating BIM and LCA enables designers to select more environmentally friendly materials and products. While LCA typically focuses on comparing the environmental impacts of two sustainable buildings rather than certification or meeting minimum sustainable requirements, this study shifts its focus to reviewing research that employs BIM to assist in the certification process and compliance with minimum sustainable requirements from building rating tools.

4. Methods

The research methodology commences with an extensive literature review. This step involves a meticulous analysis of existing literature on green building practices and the utilization of Building Information Modeling (BIM) in smart materials construction projects. Case studies and best practices are also examined. The aim of this process is to identify key elements and variables that facilitate the effective implementation of BIM in smart materials, environmentally sustainable building projects. By reviewing relevant

literature, the study builds a robust knowledge base, enabling a comprehensive understanding of past successes and the fundamental principles guiding the adoption of BIM in green building initiatives.

Following the literature analysis, the study progresses to the quantitative investigation phase. In this phase, the study examines real smart materials building projects that utilize BIM for green building techniques. Data from these projects are analyzed using statistical methods, with a focus on key sustainability metrics such as waste reduction, energy performance, resource efficiency, and collaborative decision-making. Specifically tailored to small construction projects, the analysis aims to offer empirical evidence of the positive impact of BIM implementation on these sustainability aspects. Through this analysis, the study aims to demonstrate practically how BIM can effectively support sustainability initiatives in smaller-scale building projects. Structural Equation Modelling (SEM), a highly developed statistical technique, is used in the research study's final stage. SEM enables us to thoroughly examine the hypotheses and explore the intricate relationships between different elements that affect the application of BIM for green building in small projects. We can comprehend the complex relationships between BIM adoption and sustainability outcomes better thanks to this advanced analysis. Through the application of SEM, the research can furnish industry participants with comprehensive and empirically-supported perspectives, ultimately aiding in the creation of sustainable construction methodologies customized to the particular circumstances of small-scale building undertakings.

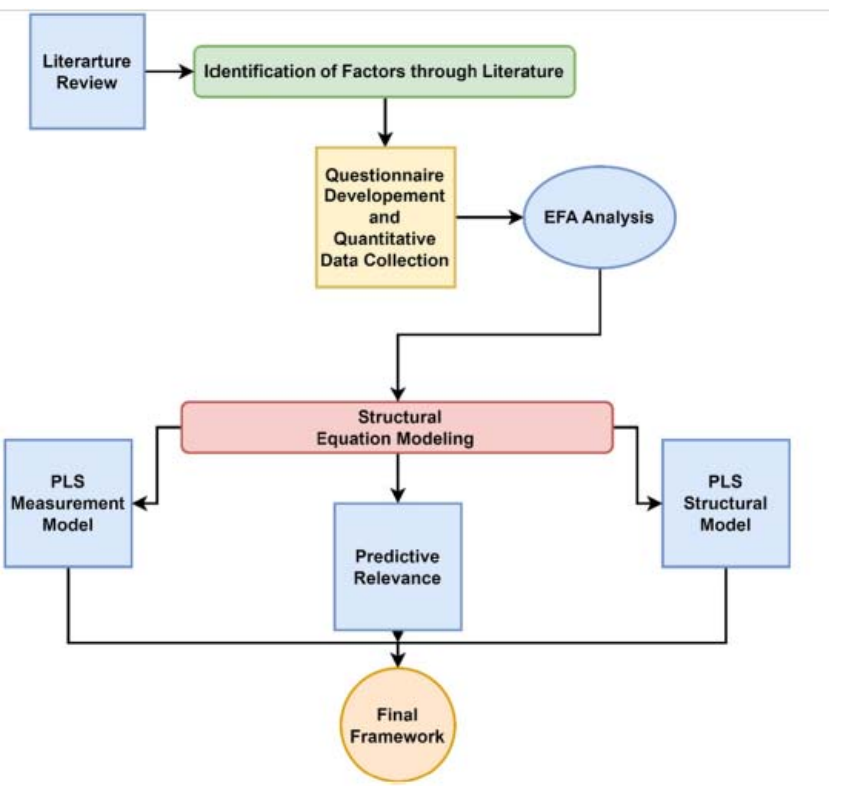

Figure 2 Research methodology

4.1 Smart materials with BIM

The integration of smart materials with Building Information Modeling (BIM) presents exciting opportunities for enhancing the sustainability and efficiency of construction projects. Smart materials are those designed with embedded sensors, actuators, or other advanced technologies that enable them to respond to external stimuli or perform specific functions. When combined with BIM, these materials can offer several benefits:

- **Real-time Monitoring and Control**: Smart materials equipped with sensors can provide real-time data on various parameters such as temperature, moisture levels, and structural integrity. This data can be integrated into the BIM model, allowing project stakeholders to monitor the performance of materials throughout the construction process and even during the operational phase of the building.
- **Optimized Building Performance**: By integrating smart materials into the BIM model, designers can simulate different scenarios and assess the impact of material choices on the building's performance. For example, BIM can be used to analyze the energy efficiency of a building by simulating the behavior of smart materials that regulate temperature or lighting based on environmental conditions.
- **Improved Decision-making**: BIM provides a collaborative platform for project stakeholders to visualize and analyze building designs. By incorporating smart materials into the BIM model, stakeholders can make more informed decisions regarding material selection, construction methods, and building systems, leading to improved sustainability and efficiency.
- **Enhanced Maintenance and Lifecycle Management**: Smart materials can facilitate predictive maintenance strategies by providing early warning signs of potential issues such as structural degradation or equipment malfunction. When integrated with BIM, this data can be used to create digital twins of buildings, allowing for better lifecycle management and optimization of maintenance schedules.
- **Reduced Environmental Impact**: Smart materials with energy-saving features or sustainable properties can contribute to reducing the environmental footprint of construction projects. By incorporating these materials into the BIM model, designers can assess their impact on energy consumption, material usage, and overall sustainability performance.

5. Data collection

The integration between BIM and simulation software enables more accurate environmental performance analysis and better-informed decision-making throughout the design process. Moreover, the interoperability between BIM and simulation tools streamlines workflows and reduces the time and effort required to perform sustainability assessments. As a result, the combination of BIM with LEED and simulation software offers a powerful framework for designing and constructing sustainable buildings. However, it is worth noting that while LEED may be one of the most frequently

integrated building rating systems with BIM, other systems such as BREEAM and Green Star also have established integrations with BIM, albeit to varying extents. Therefore, the choice of building rating system and associated BIM integration tools may depend on project-specific requirements and regional preferences.

Table 2

Overview of BIM and building rating tools

References	Group	Code	Description
[1]	Optimization of Early-stage	BIM-EO1	BIM effectively manages resources to minimize waste and promote environmentally friendly alternatives.
[2]		BIM-EO2	BIM facilitates informed sustainable design decisions, promoting the development of greener building designs
[3]		BIM-EO3	BIM enhances collaboration, making it more accessible and facilitating the attainment of sustainable objectives.
[4]		BIM-EO4	BIM enables sustainable site planning by optimizing building orientation to maximize energy efficiency.
[5,6]	Efficiency and green building analysis	BIM-EA1	BIM enables energy analysis and facilitates the identification of energy-saving methods.
[7]		BIM-EA2	BIM-guided designs result in lower greenhouse gas emissions, thereby reducing the building's carbon footprint.
[8,9]		BIM-EA3	The integration of BIM for enhanced energy efficiency contributes to a more favorable green image for the building.
[10,11]	Smart materials and assessment of life cycle	BIM-MS1	BIM aids in making environmentally responsible choices by prioritizing materials with low embodied carbon and high percentages of recycled content.
[13-15]		BIM-MS2	Using BIM to select materials with low levels of volatile organic compounds (VOCs) is an effective method for enhancing indoor air quality within buildings**.**
[16-18]		BIM-MS3	Selecting long-lasting materials is crucial to minimize the need for maintenance and replacement, thereby

References	Group	Code	Description
			optimizing resource utilization and reducing environmental impact.
[19]	Smart materials and assessment of life cycle	BIM-WB1	BIM can reduce waste in building and demolition by maximizing the utilization of each material's potential quantity.
[20,21]		BIM-WB2	A more precise estimate facilitated by BIM helps reduce surplus material and minimizes the amount of construction and demolition waste generated during the construction process.
[22]		BIM-WB3	Prefabrication integrated with BIM streamlines operations, leading to construction completed in less time.

6. Data analysis

6.1 EFA analysis

Exploratory Factor Analysis (EFA) serves as a systematic approach to uncovering the fundamental structure and relationships within a study's observed variables. It is a data reduction technique aimed at identifying latent factors or constructs that explain the variance in the data. The initial phase of EFA involves rigorous data preparation, including a thorough examination of collected responses for completeness and accuracy . Subsequently, the dataset undergoes scrubbing to address missing values adequately. Following data preparation, the suitability of the data for EFA is evaluated using measures such as the Kaiser-Meyer-Olkin (KMO) test and Bartlett's test of sphericity. These assessments provide valuable insights into sample size adequacy and the intercorrelation between variables, laying the groundwork for a robust exploratory factor analysis. Following the exploratory factor analysis (EFA), the final factor solution was interpreted to uncover latent constructs within the dataset. Variables that made significant contributions to each factor were identified, aiding in the characterization of these factors. The primary objective of employing the EFA methodology was to reveal latent constructs and elucidate the factor structure inherent in the dataset. This process facilitated the exploration of underlying dimensions and associations between variables, thereby offering valuable insights for subsequent analysis and interpretation. By identifying these latent constructs, researchers gain a deeper understanding of the complex relationships within the data, paving the way for further investigation and theoretical development.

6.2 SEM analysis

The study utilized SmartPLS 4 software to employ Partial Least Squares Structural Equation Modeling (PLS-SEM) for a comprehensive analysis of the relationships and effects among crucial factors affecting Building Information Modeling

(BIM) implementation in small construction projects, particularly focusing on green building and sustainability practices PLS-SEM was deemed appropriate for this investigation Handling Small Sample Sizes: PLS-SEM is well-suited for studies with limited sample sizes, making it an ideal choice for this research. Suitability for Exploratory Research: PLS-SEM is particularly suitable for exploratory research where constructs might not adhere to a normal distribution.

The study employed the PLS algorithm within SmartPLS 4 to examine the relationships between various factors related to BIM implementation and their impact on sustainability outcomes in small construction projects. These factors included energy efficiency analysis, resource optimization, collaboration, sustainable site planning, greenhouse gas emissions reduction, material selection, life cycle assessment, and prefabrication. To ensure the reliability and validity of the measurement model, the algorithm evaluated both convergent and discriminant validity. This was assessed by examining factor loadings, composite reliability, and average variance extracted (AVE) for each construct. High factor loadings, composite reliability values above a threshold (typically 0.7 or higher), and AVE values exceeding 0.5 indicate satisfactory convergent validity, ensuring that the measurement model accurately captures the latent variables.

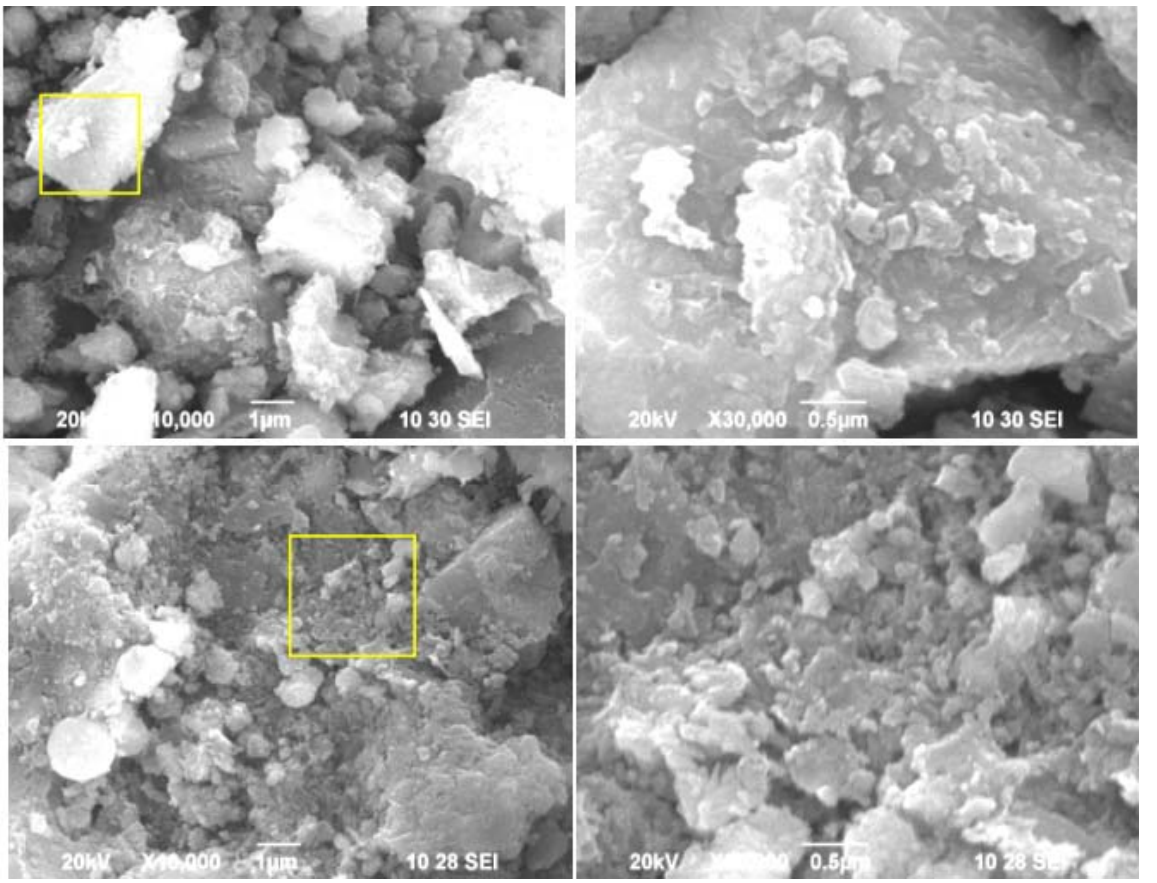

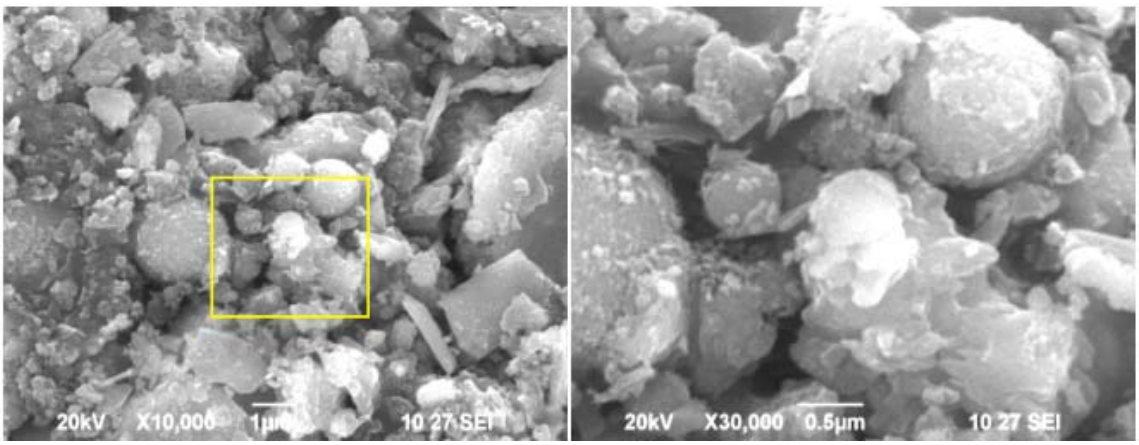

Figure 3 SEM Analysis

7.Conclusion

The integration of Building Information Modeling (BIM) with building rating tools has the potential to streamline and expedite the green certification process. However, it's apparent from the literature review that research in this area is limited, which may explain the prevalent manual approach to green building ratings. Among various building rating tools such as LEED, BREEAM, GBI, GreenRE, Green Mark, and BEAM Plus, LEED stands out as widely used for integration with BIM software, although the integration methods remain relatively underexplored. The existing research primarily focuses on leveraging BIM to enhance building sustainability by extracting information from BIM models, rather than automating the green certification process. Notably, while BIM's application in obtaining credits under energy efficiency subcategories is relatively mature, other subcategories such as water efficiency, location and transportation, material and resources, sustainable site, indoor environmental quality, innovation, and regional priority remain understudied within the context of BIM-building rating. To address these gaps, future research should delve into these underexplored subcategories to broaden the scope of BIM's utilization for green ratings. Additionally, it's worth noting that the reviewed publications predominantly concentrate on the integration of BIM and building rating tools, neglecting studies focused on utilizing BIM software to directly improve sustainability. This limitation underscores the need for expanded research efforts to explore the full potential of BIM in advancing sustainability practices within the built environment.

REFERENCES

1. Abdelaal, F., Guo, B.H.W., 2022. Stakeholders' perspectives on BIM and LCA for green buildings.
2. J. Build. Eng. Cao, Y., Kamaruzzaman, S.N., Aziz, N.M., 2022a. Building Information Modeling (BIM) Capabilities in the Operation and Maintenance Phase of Green Buildings: A Systematic Review. Buildings.
3. Cao, Y., Kamaruzzaman, S.N., Aziz, N.M., 2022b. Green Building Construction: A Systematic Review of BIM Utilization. Buildings.

4. Ekasanti, A., Dewi, O.C., Putra, N.S.D., 2021. Green BIM potential in assessing the sustainable design quality of low-income housing: a review. IOP Conf. Ser. Mater. Sci. Eng. Feng, N., 2022. The influence mechanism of BIM on green building engineering project management under the background of big data.

5. Appl. Bionics Biomech. Ferdosi, H., Abbasianjahromi, H., Banihashemi, S., Ravanshadnia, M., 2023.

6. BIM applications in sustainable construction: scientometric and state-of-the-art review. Int. J. Constr. Manag.

7. Geoghegan, H.J., Jensen, F.W., Kershaw, T., Codinhoto, R., 2022. Innovation realisation for digitalisation within Dutch small architectural practises: state of the art and future needs. Proc. Inst. Civ. Eng. Manag. Procure.

8. Law. Guo, K., Li, Q., Zhang, L., Wu, X., 2021. BIM-based Green Building Evaluation and Optimization: A Case Study.

9. J. Clean. Prod. Huang, B., et al., 2021. Contribution and obstacle analysis of applying BIM in promoting green buildings.

10. J. Clean. Prod. Ismaeel, W.S.E., Kassim, N., 2023. An Environmental Management Plan for Construction Waste Management. Ain Shams Eng.

11. J. Ismaeel, W.S.E., Lotfy, R.A.E.R., 2023. An integrated building information modelling-based environmental impact assessment framework. Clean Technol. Environ.

12. Policy. Li, H., Wang, C., 2022. The Construction of Green Building Integrated Evaluation System Based on BIM Technology.

13. Mob. Inf. Syst. Lim, Y.W., et al., 2021a. Review of BIM for Existing Building Sustainability Performance and Green Retrofit. International Journal of Sustainable Building Technology and Urban Development.

14. Lim, Y.W., Chong, H.Y., Ling, P.C.H., Tan, C.S., 2021b. "Greening existing buildings through Building Information Modelling: a review of the recent development,". Build. Environ.

15. Liu, P., Li, Y., 2023. Ecological technology of green building in the initial stage of design based on BIM technology.

16. J. Exp. Nanosci. Liu, Q., Wang, Z., 2022. Green BIM-Based Study on the Green Performance of University Buildings in Northern China," *Energy*. Sustain.

17. Soc. Maskil-Leitan, R., Gurevich, U., Reychav, I., 2020. BIM Management Measure for an Effective Green Building Project. Buildings.

18. Mohammed, A.B., 2020. Collaboration and BIM Model Maturity to Produce Green Buildings as an Organizational Strategy.

19. HBRC J. Morsi, D.M.A., Ismaeel, W.S.E., Ehab, A., Othman, A.A.E., 2022. BIM-Based Life Cycle Assessment for Different Structural System Scenarios of a Residential Building. Ain Shams Eng.

20. J. Ohueri, C.C., Bamgbade, J.A., Chuin, A.L.S., Hing, M.W.N., Enegbuma, W.I., 2022. Best practices in building information modelling process implementation in green building design: architects' insights. J. Constr.

21. Dev. Ctries. (JCDC). Olanrewaju, O.I., Enegbuma, W.I., Donn, M., Chileshe, N., 2022. Building Information Modelling and Green Building Certification Systems: A Systematic Literature Review and Gap Spotting. Sustainable Cities and Society.

22. Olawumi, T.O., Chan, D.W.M., 2021. Green-building information modelling (Green-BIM) assessment framework for evaluating sustainability performance of building projects: a case of Nigeria. Architect. Eng.

23. Des. Manag. Pu, L., Wang, Y., 2021. The Combination of BIM Technology with the Whole Life Cycle of Green Building. World J. Eng. Technol.

24. Rathnasiri, P., Jayasena, S., Siriwardena, M., 2021. Assessing the applicability of green building information modelling for existing green buildings. Int. J. Des.

25. Nat. Ecodyn. Roggeri, S., Olivari, P., Tagliabue, L.C., 2021. Green and transportable modular building: a prefabricated prototype of resilient and efficient house. In: Journal of Physics. Conference Series.

26. Solla, M., Ismail, L.H., sharainon, A., Shaarani, M., Milad, A., 2019. Measuring the feasibility of using of BIM application to facilitate GBI assessment process. J. Build. Eng.

27. Solla, M., et al., 2022. Analysis of BIM-Based Digitising of Green Building Index (GBI): Assessment Method. Buildings.

28. Waqar, A., Othman, I., Shafiq, N., Mansoor, M.S., 2023a. Applications of AI in oil and gas projects towards sustainable development: a systematic literature review.

29. Artif. Intell. Rev. Waqar, A., Khan, M.B., Shafiq, N., Skrzypkowski, K., Zag´orski, K., Zag´orska, A., 2023b. Assessment of challenges to the adoption of IOT for the safety management of small construction projects in Malaysia: structural equation modeling approach. Appl. Sci. 13 (5).

30. Waqar, A., Qureshi, A.H., Alaloul, W.S., 2023c. Barriers to Building Information Modeling (BIM) Deployment in Small Construction Projects: Malaysian Construction Industry. Sustain.

31. Waqar, A., Othman, I., Shafiq, N., Altan, H., 2023d. Sustainability Modeling the Effect of Overcoming the Barriers to Passive Design Implementation on Project Sustainability Building Success : A Structural Equation Modeling Perspective. June.

32. Waqar, A., Othman, I., Gonz´alez-Lezcano, R.A., 2023e. Challenges to the Implementation of BIM for the Risk Management of Oil and Gas Construction Projects: Structural Equation Modeling Approach. Sustain.

Redemption of the lands occupied by the photovoltaic panels in the agricultural circuit

Redarea terenurilor ocupate de panourile fotovoltaice în circuitul agricol

Florin-Alexandru Lunga[1], Bogdan-Darian Toader[1]

[1] University Politehnica Timișoara
Victoriei Square, No. 2, Timisoara, Romania
E-mail: florin.lunga@student.upt.ro, darian.toader@student.upt.ro

Coordinator: Dănuț Tokar

E-mail: daunt.tokar@upt.ro

DOI: 10.37789/rjce.2025.16.1.3

Abstract. *Nuclear energy is a source of energy that can restore large areas of land in favor of agricultural exploitation. Also, by means of nuclear energy, the required energy for the sanitation and arrangement of unexploitable land surfaces and for feeding irrigation systems can be ensured. The article makes a comparative study between renewable technologies (nuclear, wind and photovoltaic) addressing both classical high-power (LR) and small-scale systems (SMRs) located in electrical energy consumption centres. The study highlights the advantages of nuclear energy in terms of land use, agricultural production, impact on wildlife and finally the possibility of cogeneration.*

Key words: nuclear energy, RES, agricultural surfaces, thermal island

1. Introduction

Nuclear energy is relatively one of the most cost-effective and reliable energies compared to other sources. Apart from the initial cost of construction, the cost of generating electrical energy is cheaper and more sustainable than other forms of energy such as oil, coal and gas. One of the additional benefits of nuclear power is that it involves minimal risk of cost inflation compared to traditional energy sources that fluctuate regularly over periods [1]. Nuclear fission generates much more energy than fossil fuels such as coal, oil or gas. The process produces nearly 8,000 times more energy than regular fossil fuels, resulting in fewer materials used and causing less waste [1].

Nuclear energy is the lowest carbon source of energy with a lower carbon footprint than other sources such as fossil fuels [1, 2].

A typical 1,000 MW nuclear power plant (NPP) has an average need of 34 ha to operate, while for the same installed power wind systems occupy 24 ha and solar systems 92 ha, according to the Nuclear Energy Institute (NEI) [3].

The article was received on 21.03.2024, accepted on 31.01.2025 and published on 14.03.2025

Although fossil fuels are non-renewable and have high CO_2 emissions, they are still used in the production of glass, cement and pottery, as well as in medicines such as aspirin [1].

Considering these reasons, it is important to conserve fossil fuels by using them as sparingly as possible and finding alternative sources of energy to perform some of the functions that we currently rely upon fossil fuels to perform [1].

2. Comparative study between renewable energy sources (nuclear, wind and photovoltaic)

Analysing the share of electrical energy consumption in Romania (Fig. 1) as a result of efficiency measures, there is a slight decrease in electrical energy consumption in the residential sector, services and industry, as well as a slight increase in agriculture and transport [4].

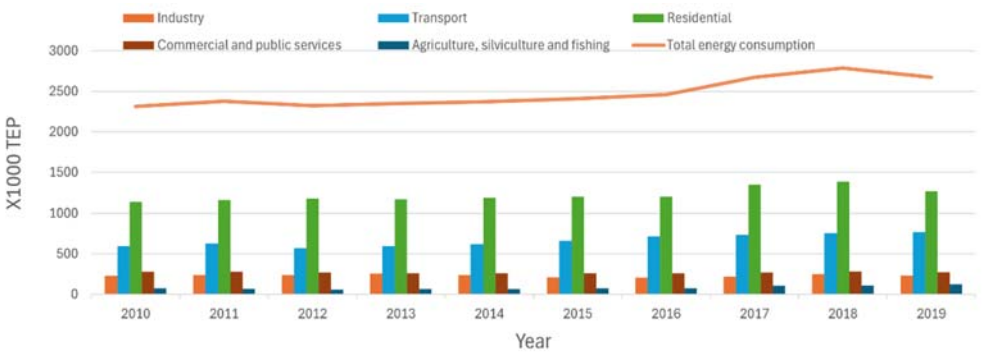

Fig. 1. Share of electrical energy consumption in Romania by sectors of activity [4]

On the other hand, the directive of the European Court of Auditors provides for the installation of 1,000,000 charging stations for electric vehicles by 2025 [5], which will put immense pressure on the Energy System (ES) of the European Union, forcing Member States to rethink their own ES. Analysing the share of energy sources participating in electrical energy production in Romania, 1/3 represents fossil fuels and 2/3 are renewable energy sources (RES) (Fig. 2) [6].

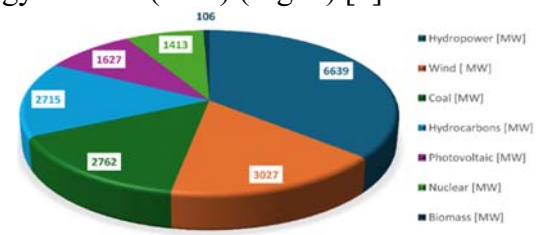

Fig. 2. Electrical energy production in Romania [6]

Romania's proposed targets for reducing greenhouse gas emissions consider three scenarios [7].

The baseline scenario for moving away from fossil fuels by 2050 calls for increasing solar and wind capacity to around 20% of the energy mix, with 27% hydrogen deployment by 2040, with a target of 30% by 2050 [7].

These commitments involve occupying large areas of agricultural land (Fig. 3, 4, 5) [7].

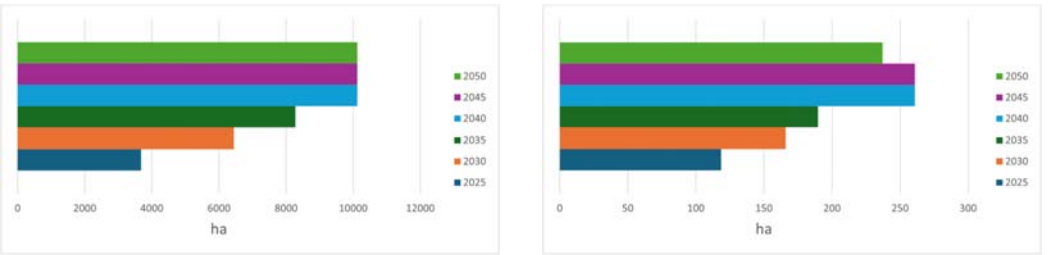

a) b)

Fig. 3. Land areas occupied by RES in the Baseline scenario. a) Solar, b) Wind [7]

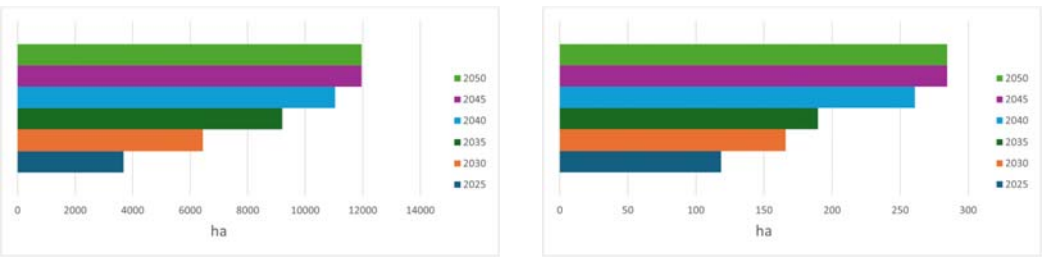

a) b)

Fig. 4. Land areas occupied by RES in the Medium scenario. a) Solar, b) Wind [7]

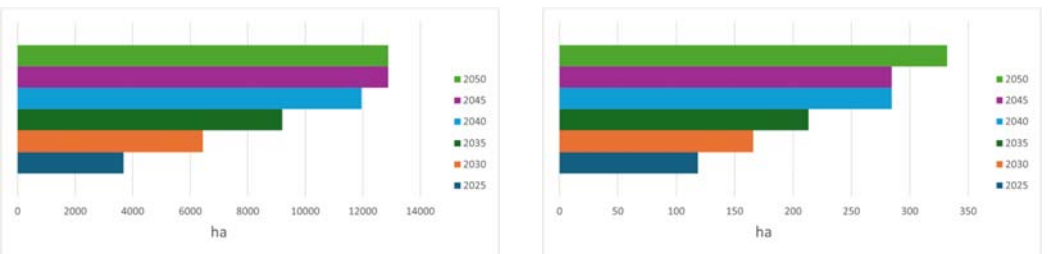

a) b)

Fig. 5. Land areas occupied by RES in the RO Neutral scenario
a) Solar, b) Wind [7]

In opposition, the fluctuating nature of solar and wind energy forces us to consider a possible alternative to them (Fig. 6) [8].

According to data recorded since 1 January to 20 March 2024, spring equinox, nuclear energy is found to be a source capable of ensuring the stable operation of the National Energy System (NES) (Fig. 6) [8].

At this moment, there are 2 functional nuclear reactors at Cernavodă (Fig. 7). By building 1 to 4 new nuclear reactors (Fig. 8, 9, 10, 11) in the system, Romania could substitute the production of electrical energy from wind (W), photovoltaic (P), coal (C) and hydrocarbons (H) together. This would lead to the unlocking of large areas of arable land [8].

Consequently, Romania should accelerate the construction works of new nuclear reactors at Cernavodă, following the example of Sweden [9, 10, 11, 12].

Another strong point of opting for the construction of additional nuclear reactors in Romania would be the fact that raw materials are no longer used for the storage of photovoltaic energy, as a result there is no more electrotechnical waste. On the other hand, ways of neutralizing radioactive waste must be considered [8].

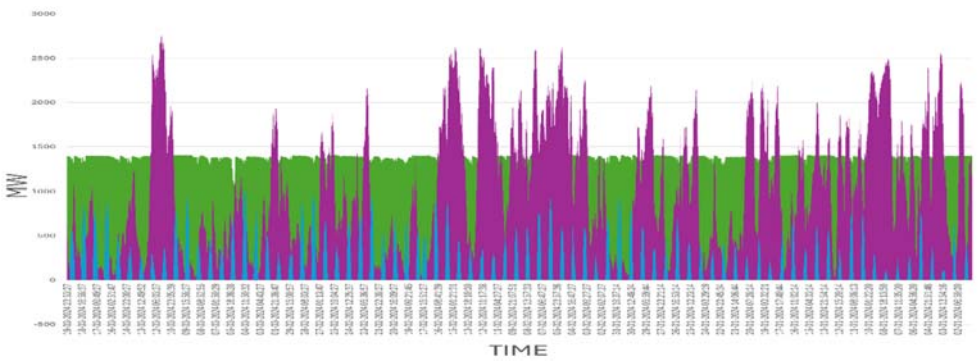

Fig. 6. RES (N, W, P) [8]

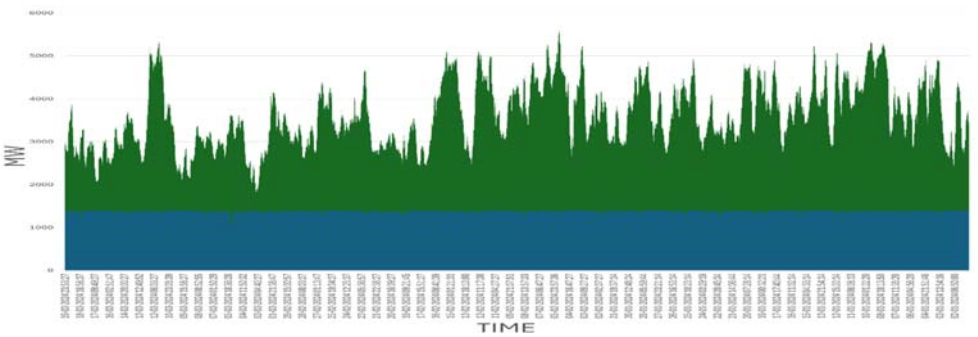

Fig. 7. Nuclear energy (2 reactors) compared to W, P, C and H together [8]

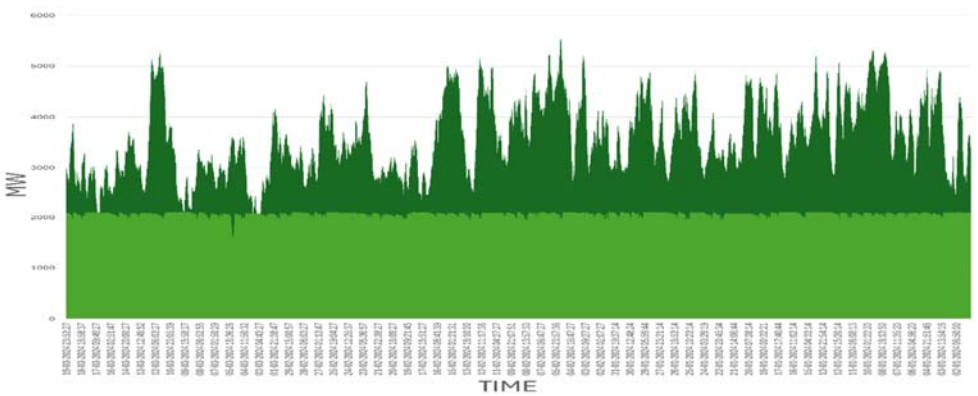

Fig. 8. Nuclear energy (3 reactors) compared to W, P, C and H together [8]

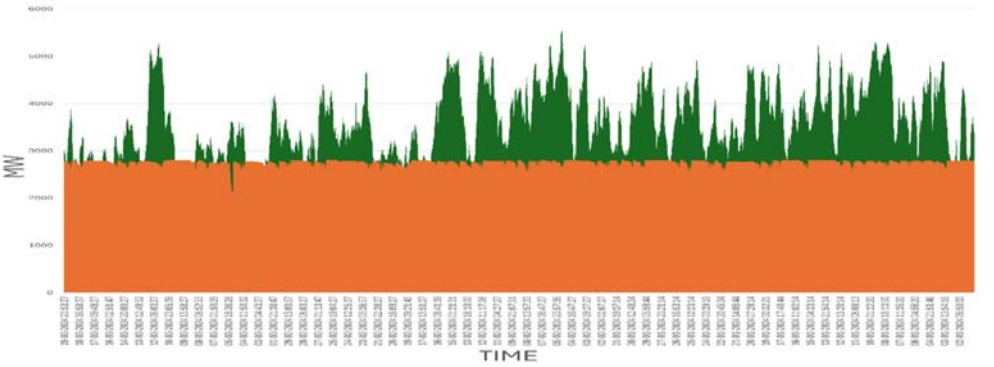

Fig. 9. Nuclear energy (4 reactors) compared to W, P, C and H together [8]

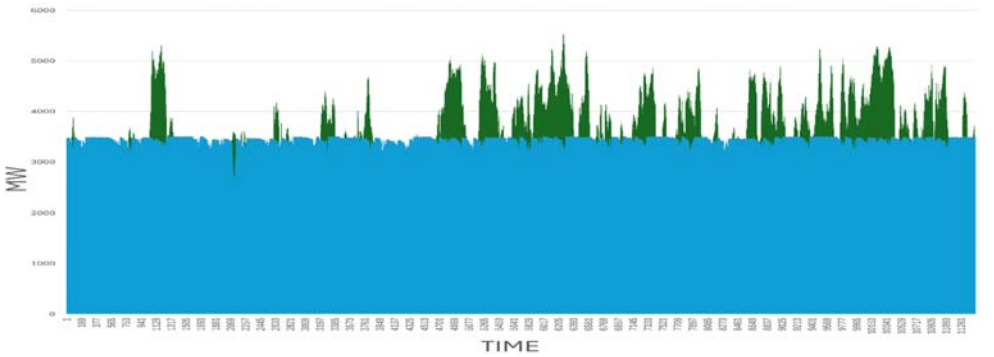

Fig. 10. Nuclear energy (5 reactors) compared to W, P, C and H together [8]

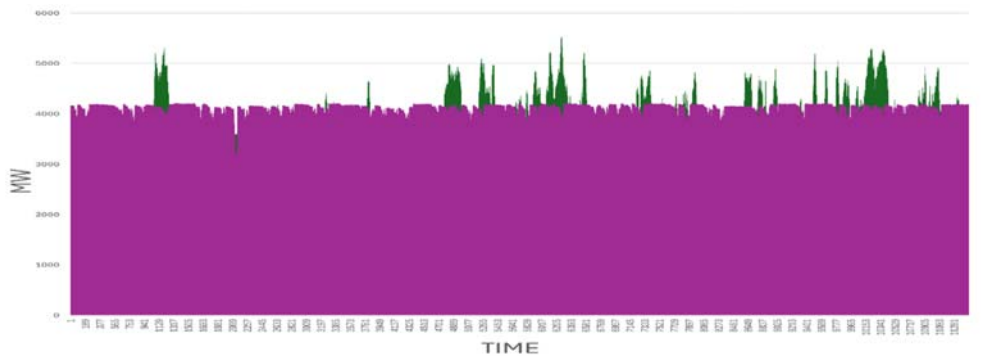

Fig. 11. Nuclear energy (6 reactors) compared to W, P, C and H together [8]

Analysing the variable character of RES, photovoltaic and wind (Fig. 6), the land areas occupied in Romania (Table 1) can assess the negative impact that these constructions have on the environment [6].

Table 1

Installed power and occupied area of RES [6]

Production type	Installed power	Occupied area
	[MW]	[ha]
Nuclear	1413	47.62
Wind	3027	71.73
Solar	1627	1496.84

It is known that during migration birds do not notice the rotational movement of the blades, producing a real carnage, and supporting photovoltaic panels requires special constructions [13].

Another aspect that should not be neglected is the thermal island effect due both to the high temperature under photovoltaic panels and to the fact that solar radiation is largely reflected from their surface (Fig. 12) [13].

Fig. 12. Resistance structures of photovoltaic panels [13]

Ensuring energy needs and achieving the targets assumed by the strategy can be achieved using nuclear energy.

The principle of electrical energy generation (Fig. 13) in NPPs is like that in thermal power plants (TPPs). The large amount of electrical energy and heat produced by NPPs, no greenhouse gas emissions, low footprint and low operating cost, recommend these systems in the energy mix [12].

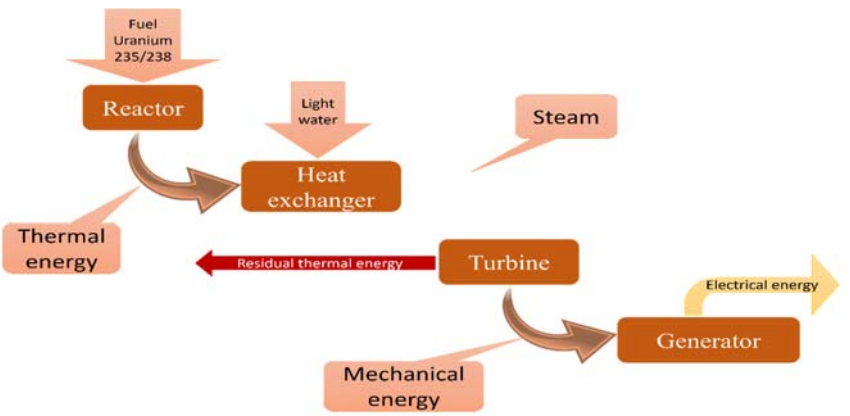

Fig. 13. Block diagram of a NPP [12]

There are 32 countries in the world that have NPPs and 4 of these: France, Slovakia, Ukraine and Belgium use nuclear energy as the primary source for electrical energy production [14]. The installed power in Romania is very small in comparison to other states, representing 0.59% (Table 2) of the installed power in the world [6].

Table 2

Technical characteristics of Cernavoda NPP Units 1 & 2 [15]

Reactor	Technology	Electrical power [MWe]	Thermal power [MWt]
Cernavoda-1	CANDU-6	706.5	2071
Cernavoda-2	CANDU-6	706.5	2071

Even though there have been a few major accidents (Fukushima, Japan in 2011, Chernobyl, Ukraine in 1986, and Three Mile Island, USA in 1979), nuclear technology is increasingly mature. Despite the known advantages, NPPs has the disadvantage of disposable radioactive waste and the imposition of safety and vulnerability restrictions to terrorist attacks. By analysing the targets in the strategy and the estimated production per hectare for different agricultural crops, the quantity not realized due to land occupation by dispatchable photovoltaic and wind systems was calculated (Fig. 14, 15, 16, 17, 18, 19) [7].

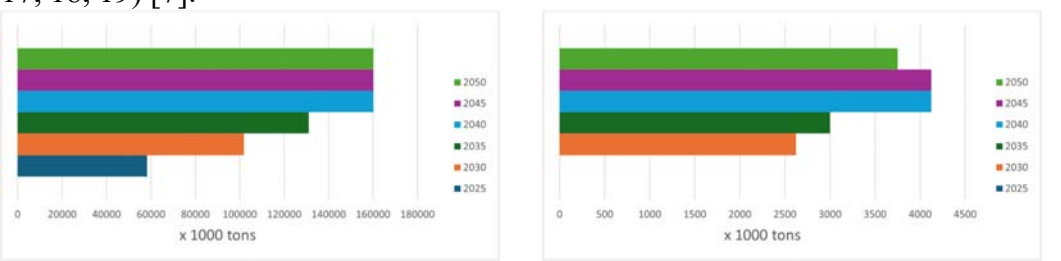

a) b)

Fig. 14. Quantities of agricultural products (potatoes) not realized as a result of land occupation by RES systems in the Baseline scenario. a) Solar, b) Wind [7]

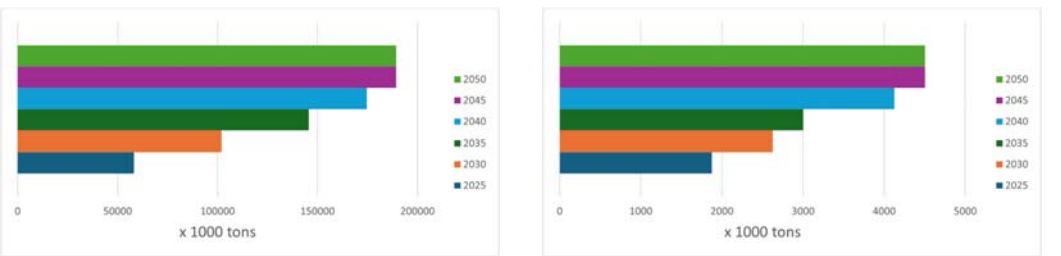

a) b)

Fig. 15. Quantities of agricultural products (potatoes) not realized as a result of land occupation by RES systems in the Medium scenario. a) Solar, b) Wind [7]

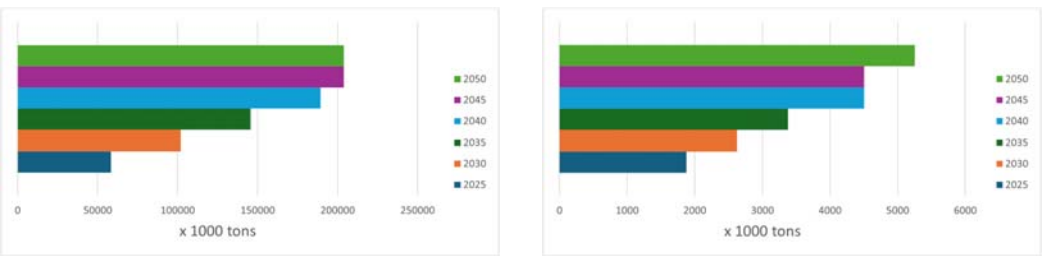

a) b)

Fig. 16. Quantities of agricultural products (potatoes) not realized as a result of land occupation by RES systems in the RO Neutral scenario. a) Solar, b) Wind [7]

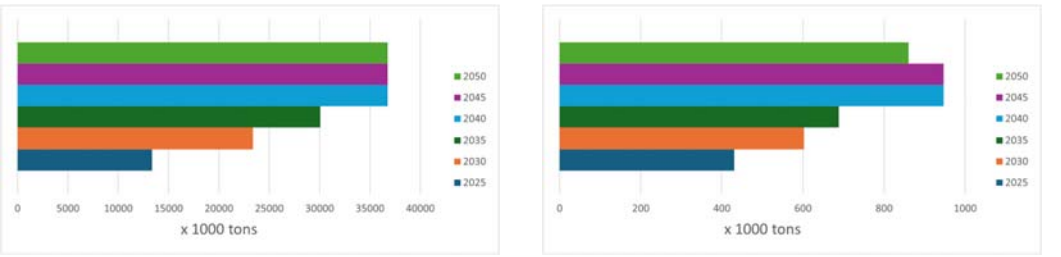

a) b)

Fig. 17. Quantities of agricultural products (cereals) not realized as a result of land occupation by RES systems in the Baseline scenario. a) Solar, b) Wind [7]

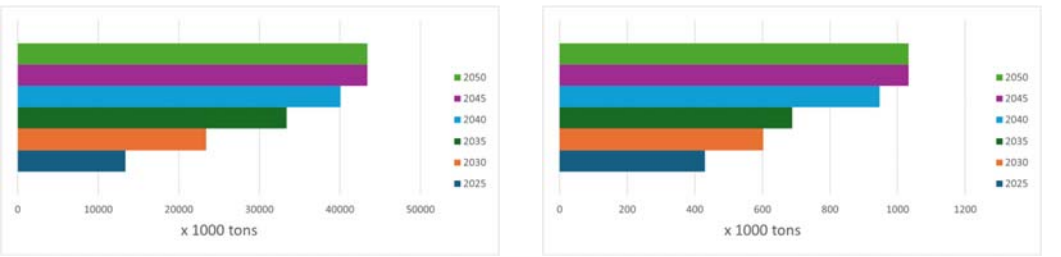

a) b)

Fig. 18. Quantities of agricultural products (cereals) not realized as a result of land occupation by RES systems in the Medium scenario. a) Solar, b) Wind [7]

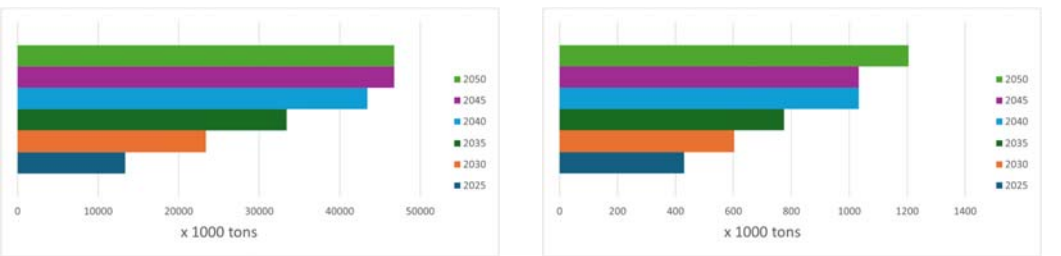

a) b)

Fig. 19. Quantities of agricultural products (cereals) not realized as a result of land occupation by RES systems in the RO Neutral scenario. a) Solar, b) Wind [7]

An emerging energy technology is small modular nuclear reactors (SMRs) suitable for areas with limited capacities and dispersed populations.

Small and medium-sized reactors, as defined by the International Atomic Energy Agency (IAEA), have installed capacities of up to 300 MWe compared to classical NPPs which have installed capacities bigger than 700 MWe [16].

SMRs differ from NPPs both by size and modularity in terms of design, installation and low fuel requirements. SMRs require less frequent refuelling, every 3 to 7 years, in comparison to between 1 and 2 years for NPPs. Some SMRs are designed to operate for up to 30 years without refuelling [16].

Furthermore, the storage of radioactive waste, the possibility of underground installation and finally the way of recovering waste thermal energy (cogeneration) represent the advantages of SMRs as opposed to conventional NPPs [16].

SMRs can be said to be a solution to eradicating energy poverty [13], as the technology is known and used in transport, medical, district heating and desalination [16]. SMRs can be appreciated as a solution for developing economies [13].

3. Conclusions

The growing need for electrical energy, but especially the achievement of the targets assumed by European countries, is not possible without the development of stable sources capable of generating large amounts of energy.

The "unloading" of transmission networks and the decentralization of electrical energy generation sources without increasing CO_2 emissions, the provision of thermal energy from reactor cooling water (technological residue) recommends SMRs as an alternative source to fossil fuels.

Even if the benefits obtained are firm, the need to ensure an emergency planning zone (EPZ) determines the implementation of specific preparation procedures and implicitly leads to increased production costs.

Although operational safety is enhanced by underground installation of this equipment in areas with low population density, public opinion is still sceptical about these systems.

This comparative study between RES (N, W, F) presents a possible solution in the future for increasing electrical energy production capacities to a low degree of land occupancy and with low CO_2 emissions, proposes even the notion of "prosumer" of electrical energy and heat.

References

[1] Martina Igini. "The Advantages and Disadvantages of Nuclear Energy." Global Commons, January 28, 2023. Accessed March 20, 2024. https://earth.org/the-advantages-and-disadvantages-of-nuclear-energy/.

[2] Clara Dassonville and Thies Siemen. *Nuclear Energy: The Pros and Cons*. Brussels, Friedrich-EbertStiftung Competence Centre for Climate and Social Justice FES Just Climate Publishing, 2023.

[3] Nuclear Energy Institute (NEI). "Nuclear energy is essential for a clean, reliable, modern grid that can support our growing electricity needs." Infrastructure. Accessed March 20, 2024. https://www.nei.org/advantages/infrastructure.

[4] National Institute of Statistics. "Final energy consumption in Romania (2010-2019)" / "Consumul final de energie în România (2010-2019)", National Institute of Statistics, June 5, 2020. Accessed March 20, 2024. https://insse.ro/cms/ro/content/statistica-energiei.

[5] European Court of Auditors. "Infrastructure for charging electric vehicles: more charging stations but uneven deployment makes travel across the EU complicated", Special Report 05/2021: Infrastructure for charging electric cars is too sparse in the EU, March 19, 2021. Accessed March 20, 2024. https://op.europa.eu/webpub/eca/special-reports/electrical-recharging-5-2021/en/.

[6] ANRE. "Installed power in electricity production capacities (in MW)" / "Puterea instalată în capacitățile de producție energie electrică (în MW)", National Energy Regulatory Authority/

Autoritatea Naţională de Reglementare în domeniul Energiei (ANRE), March 18, 2023. Accessed March 20, 2024. https://anre.ro/puteri-instalate/.

[7] Government of Romania. "Romania's Long-Term Strategy for Reducing Greenhouse Gas Emissions, Version 1.0", Long term strategy of Romania, May 5, 2023. Accessed March 20, 2024. http://www.mmediu.ro/app/webroot/uploads/files/LTS%20-%20Versiunea%201.0%20-%20Eng%20%2005.05.2023.pdf.

[8] Transelectrica. "Graph of National Power System (NPS) production, consumption and balance" / "Grafic producția, consumul și soldul Sistemului Energetic Național (SEN)", Transelectrica, March 20, 2024. Accessed March 20, 2024. https://www.transelectrica.ro/widget/web/tel/sen-grafic//SENGrafic_WAR_SENGraficportlet.

[9] Roxana Petrescu. "Sweden reopens nuclear chapter to cover significant increase in energy demand by 2040. Relinquishes 100% green and goes 100% fossil-free" / "Suedia redeschide capitolul nuclear pentru a acoperi creşterea semnificativă a cererii de energie la nivelul anului 2040. Renunţă la 100% verde şi trece la 100% fără fosili", Finance Newspaper, June 28, 2023. Accessed March 20, 2024. https://www.zf.ro/companii/suedia-redeschide-capitolul-nuclear-pentru-a-acoperi-Growth-21973765.

[10] World Nuclear News. "Changes to Swedish law proposed to enable nuclear new build", World Nuclear News, January 12, 2023. Accessed March 20, 2024. https://world-nuclear-news.org/Articles/Changes-toSwedish-law-proposed-to-enable-nuclear.

[11] Johnson, Simon. "Swedish parliament passes new energy target, easing way for new nuclear power", Reuters, June 20, 2023. Accessed March 20, 2024. https://www.reuters.com/sustainability/climateenergy/swedish-parliament-passes-new-energy-target-easing-way-new-nuclear-power-2023-06-20/.

[12] Florin-Alexandru Lunga, Bogdan-Darian Toader and Dănuț Tokar. "Sustainability of Nuclear Energy as a Source of the Future", in Hidraulica, No. 4, pp. 50-57, 2023..

[13] Simion Baciu, Eugen Bârsan, Mircea Hordilă, Cristian Ivășcanu, Ionuț Nicoraş, Adriana Tokar and Dănuț Tokar. "Environmental comfort versus energy poverty." Student Scientific Bulletin, Partnership developed for Student Counseling and Practice in order to increase their employability – Conpractis 1 (2015): 168-172.

[14] International Atomic Energy Agency (IAEA). "Nuclear Share of Electricity Generation in 2022", World Statistics, June 8, 2023. Accessed March 20, 2024. https://pris.iaea.org/pris/worldstatistics/nuclearshareofelectricitygeneration.aspx.

[15] Nuclearelectrica. "Cernavoda NPP Units 1 & 2, Romania - Safety features of CANDU 6 design and stress test summary report" Nuclearelectrica, March 20, 2024. Accessed March 20, 2024. https://www.nuclearelectrica.ro/cne/wpcontent/uploads/sites/2/2015/10/SafetyFeaturesOfCANDUDesign_CNECernavoda.pdf.

[16] International Atomic Energy Agency (IAEA). Advances in Small Modular Reactor Technology Developments. Vienna, IAEA Department of Nuclear Energy, 2018.

Geopolymer concrete as an effective technical variant for reducing CO_2 emissions in the atmosphere during preparing construction materials

Beton geopolimeric ca variantă tehnică eficace pentru reducerea emisiilor de CO_2 în atmosferă în timpul pregătirii materialelor de construcție

Lucian Paunescu[1], Bogdan Valentin Paunescu[2], Enikö Volceanov[3,4], Adrian Ioana[5]

[1]Daily Sourcing & Research SRL
95-97 Calea Grivitei street, sector 1, Bucharest 010705, Romania
E-mail: lucianpaunescu16@gmail.com

[2]Consitrans SA
56 Polona street, sector 1, Bucharest 010504, Romania
E-mail: pnscbogdan@yahoo.com

[3]Metallurgical Research Institute SA
39 Mehadia street, sector 6, Bucharest 060543, Romania
E-mail: evolceanov@yahoo.com

[4]University ”Politehnica” of Bucharest, Faculty of Science and Materials Engineering
313 Independence Splai, sector 6, Bucharest 060042, Romania
E-mail: evolceanov@yahoo.com

[5]University ”Politehnica” of Bucharest, Faculty of Science and Materials Engineering
313 Independence Splai, sector 6, Bucharest 060042, Romania
E-mail: adyioana@gmail.com

DOI: 10.37789/rjce.2025.16.1.4

Abstract. *The improved version of geopolymer concrete manufacturing based on fly ash and granulated blast furnace slag was made by correlating the high mechanical strength of the hardened material with the medium level-workability of the fresh material. The fly ash/slag ratio in the composition of the substitute binder for Portland cement was reduced to the limit where the workability was affected, but this reduction was compensated by fluidizing additive (calcium lignosulfonate) addition. Due to the correlation of mechanical properties and those of fluidity, high compression and flexural strengths were obtained (57.4 and 10.1 MPa) after curing and 28 days-storage.*

Key words: *geopolymer concrete, alkaline activator, curing process, calcium lignosulfonate, mechanical strength, workability.*

The article was received on 27.11.2023, accepted on 05.02.2025 and published on 14.03.2025

Rezumat. *A fost realizată o versiune îmbunătățită a betonului geopolimeric fabricat pe bază de cenușă zburătoare și zgură de furnal granulată prin corelația rezistenței mecanice înalte a materialului întărit cu lucrabilitatea de nivel mediu a materialului proaspăt. Raportul cenușă zburătoare/zgură în compoziția liantului înlocuitor al cimentului Portland a fost redus la limita la care lucrabilitatea a fost afectată, dar această reducere a fost compensată de adaosul aditivului fluidizant (lignosulfonat de calciu). Datorită corelației proprietăților mecanice si acelea ale fluidității, au fost obținute rezistențe înalte la compresie și încovoiere (57,4 și 10,1 MPa) după întărire și stocare pentru 28 zile.*

Cuvinte cheie: beton geopolimeric, activator alcalin, proces de întărire, lignosulfonat de calciu, rezistență mecanică, lucrabilitate.

1. Introduction

In the current context of dangerous rate of destructing the protective ozone layer of our planet due to excessive emissions of greenhouse gases (mainly CO_2), humanity's concern for stopping or limiting this possible ecological disaster has already reached a high level since the beginning of the new millennium.

One of the industrial activity fields deeply involved in CO_2 emissions and responsible for up to 7 % of the entire CO_2 amount released worldwide is the construction material industry and primarily the manufacture of ordinary Portland cement as the essential raw material of the concrete manufacturing process [1, 2]. Also, the cement making is a high energy-intensive process, the manufacture of one ton of Portland cement requiring about 4 GJ [3] in form of fossil fuels, which generate carbon dioxide by burning.

The modern use of Portland cement as the dominant binder in the production of construction concrete is already over 180 years old [4]. During all this time, due to humanity's lack of concern for the high consumption of hydrocarbons and the dangerous emissions of pollutants in the atmosphere, the industry, in general and the cement industry, in particular, have experienced a long period of development, suddenly interrupted starting from the last decades of the last century.

Reducing the carbon footprint of cement has been tried by several researchers' teams using different cementitious materials such as fly ash, metallurgical slag, rice husk ash, red mud, metakaolin, having the role of partially replacers for the cement intended for manufacturing the concrete [3, 5-8].

According to Juenger et al. [4], recently, there is an unprecedented increase in the interest of researchers from all over the world for developing, testing, and applying new alternatives to ordinary Portland cement. Thus, calcium aluminate cement, calcium sulfo aluminate cement, super sulphated cements, and alkali-activated binders were analyzed in this paper.

According to [9, 10], the use of geopolymeric materials (high alumina and silica contents) favours reducing CO_2 emissions by 73 % and at the same time, the required energy consumption is reduced by 43 % compared to the use of Portland cement as a binder in the concrete manufacturing.

The development of a very effective process in ecological terms based on turning alumino-silicate materials (waste or natural) in alkaline solution activator into geopolymeric materials with excellent physical-mechanical characteristics was achieved at the end of the 20th century through remarkable invention of the French researcher J. Davidovits [11]. He has identified the geopolymerization reaction of alumina and silica-rich materials into an alkaline solution of sodium or potassium silicate and hydroxide [11, 12]. The curing process of geopolymer concrete can be carried out, according to the inventor J. Davidovits, at ambient temperature or at high temperature. The geopolymerization process is favoured by increasing the temperature, leading to the significant improvement of mechanical strength properties in a much lower time range compared to hardening at ambient temperature [12].

In the work [13], several versions for preparing geopolymer concrete by curing at ambient temperature were experimented using Taguchi method as a quality control procedure aiming at reducing final product failures. Ground granulated blast furnace slag was utilized with the role of alumino-silicate binder. The alkaline activator was a liquid solution composed of sodium silicate and sodium hydroxide in the ratio 2.5, in which the molar concentration of NaOH was 14M. After 7 days to the increase of setting time (and therefore of workability) affected by the use of blast furnace slag, but the compression strength value decreased due to reducing the mixture calcium content of concrete storage, the highest compression strength (60.4 MPa) was obtained. The partially replacing the slag with variable ratios of fly ash, metakaolin, and silica fume, respectively, has contributed.

Fly ash and ground granulated blast furnace slag (added in ratios up to 20 % of the entire binder amount) were alumino-silicate wastes used in the experiment presented in [14]. The alkaline activator was a liquid solution including Na_2SiO_3 and NaOH, the activator/binder ratio being kept constant at 0.35. The curing process was performed at room temperature. The results showed that the compression strength of geopolymer concrete increased from the early age. The increase of the slag amount added to the starting mixture has also contributed to the increase of the concrete mechanical strength. Drying shrinkage, void volume, and sorption had almost similar values to concrete specimens made with Portland cement. Comparing the results of the geopolymer concrete with those of the reference concrete based on Portland cement, the authors showed that the fly ash-slag combination and curing at ambient temperature ensure the durability of the new material at a similar level to that of the reference concrete.

A research team including authors of the current paper previously conducted tests aiming at the production of geopolymer concrete using fly ash and blast furnace slag as binders, activated in Na_2SiO_3 and NaOH solution [15]. The paper originality was the increase of slag ratio range (15-25 %) in the binder mixture, for increasing the compression strength despite the decrease in workability. The fresh geopolymer obtained by mixing the raw material components and pouring into a mold was cured with hot air at 80 °C. After 7 days, the compression strength reached 55.2 MPa corresponding to 25 % slag ratio in the binder amount, but the workability test

decreased from 70 to 45 mm. The adopted optimal version was that with 80 % fly ash and 20 % slag. The compression strength for this version reached 53.3 MPa and the fresh concrete workability was 58 mm (corresponding to a medium workability value).

Special interest was given by Hamidi et al. [16] on the concentration of the NaOH aqueous solution as a component of the alkaline activator. Its influence on the mechanical resistance of concrete, especially on the flexural strength, was experimentally determined in the work mentioned above. Under the conditions of using fly ash as the main alumino-silicate binder in the concrete manufacturing process, the optimal concentration of NaOH was determined to be 12M. The curing process of the fresh mixture was performed at 60 °C for 1 day.

The temperature and duration of the curing process of the fresh geopolymer as well as the concentration of the NaOH solution were identified in the work [17] as having significant effects on the compression strength value. Increasing the mentioned parameters led to improving the compression resistance. On the other hand, increasing the water/geopolymer ratio led to the reduction of compression strength value. The role of the superplasticizer based on naphthalene on increasing the workability of fresh concrete was also determined.

The influence of the main known curing techniques of geopolymer concrete (with steam, hot air, and at room temperature) on its mechanical characteristics were analyzed in the paper [18]. The composition of the material mixture included low calcium fly ash, ground blast furnace slag, sand as the fine aggregate, coarse aggregate (below 20 mm particle size), and alkaline activator solution containing Na_2SiO_3 and NaOH mixture. The fly ash amount varied between 392.4-436 $kg \cdot m^{-3}$, while the slag amount had values in the range 0-43.6 $kg \cdot m^{-3}$. The Na_2SiO_3/NaOH ratio was 2.5. The hot air curing method allowed to reach the highest level of compression strength (24.5-28.3 MPa). The curing at ambient temperature reached the highest compression strength after 12 days compared to its value after 3 days, registering maximum 25.5 MPa.

According to the results obtained in the own previous tests [15] as well as those of other authors [17], the increase in the mechanical strength of geopolymer concrete has as a secondary effect the decrease of workability properties. This worsening of the fresh material-flow characteristics can be counteracted by using an adequate fluidizing additive. The authors of the paper [17] chose naphthalene-based superplasticizer suitable for high-strength, steam cured, fluid, waterproof, plasticized or reinforced concretes, being manufactured in China [19].

The authors of the current paper adopted a calcium lignosulfonate (LSC) fluidizing additive, extracted from the sulphite lye resulting from the manufacture of cellulose as a by-product. This type of additive is a polymer with a high molecular mass and a three-dimensional structure. Although LSC was intended to improve the properties of mortars and cement-based Portland concretes, its use was also extended to new geopolymers, considering the similarity of alumino-silicate materials with pozzolanic properties used as substitutes for cement and the ordinary Portland cement in the composition of traditional concrete. According to [20], in general, fluidizing additives contribute to the slight increase of apparent density due to the improvement

of workability and the reduction of the working water requirement. Also, the mechanical strength of concrete is increased, allowing the reduction of the dosage of cementitious materials replacing the cement. The improvement of concrete strength after 7 and 28 days can increase by 10-20 % compared to concrete without fluidizing additive. According to the same reference, the presence of fluidizing additives could improve slow flow, especially at early ages. Capillary sorption and concrete permeability are reduced due to the presence of fluidizing additives as a result of reducing the water requirement and increasing the structural homogeneity. The resistance to corrosive attack should be improved as a result of the decrease in permeability.

2. Materials and methods

The solids adopted in this experiment as materials for preparing mixtures for producing the geopolymer concrete were: fly ash, granulated blast furnace, both as binders from residual alumino-silicate materials, Na_2SiO_3 and NaOH in aqueous solution constituting the alkaline activator, sand as fine aggregate, gravel as coarse aggregate, and calcium lignosulfonate as a fluidizing additive.

Coal fly ash, a well-known by-product of the coal burning process in thermal power plant boilers, trapped after the purification of residual gases in electrofilters, was previously supplied by Paroseni-Thermal Power Station and preserved. Having the initial size of particles below 200 μm, it was ground in a ball mill and selected after sieving to sizes below 80 μm.

Granulated blast furnace slag in the form of 2-6 mm-granules was supplied by ArcelorMittal Galati (Romania) over 25 years ago being preserved and used in several experiments. The fine grinding process of the slag allowed to obtain a powder with dimensions less than 100 μm.

Chemical composition of coal fly ash and granulated blast furnace slag was determined in the Romanian Metallurgical Research Institute and are shown in Table 1.

Table 1

Chemical composition of fly ash and blast furnace slag

Composition	Coal fly ash (%)	Blast furnace slag (%)
SiO_2	48.1	36.4
Al_2O_3	26.4	11.6
CaO	3.6	41.8
MgO	3.2	5.8
MnO	-	0.6
Fe_2O_3	8.6	0.8
Na_2O	6.0	0.3
K_2O	4.1	0.4

Sodium silicate (Na_2SiO_3), known as water glass, is soluble in water creating an alkaline solution. In general, it is used as a binder and can contribute to improving the mechanical resistance of ceramic and composite materials [21]. Commercially, it is available in the form of liquid solution with concentrations around 40 %.

Sodium hydroxide (NaOH), known as caustic soda, contains 16.4 % Na_2O, 34.3 % SiO_2, and 49.3 % H_2O. It exists in solid state and is a very water-soluble material. Commercially, it is available in pellet form (with high purity of 98 %). Together with water glass, it forms an excellent alkaline activator [22] also used in this experiment.

Quartz sand (with the density of 1430 $kg \cdot m^{-3}$) was chosen as fine aggregate, having dimensions less than 1.7 mm selected by sieving.

The coarse aggregate was constituted using natural gravel with the density of about 2800 $kg \cdot m^{-3}$. The maximum size of this aggregate was limited to 20 mm.

Calcium lignosulfonate (LSC) as a fluidizing additive was already mentioned above, its main role being to improve the fresh material-flow features. Generally, calcium lignosulfonate is available in the form of a fine powder (average density of 1200 $kg \cdot m^{-3}$), soluble in ordinary water. The authors' team benefited from a batch of this type of additive previously procured from the Romanian chemical industry.

Unlike the first article of the authors' team from 2022 [15], in the current paper some important changes were made in the starting composition of mixture for manufacturing the geopolymer concrete. Keeping constant the total amount of the alumino-silicate binder (substitute for Portland cement), the weight ratio of fly ash and granulated blast furnace slag was changed, using the following ranges of values: 77-83 wt. % for fly ash and 17-23 wt. % for slag. Na_2SiO_3 and 12M NaOH were the components of the alkaline activator. The weight ratio between the activator and the alumino-silicate binder was adopted at a constant value of 0.358. According to the literature [23], the water addition into the binder mixture is important. A low value of the water/geopolymer binder ratio (0.25 wt. %) leads to obtaining a very viscous and stiff mixture, therefore with inadequate workability, but ensures excellent mechanical strength of the concrete. By increasing the water/binder ratio, the workability of the fresh material improves, but the compression strength decreases. Experimentally, the ratio of 0.28 was adopted, meaning an added water amount of 126 $kg \cdot m^{-3}$. Unlike the reference work [15], the main novelty of the mixture composition for the acceptable correlation of the two features of geopolymer concrete (strength and workability) was the addition of calcium lignosulfonate (LSC) as a fluidizing additive. According to [24], its weight proportion must be below 1 wt. % of the binder amount, the paper referring to the traditional concrete binder, i.e. the Portland cement. From the authors' own experience, a maximum value of 0.31 wt. % is more advisable in the case of geopolymer concrete, meaning an additive amount of 1.4 $kg \cdot m^{-3}$. The two types of aggregate chosen in this experiment (quartz sand as fine aggregate and natural gravel as coarse aggregate) had the usual role in any type of concrete, including geopolymer concrete [25]. The weight ratio between the entire amount of aggregate and the alumino-silicate binder was adopted at the value of 4.8. The binder amount being 450 $kg \cdot m^{-3}$, it results that the total aggregate was 2160 $kg \cdot m^{-3}$. Choosing the weight proportion of 35 % for fine aggregate and 65 % for coarse aggregate respectively, the

corresponding amounts of the two types of aggregate were determined: 756 kg·m^{-3} (quartz sand) and 1404 kg·m^{-3} (coarse aggregate).

The experiment presented below contains four experimental versions marked V1-V4 (Table 2), in which the amounts of fly ash and granulated blast furnace slag ratio is reduced from 4.88 (V1) to 3.35 (V4), the other values of mixture component amounts being kept constant.

Table 2

Composition of experimental versions of geopolymer concrete

Composition	V1 (kg·m^{-3})	V2 (kg·m^{-3})	V3 (kg·m^{-3})	V4 (kg·m^{-3})
Fly ash	373.5	364.5	355.5	346.5
Granulated blast furnace slag	76.5	85.5	94.5	103.5
12M NaOH	46	46	46	46
Na_2SiO_3	115	115	115	115
Quartz sand	756	756	756	756
Coarse aggregate	1404	1404	1404	1404
Supplementary water added	126	126	126	126
Calcium lignosulfonate	1.4	1.4	1.4	1.4

The conversion of alumino-silicate materials (mostly industrial waste such as coal fly ash, metallurgical slag, red mud, rice husk ash, etc.) into products with special mechanical and physical characteristics called geopolymers, as a result of developing the geopolymerization reaction activated by an alkaline activator, constitute the basic elements of the remarkable invention of the French researcher J. Davidovits mentioned above. Alumino-silicate materials have pozzolanic properties having ability to replace the traditional Portland cement as a binder in geopolymer concrete manufacturing.

The geopolymerization process is based on a complex chemical reaction between an alkali solution and the alumino-silicate material and forms a three-dimensional polymeric chain and ring structure of Si–O–Al–O bonds. The reaction, that can occur at ambient temperature, is developed in three main stages: dissolution of alumino-silicate material into aluminates and silicates species, condensation of monomers (when the setting time is beginning), and the monomer polymerization into an amorphous inorganic polymer [26].

The adopted working method has included firstly preparing the alkaline activator mixture containing sodium silicate solution (Na_2SiO_3) and water-soluble NaOH pellets dissolved in distilled water (with 12M molarity). The activator homogenization was performed by mechanical stirring in a quartz vessel for 3 min. Separately, the preparation of the solid mixture was carried out in another vessel. First, the mixture containing ground fly ash, ground granulated blast furnace slag, and calcium lignosulfonate was mechanically mixed for 5 min and then fine sand (below

1.7 mm), coarse aggregate (below 20 mm), and supplementary water were introduced over the first solid mixture. After the homogenization of the two solid mixtures for 3 min, the alkaline activator was poured over these. A last mixing together of the solid and liquid materials was performed for about 5 min, until a paste was obtained. The paste, representing fresh geopolymer concrete, was poured into cubic and rectangular molds, placed in a thermally insulated enclosure and heated with hot air at 80 ℃ from an electric air preheater. The duration of the curing treatment of the fresh geopolymer was 24 hours. The characteristic peculiarities analysis of the hardened geopolymer concrete was performed after 7 and 28 days of storage of specimens removed from the molds.

Characterization methods of geopolymer concrete specimens were the following. The fresh geopolymer concrete workability was analyzed according to ASTM C 143-10, Standard for concrete slump test, with the slump test apparatus. Water-absorbing was determined by the immersion method of specimen under water (ASTM D570) after its storage for 28 days [27]. The geopolymer concrete density was measured by Archimedes' method by the water intrusion technique (ASTM D792-20). The compression strength was identified with 100 kN-compression fixture Wyoming Test Fixture [28] and the flexural strength was measured by carrying out the three-point bend test on the specimen (SR EN ISO 14125: 2000). The microstructural appearance of geopolymer concrete specimens was examined with the Biological Microscope model MT5000 with image captured with a Nikon Coolipix 3 mp Camera, 1000 x magnification.

3. Results and discussion

The workability of fresh geopolymer concrete samples was determined by slump tests and the conclusion was that in the four experimental versions its value significantly changed by increasing the weight ratio of slag in the binder composition, respectively by decreasing the fly ash/slag ratio from 4.88 to 3.35, according to the data in Table 3.

Table 3

Results of the workability test

Experimental version	V1	V2	V3	V4
Fly ash/slag ratio	4.88	4.26	3.76	3.35
Workability slump test (mm)	75 (medium)	69 (medium)	57 (medium)	46 (low)

According to the Standard for concrete slump test (ASTM C 143-10), the first three specimen versions had medium workability (within the limits of 57-75 mm), while the V4 version had low level of workability (46 mm). The mentioned standard delimits the medium level between 50-100 mm and low level in the range of 25-50 mm.

The hardened geopolymer concrete after the curing process at 80 °C for 1 day and the storage for 7 and 28 days gained compactness and high mechanical strength, especially after 28 days. The specimens were obtained by pouring the fresh material into cubic shapes with the side dimension of 100 mm (for measuring the compression strength) and rectangular shapes with dimensions of 100 x 100 x 350 mm (for measuring the flexural strength) [29]. The appearance of the cubic specimens made in the four experimental versions is shown in Fig. 1.

V1 V2 V3 V4

Fig. 1. Appearance of the cubic shape specimens
V1 – version 1; V2 – version 2; V3 – version 3; V4 – version 4.

The outer surface appearance of specimens does not visibly differ. However, their physical and mechanical features as well as the microstructural aspects have distinct peculiarities.

The density of geopolymer concrete specimens, measured on cubic shape samples after 28 days-hardening, reached high values within the limits of 2488-2506 $kg \cdot m^{-3}$, the tendency of slight increase in density being noted in the case of reducing the fly ash/slag ratio, i.e. increasing the weight ratio of granulated blast furnace slag in the binder composition from 17 to 23 wt. %. The compression strength of specimens reached very high levels, especially after 28 storage-days of over 50 MPa (between 53.9-59.7 MPa), its increase being the result of blast furnace slag addition together with fly ash in the alumino-silicate binder composition. The flexural strength also reached high values after 28 days between 7.8-12.1 MPa. The tests on the geopolymer concrete water-absorbing capacity showed that the absorption degree was limited to very low water proportions (around 1 wt. %) and practically, the addition of slag along with fly ash did not influence this geopolymer characteristic.

The centralized presentation of the main characteristics of geopolymer concrete samples made in this experiment is carried out in Table 4.

Table 4

Main physical-mechanical features of specimens

Characteristic	V1	V2	V3	V4
Density after 28 days ($kg \cdot m^{-3}$)	2488	2495	2501	2506
Compression strength (MPa)				

Characteristic	V1	V2	V3	V4
- after 7 days - after 28 days	31.8 53.9	32.6 55.4	34.0 57.4	36.1 59.7
Flexural strength (MPa) - after 7 days - after 28 days	 3.8 7.8	 4.9 8.7	 6.6 10.1	 8.0 12.1
Water-absorbing after 28 days (vol. %)	1.1	1.0	0.9	0.9
Workability level (mm)	75 (medium)	69 (medium)	57 (medium)	46 (low)

As stated above, in this experiment the aim was to find the optimal correlation between the mechanical strength of the hardening geopolymer concrete and the fresh geopolymer workability. Analyzing the data in Table 4, authors' team considered that a very good correlation between the two characteristic types was obtained in the experimental version V3. Having a fly ash/slag ratio of 3.76, which includes 79 % fly ash and 21 % granulated blast furnace slag, the workability of the fresh material was determined by slump test at 57 mm, considered as a medium level workability according to the standard. On the other hand, the compression strength reached the maximum value of 57.4 MPa after 28 days, while the strength after 7 days was 34.0 MPa. Also, the flexural strength reached 10.1 MPa after 28 days and 6.6 MPa after 7 days, which means excellent strength values.

The microstructural appearance of geopolymer concrete specimens is shown in Fig. 2.

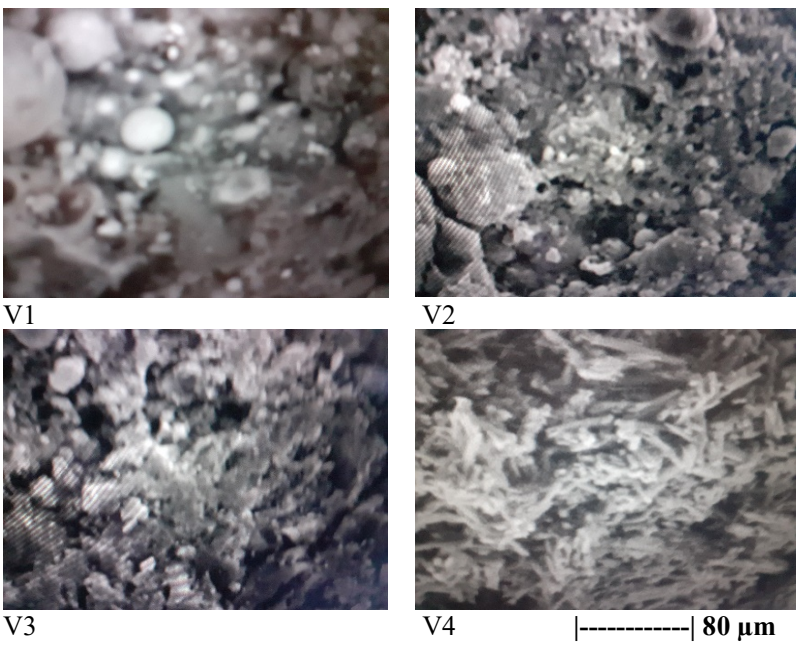

Fig. 2. Microstructural appearance of geopolymer concrete specimens
V1 – version 1; V2 – version 2; V3 – version 3; V4 – version 4.

The pictures in Fig. 2, present the changes at the microstructural level caused by increasing the proportion of ground granulated blast furnace slag in composition of the binder dominated by the fly ash component. The typically spherical grains of ash are clearly predominant in pictures V1 and V2, instead, in picture 4 they almost completely disappear, leaving the place of a typical microstructure for metallurgical slag.

Fly ash is the most important alumino-silicate binder due to its pozzolanic properties, which makes it suitable for replacing the ordinary Portland cement. The manufacture of fly ash-based geopolymer, one of the important ideas of the geopolymer creator (J. Davidovits), imposes as a main condition of the coal fly ash characteristics for contributing to the development of the geopolymerization reaction in alkaline medium, the low content of lime (CaO). Class F-fly ash represents the appropriate group, which includes the ash from burning anthracite (bituminous coal). According to the existing standards, class F contains between 1-10 % CaO, its values as low as possible (below 5 %) being preferable. Fly ash purchased from Paroseni during a period when the Thermal Power Pant was operating with anthracite has in its composition 3.6 % CaO (according to Table 1).

Fly ash with low calcium content after grinding below 80 μm is known as a fine powder with spherical granules having pozzolanic properties quite similar to Portland cement, which it can replace. These properties facilitate the reaction of fly ash, in the presence of water, with calcium hydroxide forming hydrated calcium silicates as well as calcium aluminates. Thus, the liquid phase created in the paste due to the hydration process is saturated with calcium hydroxide, reacting with fly ash in addition to the alkaline salts. The use of fly ash and ground granulated blast furnace slag has an important impact on the properties of concrete (or geopolymer concrete) due to the filling and rheological effects]5].

Due to the viscous peculiarity of the NaOH solution used as an alkaline activator in the manufacture of geopolymer concrete, the geopolymer rheology is quite variable. The slump value of the fresh material decreases by increasing the weight proportion of granulated blast furnace slag and the molarity of NaOH [3].

Because the fly ash reactivity is not suitable to be activated at room temperature by alkaline activators, the temperature of its curing process requires higher temperatures (60-85 °C). Thus, incompletely reacted gels affect the full development of the geopolymerization reaction. Experimentally, it was found that granulated blast furnace slag can improve the characteristics of fly ash-based geopolymer concrete by curing at room temperature probably due to the high content of CaO (over 40 %) in the slag composition [9].

The comparison with other works presented in the literature confirmed the originality of the current work. Few published articles refer to results obtained in the field of geopolymer concrete based on fly ash and granulated blast furnace slag because, although the addition of slag increases the geopolymer mechanical strength, the workability of the fresh material is affected, worsening the practical application conditions. The paper [30] is an example in this sense. The compression and flexural

strengths reported in this work are lower than those obtained in the current work. Compared to the reference article [15], published by the same authors' team in 2022, the mechanical performances of the geopolymer concrete were improved firstly, by using a fluidizing additive (calcium lignosulfonate) that allowed obtaining an optimal correlation between strength and workability. In addition, the increased duration of concrete storage up to 28 days allowed obtaining superior mechanical performances compared to the reference article.

4. Conclusions

The objective of the current paper was the production of geopolymer concrete based on two alumino-silicate wastes used as a substitute binder for traditional cement (fly ash and granulated blast furnace slag), in which the slag proportion was over 20 wt. %, which normally negatively affects the workability of the fresh material, but greatly increases the mechanical resistance of the hardened geopolymer. The work originality consisted in finding the optimal correlation between the increase in geopolymer strength due to the decrease of the fly ash/slag ratio and the contribution of the fluidizing additive (calcium lignosulfonate) on increasing the material fluidity to an acceptable medium level. The basic principles of turning alumino-silicate materials into geopolymers with special properties, through the geopolymerization reaction in the presence of the liquid alkaline activator, provided in the remarkable recent invention of the researcher J. Davidovits, were preserved in this experiment. The results showed excellent mechanical performances of the geopolymer concrete obtained as a result of the curing process at 80 °C for 1 day, continued by the specimen storage for 7 and 28 days, under the conditions that the level of workability determined by the slump test was acceptable at an average value according to the standard. Thus, very high compression and flexural strengths were obtained (57.4 and 10.1 MPa, respectively, after the storage for 28 days as well as 34.0 and 6.6 MPa after the storage for 7 days). Results were better compared to those of other works from the literature. Although the whole range of inventions related to geopolymer concretes and mortars patented by J. Davidovits in the last three decades have a very comprehensive character, numerous versions of preparing these innovative materials have not yet been experimentally verified, so there is a wide availability for new experiments in the future.

References

[1] L.N. Assi, M. Al-Bazoon, K. Carter, R. Anay, „Geopolymer Concrete Can Be the Solution for Sustainable Infrastructure", Proceedings to the Conference The 13th Annual Inter-University Symposium on Infrastructure Management (AISIM), Indiana-Purdue University, Indianapolis, Indiana, the United States, 2017.

[2] J.X. Peng, L. Huang, Y.B. Zhao, P. Chen, L. Zeng, W. Zheng, „Modelling of Carbon Dioxide Measurement on Cement Plants", Advanced Materials Research, vol. 610-613, pp. 2120-2128, 2012. https://doi.org/10.4028/www.scientific.net/AMR.610-613.2120

[3] M.G. Girish, K.S. Kiran, N. Gopinatha, „Synthesis of Fly-Ash and Slag Based Geopolymer Concrete for Rigid Pavement", Materials Today: Proceedings, vol. 60, Part 1, pp. 46-54, 2022. https://doi.org/10.1016/j.matpr.2021.11.332
[4] M.C.G. Juenger, F. Winnefeld, J.L. Provis, J.H. Ideker, „Advances in Alternative Cementitious Binders", Cement and Concrete Research, Elsevier, vol. 41, no. 12, pp. 1232-1243, 2011. https://doi.org/10.1016/j.cemconres.2010.11.012
[5] Z. Giergiczny, „Fly Ash and Slag", Cement and Concrete Research, Elsevier, vol. 124, 2019. https://doi.org/10.1016/j.cemconres.2019.105826
[6] M. Amin, B.A. Abdelsalam, „Efficiency of Rice Husk Ash and Fly Ash as Reactivity Materials in Sustainable Concrete", Sustainable Environment Research, Springer, vol. 29, no. 30, 2019. https://sustainenvironres.biomedcentral.com/articles/10.1186/s42834-019-0035-2
[7] S. Cheng, Z. Shui, T. Sun, R. Yu, G. Zhang, S. Ding, „Effects of Fly Ash, Blast Furnace Slag and Metakaolin on Mechanical Properties and Durability of Coral Sand Concrete", Applied Clay Science, Elsevier, vol. 141, pp. 111-117, 2017. https://doi.org/10.1016/j.clay.2017.02.026
[8] J. Singh, S. Naval, „Partial Replacement of Cement with Red Mud in Concrete-A Review", Sustainable Environment and Infrastructure, pp. 51-70, Part of the Lecture Notes in Civil Engineering book series (LNCE), vol. 90, 2020.
[9] P. Zhang, Z. Gao, J. Guo, S. Shaowei Hu, Y. Yifeng Ling, „Properties of Fresh and Hardened Fly Ash/Slag Based Geopolymer Concrete: A Review", Journal of Cleaner Production, Elsevier, vol. 270, 2020. https://doi.org/10.1016/j.clepro.2020.122389
[10] C. Meyer, „The Greening of the Concrete Industry", Cement and Concrete Composites, Elsevier, vol. 31, no. 8, pp. 601-605, 2009.
[11] J. Davidovits, M. Davidovits, N. Davidovits, „Process for Obtaining a Geopolymeric Alumino-Silicate and Products thus Obtained", US Patent no. 5342595, 1994.
[12] J. Davidovits, „Geopolymers: Inorganic Polymeric New Materials", Journal of Thermal Analysis and Calorimetry, vol. 37, no. 8, pp. 1633-1656, 1991. https://doi.org/10.1007/BF.01912193
[13] N.S. Muhammad, A. Hadi Nabeel, M. Farhan, M. Neaz Sheikh, „Design of Geopolymer Concrete with GGBFS at Ambient Curing Condition Using Taguchi Method", Construction and Building Materials, vol. 140, pp. 424-431, 2017. https://doi.org/10.1016/j.conbuildmat.2017.02.131
[14] P. Sarathi Deb, P. Kumar Sarker, „Properties of Fly Ash and Slag Blended Geopolymer Concrete Cured at Ambient Temperature", Proceedings to the 7th International Structural Engineering and Constructions Conference (ISEC-7), Honolulu, Hawaii, the United States, June 2013.
[15] L. Paunescu, B.V. Paunescu, E. Volceanov, G. Surugiu, „Geopolymer Concrete-A Suitable Nonconventional Alternative Solution for the Global Reduction of CO_2 Emissions in Manufacturing the Concrete", Nonconventional Technologies Review, vol. 26, no. 4, pp. 25-30, 2022.
[16] R.M. Hamidi, Z. Man, K. Azizi Azizly, „Concentration of NaOH and the Effect on the Properties of Fly Ash Based Geopolymer", Procedia Engineering, Elsevier, vol. 148, pp. 189-193, 2016. https://doi.org/10.1016/j.proeng.2016.568
[17] R.V. Prakash, V.D. Urmil, „Parametric Studies on Compressive Strength of Geopolymer Concrete", Procedia Engineering, Elsevier, vol. 51, pp. 210-219, 2013. https://doi.org/10.1016/j.proeng.2013.01.030
[18] S. Kamaravel, „Development of Various Curing Effect of Nominal Strength Geopolymer Concrete", Journal of Engineering Science and Technology Review, vol. 7, no. 1, pp. 116-119, 2014. https://doi.org/10.25103/jestr.071.19
[19] *** Sodium Naphthalene Sulfonate, Kingsun, China, 2023. https://kingsunchemical.com/sodium-naphthalene-sulfonate-formaldehyde
[20] V. Moldovan, „Aditivi in betoane", Editura Tehnica, Bucuresti, Romania, 1978, pp. 139-157.
[21] A. Ayadi, N. Stiti, F. Benhaoua, K. Boumchedda, Y. Lerari, „Elaboration and Characterization of Foam Glass Based on Cullet with Addition of Soluble Silicates", AFI Conference Proceedings

of the International Conference on Advances in Materials and Processing Technologies, vol. 1315, no. 1, 2011. https://doi.org/10.1063/1.3552401

[22] P. Prochon, Z. Zhao, L. Courard, T. Piotrowski, F. Michel, A. Garbacz, „Influence of Activators on Mechanical Properties of Modified Fly Ash Based Geopolymer Mortars", Materials (Basel), vol. 13, no. 5, 2020. https://doi.org/10.3390/ma13051033

[23] S.V. Patankar, S.S. Jamkar, Y.M. Ghugal, „Effect of Water-to-Geopolymer Binder Ratio on the Production of Fly Ash Based Geopolymer Concrete", International Journal of Advanced Technology in Civil Engineering, vol. 1, no. 4, 2012. https://interscience.in/ijatce/vol1iss4/15

[24] J. Sharma, R. Nisha, „Ligno Sulphonate: An Additive in Concrete", International Journal of Advance Research in Science and Engineering, vol. 6, no. 9, 2017. ISSN: 2319-8354.

[25] B.S. Thomas, J. Yang, A. Bahurudeen, S.N. Chinnu, J.A. Abdalla, R.A. Hawileh, H.M. Hamada, „Geopolymer Concrete Incorporating Recycled Aggregates: A Comprehensive Review", Cleaner Materials, vol. 3, 2022. https://doi.org/10.1016/j.clema.2022.100056

[26] I. Ozer, S. Soyer-Uzun, „Relations between the Structural Characteristics and Compressive Strength in Metakaolin Based Geopolymers with Different Molar Si/Al Ratios", Ceramics International, vol. 41, pp. 10192-10198, 2015. https://doi.org/10.1016/j.ceramint.2015.04.125

[27] A. Mishra, D. Choudhary, N. Jain, M. Kumar, N. Sharda, D. Dutt, „Effect of Concentration of Alkaline Liquid and Curing Time on Strength and Water Absorption of Geopolymer Concrete", Journal of Engineering and Applied Sciences, Asian Research Publishing Network, vol. 3, no. 1, pp. 14-18, 2008, ISSN: 1819-6608.

[28] A.A. Dyg Siti Quraisyah, K. Kartini, M.S. Hamidah, „Water Absorption of Incorporating Sustainable Quarry Dust in Self-Compacting Concrete", 4th International Symposium on Green and Sustainable Technology (ISGST), Kampar, Malaysia, October 3-6, 2021, IOP Conf. Series: Earth Environmental Science, vol. 945, IOP Publishing Ltd., 2021. https://doi.org/10.1088/1755-1315/945/1/012037

[29] S. Kushwah, M. Mudgal, R. Kumar Chouhan, „The Process, Characterization and Mechanical Properties of Fly Ash-Based Solid Form Geopolymer via Mechanical Activation", South African Journal of Chemical Engineering, Elsevier, vol. 38, pp. 104-114, 2021.

[30] J. Li, X. Dang, J. Zhang, P. Yi, Y. Li, „Mechanical Properties of Fly Ash-Slag Based Geopolymer for Repair of Road Subgrade Diseases", Polymers (Basel), MDPI, Basel, Switzerland, vol. 15, no. 2, 2023. https://doi.org/10.3390/polym15020309

Investigating the Instability of a Retaining Wall: Construction Concerns and Design Revisions

Investigarea instabilității unui zid de sprijin: preocupări de construcție și revizuiri de proiectare

Houssam KHELALFA [1, 2*], Fethi Boulkhiout [1], Youcef Kaikea [1]

[1]LGCE, University of Jijel, Jijel, Algeria
[2]Faculty of Engineering and Technology, Selinus University of Science and Literature (SUSL), Bologna, Italy

E-mail: *khelalfahoussam@gmail.com*

DOI: 10.37789/rjce.2025.16.1.5

Abstract :
This article examines a partially overturned retaining wall designed to protect the Taher Treasury Administration in Jijel Province, Algeria, from the sliding of the slope on which it is constructed. Although the wall remained intact, it led to the project being suspended by local authorities due to concerns about its stability. Despite several expert assessments, the root cause was not identified, necessitating in-depth analysis. Field investigations revealed unexpected results: the presence of a plastic sheet behind the wall hindered the drainage of rainwater and exacerbated the pressures on the surface layer of the backfill material. In particular, the wall's anchoring proved insufficient, barely affecting the intermediate layer. This configuration was critical for understanding the dynamics of soil pressures leading to superficial and partial sliding, which impacted the retaining wall's stability. Comparisons between field observations and our numerical model highlighted discrepancies in design dimensions and construction practices. Our revised model proposes a larger, deeper, and better-anchored retaining wall configuration, contrasting with the initial designs. This study concludes that errors in both design calculations and construction implementation contributed to the wall's instability, underscoring the importance of meticulous planning and adherence to geotechnical principles in future projects.

Keywords: Diagnosis, partial and superficial sliding, Retaining wall, lateral detachment, overturning, investigations, numerical simulation.

Introduction :

Geotechnical failures can have significant impacts on structures and represent a major challenge in civil engineering and risk management worldwide [1-5]. These often catastrophic events have devastating economic, environmental, and social consequences [6-10]. To improve the prevention, response, and mitigation of

The article was received on 24.07.2024, accepted on 12.12.2024 and published on 14.03.2025

geotechnical disasters, it is crucial to understand the causes, mechanisms, and impacts of these failures [11]. The importance of geotechnical stability lies in its ability to prevent geotechnical and structural failures that can lead to disasters such as landslides, foundation collapses, or dam breaches [12-17]. To achieve this, engineers conduct geotechnical investigations [18-21], including in situ and laboratory tests [22-24], as well as numerical analyses to model the behaviour of soils and structures [25 - 29].

If a failure occurs, it is undeniable evidence that the engineering of the failed structure was incorrect or incomplete. Today, geotechnical engineers conduct thorough investigations of failures and hypothesize how the failure was initiated and progressed [30-32]. These investigations involve reverse engineering design and construction problems [33, 34], where the engineer must develop possible scenarios and test them through analysis [35, 36]. In many cases, failures are not due to a single deficiency but rather to an unfortunate combination of factors, making the prognosis even more challenging [37, 39]. In addition, the variability of soil parameters and the resulting uncertainty are fundamental aspects of geotechnical engineering [40]. Understanding and quantifying this variability and uncertainty is essential for improving the reliability of geotechnical predictions and making informed decisions in the design, construction, and management of geotechnical infrastructure.

The stability of retaining walls is crucial in geotechnical engineering to protect infrastructures against landslides [41]. Our article aims to study geotechnical stability and conduct a diagnosis to find the cause of the superficial and partial sliding that led to the overturning of a retaining wall, with the goal of proposing reinforcement solutions for this wall installed on the slope of the Treasury Project in Taher, Jijel Province in Algeria. Since the sliding has already occurred, the objective of this study is to analyze the causes that led to the instability, and then propose an adequate reinforcement system, while describing the procedure for its implementation. To carry out this study, our article focuses on the geotechnical, geological, and hydrogeological study of the sliding site. It also includes the verification of the initial study's calculations, which failed, using the PLAXIS 2D program, as well as an in-depth study of reinforcement options and verification of the sliding site's stability. Finally, our work concludes with a general summary of what we have learned and compiled in terms of study and reinforcement methods for landslides.

Position of the retaining wall and verification of slope stability:

The site intended for the construction of a municipal revenue office in the city of Taher, in the Jijel province of Algeria, is located at the foot of a small slope (figure1). This slope has experienced some movements, causing the existing retaining wall to partially overturn and shift laterally.

Figure 1 : position of the retaining wall.

The stability check consists of both checking the stability of the slope on the one hand and determining the direct causes of the movements of the existing retaining wall on the other hand (figure 2).

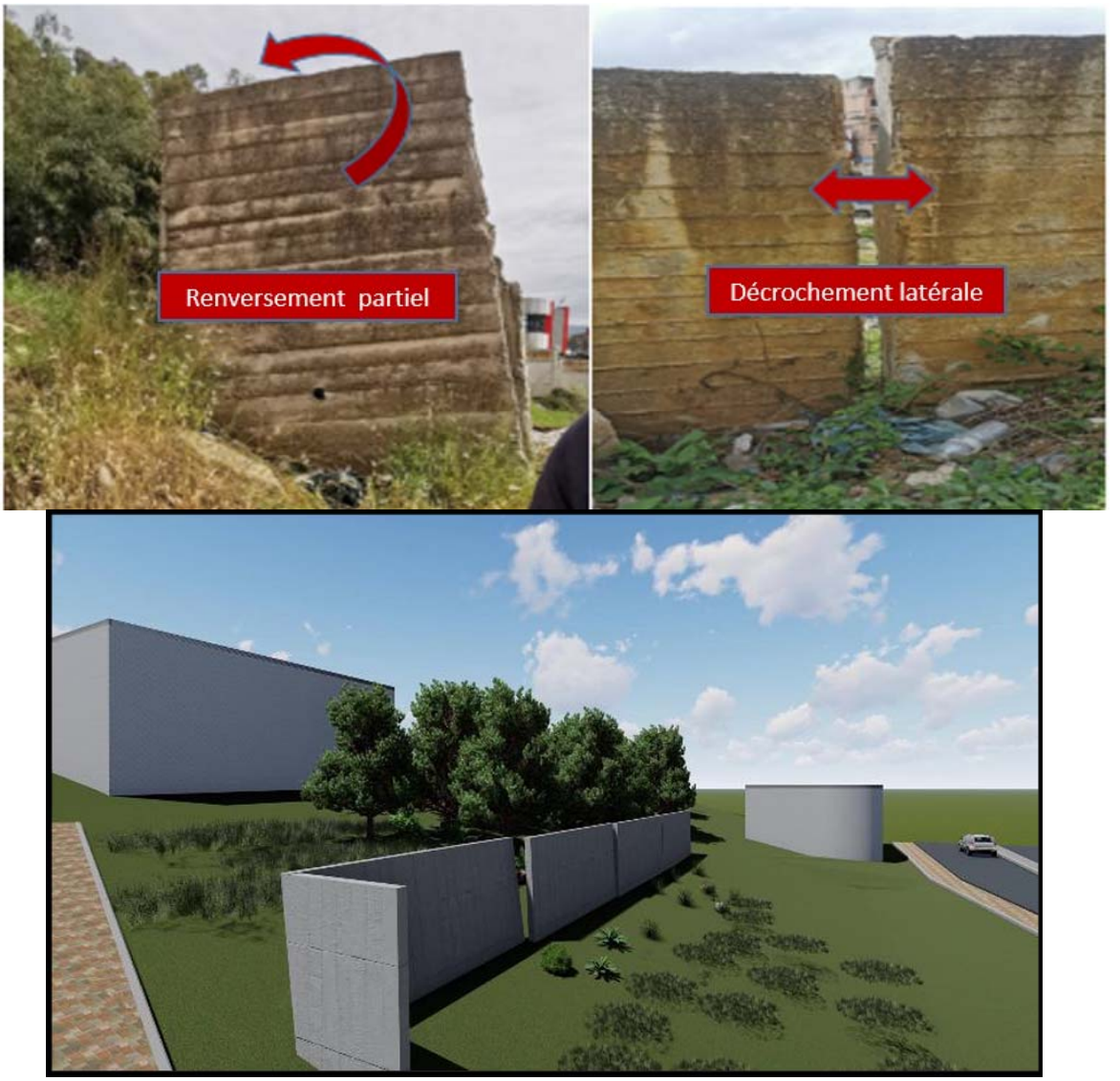

Figure 2: a) deformation on the retaining wall (partial overturning and lateral detachment) b): 3D photo of the site.

The lithology of the slope (figure 3) is characterized by a layer of backfill with a variable thickness ranging from 1.0 to 6.0m (the highest elevation is detected at the top of the slope), this deposit resting on a sandy clay and a clayey marl. Then in depth a marl is found.

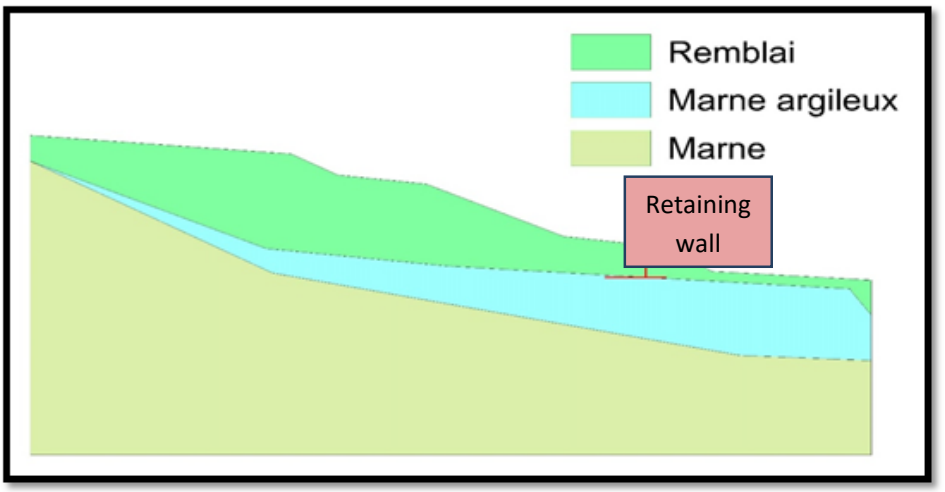

Figure 3 ; Lithological section of the project site.

The manual calculation of the stability of a slope (Figure 4) is done by trial and error, finding the most unfavorable slip line while strictly adhering to the geometry, geotechnical characteristics, and hydraulic properties of the embankments [51]. This section presents the manual calculation results of our slope failure using the Fellenius and Bishop limit equilibrium methods.

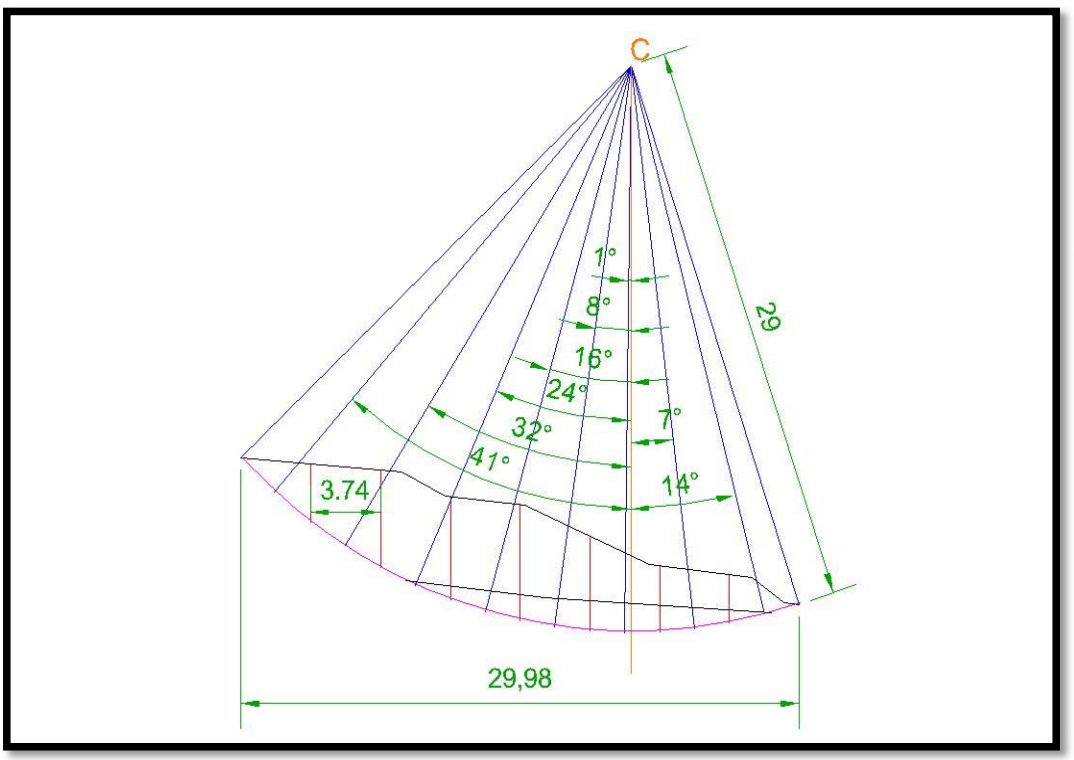

Figure 4 : Calculation of the slip circle by the slice methods, - Coordinates of the slip circle are; Center of the circle (25m; 38m), Radius 29m, B= 3.74 and L=29.98-.

The slice methods (Fellenius and Bishop) are the simplest and most practical due to their ease of implementation and reliability, always providing the best results for the safety factor [52, 53]. From the results obtained in Table (1), we observed that: The safety factor FS calculated by the Bishop method is higher than that calculated by the Fellenius method. Additionally, both safety factors FS (calculated by Bishop and Fellenius) are less than 1, indicating that the slope is unstable.

Table 1 :

Values of the safety factor calculated by different methods.

Fellenius	Bishop
0.70	0.81

Geology, Topography and Morphology of the Site, Climatological Context, Hydrology and Hydrogeology:

The set of topographic, morphologic, geological, geomorphological, and hydrological data allowed us to draw the following conclusions: the site intended for the construction of a municipal revenue office is located in the main agglomeration of the commune of Taher. Topographically, the site's relief has an irregular shape. The project is situated at the foot of a slope with an average to steep incline oriented towards the west, containing several small slopes. The overall slope ranges from 25% to 30%. The local geology consists of lithological formations from the Pliocene [54]. In terms of hydrology, the intensity of the hydrographic network is moderate, with a thalweg located at the foot of the slope, near the site, to the west. Climatologically, the study region is considered one of the rainiest. It has a temperate Mediterranean climate, with rainy and cold winters and hot, humid summers.

Correlation of dynamic penetration tests and borehole sections:

We found it useful to establish a correlation that allows for the comparison of penetrometric diagrams based on the penetration resistance criterion, with the depth of the resistant layer as it appears from the cross-sections made on the boreholes. The best way to proceed is to draw profiles that intersect the terrain in several directions. Thus, on the layout plan, profiles designated by double alphabetic letters are drawn: (A-A'): (S2, S3)-(P2, P4, P6)**.**

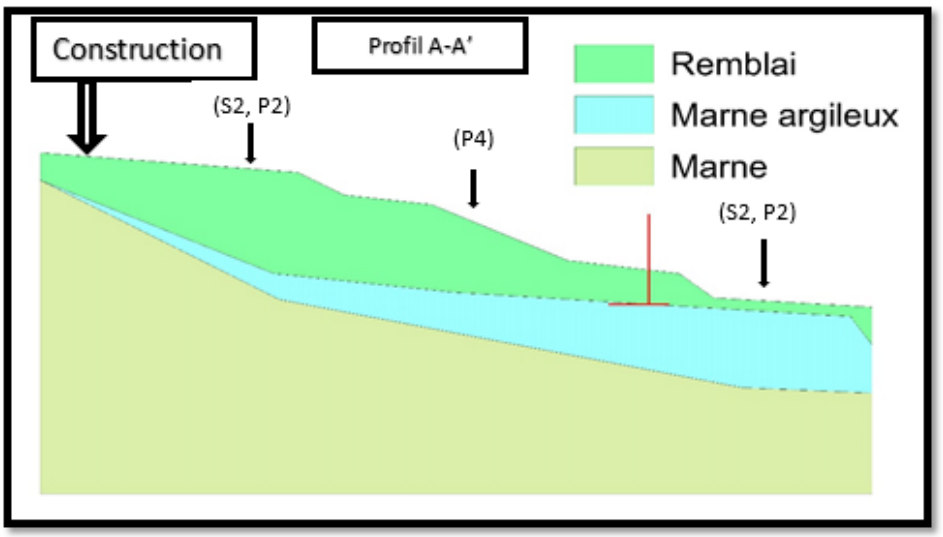

Figure 5: the A-A' profile.

The profile has a relief with a moderate to steep slope oriented towards the West. Geologically, it consists of clayey marl and sandy clays resting at depth on marls. This in-place formation is overlain by a thick layer of fill with a thickness of up to 6.0 meters. Dynamic penetration tests at this profile revealed variable resistances, very low in the fill with values of 10 to 20 bars, moderate in the clayey marl with Rp values ranging from 40 to 60 bars, and high in the marl at depth with values exceeding 100 bars. The piezometers installed at this profile revealed a low presence of groundwater, which consists of infiltration water from upstream areas.

Interpretations of physical parameters results

Water retention measurements (table 2) were carried out on different samples, yielding variable values. For clayey marl, the water retention is between 20% and 23%, and for marl, it is between 11% and 13%. The degree of saturation for clayey marl ranges from 68% to 79%, indicating a naturally moist state, while for marl, it is between 53% and 61%, indicating a moderately moist formation.

The dry density value for clayey marl is 1.50 t/m³, while for marl, it is slightly better, ranging from 1.68 to 1.76 t/m³. The apparent wet densities are as follows: for clayey marl, it ranges from 1.81 to 1.85 t/m³, and for marl, it ranges from 1.88 to 1.97 t/m³ (table 2). According to geotechnical standards, these soils are classified as semi-dense for clayey marl and dense for marl at depth.

Grain size tests were conducted for the different soil types. For clayey marl, the test showed that this formation has a fine texture, with 79% passing the 80 µm sieve and 94% passing the 2 mm sieve. For marl, more than 87% passes the 80 µm sieve (table 2).

Plasticity tests using the Casagrande apparatus on clayey marl gave a liquid limit value ranging from 42% to 44%, with a plasticity index between 22% and 23%. According to the Casagrande chart, this indicates a low plasticity soil. For marl, the

liquid limit values are closer, ranging from 45% to 47%, and the plasticity index is around 24% to 25% (table 2). According to the Casagrande chart, these formations are of low to medium plasticity.

Soil activity is defined by the ratio of the plasticity index to the percentage of particles smaller than 2 μm. The soil consisting of marl has an average plasticity index of 24.97% and an average percentage of particles smaller than 2 μm of about 78.66%, giving an average activity (Ac) of around 0.31. According to Skempton, this indicates that the soil is inactive.

Table 2:

The results of the physical characteristics of the site layers.

Drilling		Identification							
N° drilling	depth (m)	**W** (%)	γ(t/m^3)	γ**d** (t/m^3)	Sr (%)	2 (mm)	0.08 (mm)	WL (%)	IP (%)
S1	2.5/3.0	28	1.78	1.37	83	/	/	/	/
	7.5/8.0	11	1.97	1.76	58	98	88	47	25
S2	7.5/8.0	13	1.93	1.70	61	97	89	46	24
S3	2.0/2.5	20	1.81	1.51	68	94	79	44	23
	5.0/5.5	12	1.95	1.72	60	95	87	45	24
S4	3.0/3.5	23	1.85	1.50	79	94	80	42	22
	6.0/6.5	11	1.88	1.68	53	97	88	47	24

Interpretations of mechanical parameters results

The characteristics of soils, including shear resistance and compressibility, directly determine the bearing capacity of soils in relation to acceptable deformation (settlement). To assess these characteristics, we used the Casagrande apparatus for shear tests and the Terzaghi oedometer for compressibility tests. Shear tests were conducted according to the standard NF P94-071-1, of the UU type, using a direct shear machine at a speed of 1.2 mm/min (see Table 3). Shear tests were performed on samples taken from the borings, using a shear machine and a Casagrande apparatus, where 60 mm diameter samples were sheared at a rate of 1 mm/min. The cohesion values for the clayey marls range from 0.30 to 0.35 bars, and the friction angle values range from 7° to 8°. These characteristics clearly indicate that this formation has a relatively medium cohesion and friction angle. For the deeper marl, the cohesion values range from 0.55 to 0.61 bars, and the friction angle values range from 8° to 10°. For the deposit, the intrinsic characteristics are low.

Table 3 :

Shear test results.

Drillig		Shear	
N° drilling	Depth(m)	C_{cc}(bars)	φ_{uu} (°)
S1	2.5/3.0	0.23	6
	7.5/8.0	0.57	10
S2	7.5/8.0	0.61	9
S3	2.0/2.5	0.3	8
	5.0/5.5	0.55	8
S4	3.0/3.5	0.35	7
	6.0/6.5	0.6	8

To assess the soil's propensity for settlement, compressibility tests were conducted on pre-saturated samples using the LPC procedure (incremental loading test). The consolidation pressure values for the clayey marls ranged from 1.64 to 1.71 bars, indicating that this formation is overconsolidated. The compressibility coefficients were moderate, ranging from 21% to 23%, which shows that the formation is moderately compressible. The swelling indices were below the 4% threshold, indicating that the formation is non-swelling. For the deeper marl samples, the values for consolidation pressure (Pc) ranged from 2.36 to 2.6 bars, the compressibility coefficient (Cc) from 15% to 18%, and the swelling index (Cg) from 2.6% to 3.6% (see Table 4). According to geotechnical standards, this formation is overconsolidated, has low compressibility, and is non-swelling.

Tableau 4:

Oedometer test results.

Drilling		Oedometer		
N° drilling	Depth (m)	σc (bars)	Cc (%)	Cg (%)
S1	7.5/8.0	2.48	16.59	2.6
S2	7.5/8.0	2.60	15.83	3.3
S4	2.0/2.5	1.71	23.37	3.6
	5.0/5.5	2.59	18.09	3.3
S5	3.0/3.5	1.64	21.61	3.3
	6.0/6.5	2.36	17.34	3.6

Interpretations of chemical results

Chemical analyses revealed a variable presence of carbonate, ranging from 31% to 48%. These analyses did not indicate any presence of sulfates; however, the soil is non-aggressive.

Tableau 5:

Presente l'interpretation des résultats chimique :

Samples	% of carbonates CaCo3	% of insolubles	% of gypsum $CaCo_4 2H_2O$	Sulfates SO4-103 mg/kg
S1(7.0/7.5m)	45.8	55	nil	nil
S2(7.0/7.5m)	47.5	52.4	nil	nil
S3(2.5/3.0m)	31.0	69	nil	nil
S4(3.0/3.5m)	33.5	66.3	nil	nil

The examination of all physical, mechanical, and chemical characteristics provides the following assessments: The analyzed soils are composed of formations with varying consistencies. The clayey marl formation is characterized by a fine texture, semi-dense dry density, and a naturally wet moisture content, indicating low plasticity. The marl found at depth is classified as slightly moist and dense. Mechanically, both the clayey marl and marl exhibit average cohesion and friction angle values. In terms of compressibility, these formations are overconsolidated, low to moderately compressible, and non-swelling. Chemically, the soils contain no sulfates, indicating no aggressiveness, thus normal cement is appropriate for infrastructure concrete.

Numerical simulation of the revised retaining wall:

The behaviour of soils under stress is often unpredictable and nonlinear [42]; this requires extraordinary efforts [43-45]. The undeniable advantage of numerical methods is their ability to solve problems that cannot be resolved analytically and to find approximate solutions [46-47]. The modelling of geotechnical structures using numerical methods is made possible by a set of assumptions regarding the geometry of the structure and its environment [48], the materials and their behaviours, the loads, the boundary conditions, and the initial conditions [49].

PLAXIS 2D is a two-dimensional finite element method (FEM) program specifically designed to perform deformation and stability analyses for various types of geotechnical applications. Real situations can be represented by a plane or axisymmetric model. The program uses a user-friendly graphical interface that allows users to quickly generate a geometric model and a finite element mesh based on the vertical cross-section of the structure to be studied [50].

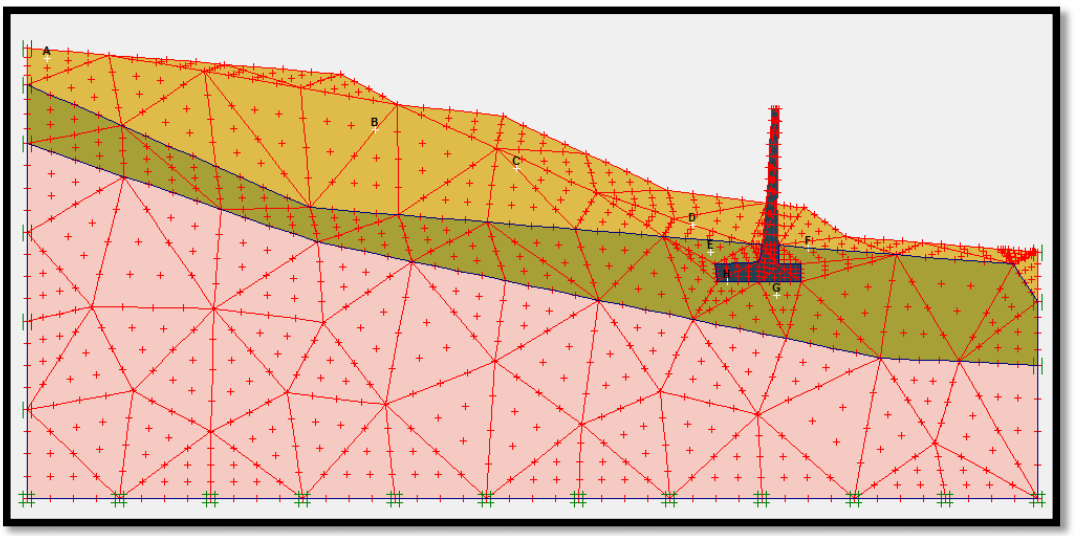

Figure 6: Designed Model and Behaviour *Tracking Points in our Model.*

Our modelling framework (Figure 6) has a total width of 40 meters and a height of 19 meters. It includes three different layers in its lithology, from top to bottom: a fill layer, a silty clay layer, and a clay marl layer, respectively (table 6). To revise the dimensions of the initial retaining wall, we modelled it with real dimensions instead of using plate elements to accurately observe its full-scale behaviour. The new height is 5.4 meters instead of the previous 4.6 meters, and the thickness is 0.4 meters instead of the previous 0.2 meters. Its foundation is anchored in the intermediate layer at a depth of 1 meter instead of the previous 0.4 meters in the superficial layer, with a front base of 2 meters and a rear base of approximately 1 meter. Our model is generated using a 15-node triangular mesh and is constrained by a system of boundary conditions to control the distribution of stresses and deformations, as well as to avoid undesirable effects at the model's boundaries. Our numerical modelling proceeds through four main phases to approximate real-time behaviour: Phase 1 involves the initial plastic phase, where there is no retaining wall over a period of seven (7) days. Phase 2 represents the installation of the retaining wall, adjusted over ninety (90) days, including the application of building loads above the slope (16 kN/m²) and traffic loads (6 kN/m²) below the slope. Phase 3 is the consolidation phase, adjusted for one hundred and twenty (120) days, to calculate the deformations of our system. Finally, Phase 4 involves calculating the Phi/c reduction to determine the safety factor of our system.

Table 6 :

The characteristics of the different soil layers.

Parameters		Backfill layer	Clayey marl	Marl
Behaviour		Mohr-Coloumb		
Type		Drained	Undrained	Undrained
ɣunsat	[kN/m³]	15,000	13,700	16,800
ɣsat	[kN/m³]	18,000	17,800	18,800
kx	[m/min]	8,000E-03	8,000E-03	8,000E-03
ky	[m/min]	8,000E-03	8,000E-03	8,000E-03
Eref	[kN/m²]	2,660E+04	6,400E+04	6,450E+04
Eoed	[kN/m²]	3,941E+04	9,483E+04	1,035E+05
υ	[-]	0,33	0,33	0,350
Gref	[kN/m²]	1 E+04	2,406E+04	2,389E+04
cref	[kN/m²]	5	12	20
ϕ	[°]	20	38	15
ψ	[°]	0	0	0

To monitor the deformations in our numerical model, we selected points A, B, C, D, and E on the surface of the fill layer, as well as points F and G below the retaining wall, to thoroughly understand the deformations around the retaining wall (Figure 6). Additionally, to track the stresses in our model, we adopted points I, J, K, L, M, and N in the fill layer, as well as points O, P, and Q around the retaining wall in the intermediate layer.

Results :

After the calculation, we found a total deformation of 444.73 x 10^3 with a scale effect of 2.10^-6, which gives us a total deformation of 0.89 m. It can be observed that this displacement occurs only in the surface layer of the backfill, with a direction going from the top of the slope to the foot of the slope, before the retaining wall, without any effect on the wall itself (Figure 7).

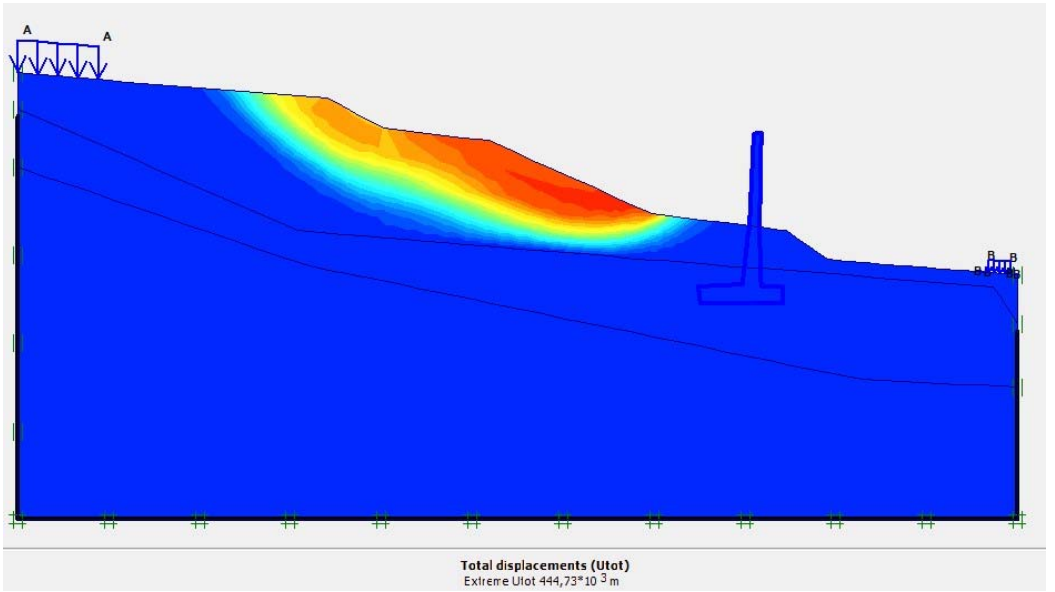

Figure 7: Total deformation of 0.89 m.

Thus, we observed that significant displacement occurs at tracking point A, located above (at the head of) the slope in the surface layer, and at point D, located directly behind the retaining wall. The other tracking points in the model can be considered negligible (Figure 8).

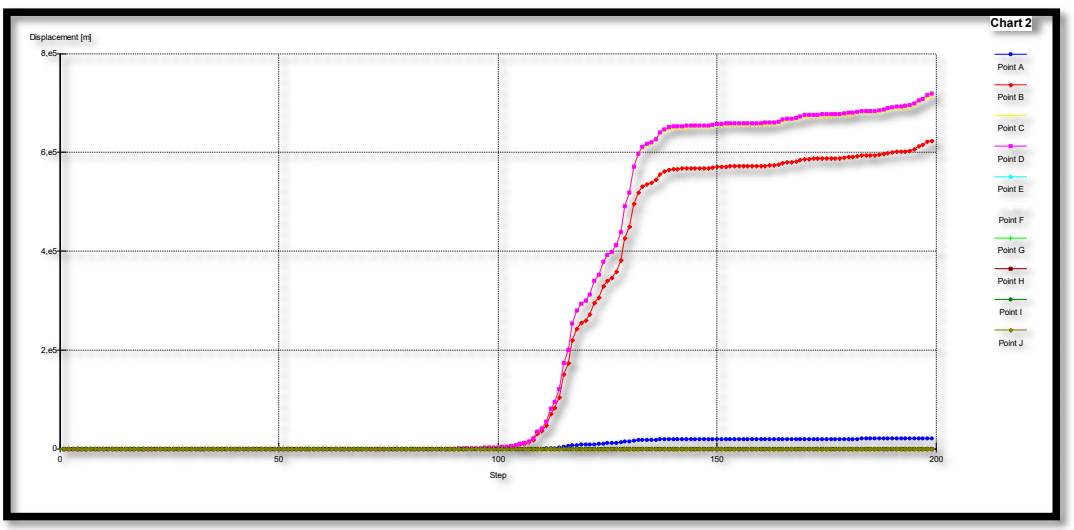

Figure 8: Deformation curves at the different monitoring points.

The safety factor calculated before the installation of the retaining wall is 0.58 (the red curve in Figure 9), which required us to find a solution to stabilize the slope. We chose the same solution proposed by the initial design office to determine if the problem lay in the study or in the execution, and thus conclude on the appropriate solution based on our expertise. The safety factor calculated by our model after the

installation of the retaining wall is 2.11 (the blue curve in Figure 9). This safety factor value indicates that the retaining wall is largely stable and that the deformations occurring behind the wall do not affect its stability, which lends credibility to our model.

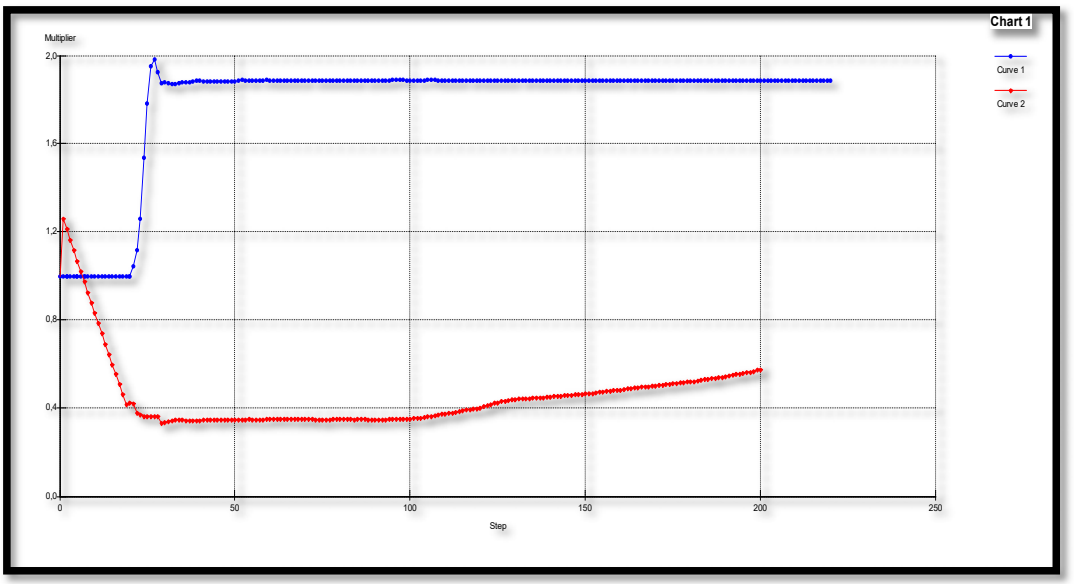

Figure 9: Safety factor before installation (red) with a value of 0.58 and after installation of the retaining wall with a value of 2.11.

Discussion

The wall intended to support the administration of the Treasury of Taher in the province of Jijel in Algeria against the sliding of the embankment behind the Treasury is partially overturned without visible deformation, which led the project owner (APC of Taher) to suspend the project by freezing the allocated funds and to open an inspection to determine the real cause of the problem, whether in the initial study or in the poor execution. Despite the counter-expertise carried out by several engineering offices and civil engineering experts on the ground, no satisfactory solution has been found to solve this problem. This prompted us to undertake investigation to identify the real source of the problem.

Figure 10: the investigation site.

Upon visiting the site and conducting our diagnostic of the wall (see photos in Figure 10), we discovered the presence of a plastic sheet - plastic tarpaulin - behind the wall, along half of the slope, sealing the surface layer of the backfill and blocking the dissipation of rainwater upwards. This created pressure on the wall in the surface layer, particularly at monitoring point D in our model. We also noticed that the retaining wall is anchored only in the backfill layer and barely touches the intermediate layer. This led us to realize that the pressure exerted by the soil under the rear footing of the retaining wall after significant rainfall can cause superficial and partial sliding in the area of point D in our model, resulting in a partial and slight overturning of the left part of the retaining wall without visible deformation (see Figure 11 for photos of the plastic sheet and the toppled wall).

Figure 11 : plastic tarpaulin.

By comparing these observations with the predictions from our model, we find a logical correlation, particularly at point D as previously mentioned, as well as at point A where we observed deformations in the foundations of buildings at the top of the slope (see Figure 8 for deformation curves and Figure 12 for photos of the deformed houses).

Figure 12 : distorted house photos.

It should be noted that our retaining wall model is larger than that of the initial design office, with an increased height of 0.80 m, a greater thickness of 0.20 m, and a deeper foundation of 0.60 m, anchored down to the intermediate layer. This provides greater stability to our model compared to that of the design office.

Figure 13 : photo of the adjacent administration.

In summary of our diagnosis and expertise, we identify errors both in the study and in the execution. In the study, the design office failed to correctly size and provide adequate anchoring for the base of the wall, which should have been deeper down to the intermediate layer. Additionally, there appear to be potential errors in the execution, particularly concerning site preparation and the inappropriate use of a plastic sheet instead of a geotextile to facilitate the drainage of the backfill. This conclusion is supported by the intact state of the adjacent administration, visible in the condition of its services, which shows no signs of sliding (see Figure 13 for photos of the adjacent administration). It is noteworthy that this administration is located lower than the Treasury and had excavated a thinner superficial layer of backfill.

Conclusion:

This in-depth study on the stability of a retaining wall in Jijel Province, Algeria, reveals several critical aspects in the design and execution of urban constructions. The partial overturning of the wall, without apparent deformation, was a major concern that led to the suspension of the Taher Treasury Project. Evaluations highlighted deficiencies in both the initial study and on-site execution. The identification of a plastic sheet behind the wall, hindering proper rainwater drainage, was a significant discovery. This situation exacerbated pressures on the superficial layer of the backfill, contributing to the observed superficial sliding. Additionally, the insufficient anchoring of the wall in the intermediate layer compromised its stability under local geotechnical conditions.

The comparison between field observations and our full-scale, real-time numerical model—different from the initial failed model, which was only plate-element based—emphasized the importance of a robust design with adequate dimensions and appropriate anchoring. Our proposed revised model, larger, deeper, and better anchored, aims to rectify the identified shortcomings, offering better resilience against slope sliding risks.

Ultimately, this study underscores the crucial importance of rigorous geotechnical planning and adherence to standards in urban projects. The lessons learned from this analysis should guide future decisions to avoid similar failures, ensuring stability during construction and the durability of buildings in morphologically challenging and geotechnical complex urban areas.

References

[1] Castro-Nova, I., Gad, G. M., Touran, A., Cetin, B., and Gransberg, D. D., Evaluating the Influence of Differing Geotechnical Risk Perceptions on Design-Build Highway Projects, Journal of Risk and Uncertainty in Engineering Systems, Part A: Civil Engineering, ASCE, 4(4), 04018038, August, 2018.
[2] Christian, J. T., and Baecher, G. B., Unresolved Problems in Geotechnical Risk and Reliability, Geo-Risk 2011: Risk Assessment and Management, Atlanta, Georgia, United States. doi: 10.1061/9780784411834. June 26-28, 2011.
[3] Assaf, S. A., and Al-Hejji, S., Causes of Delay in Large Construction Projects, International Journal of Project Management, Elsevier, 24(4), 349-357, May, 2006.
[4] Day, R. W., Geotechnical Engineering: A Risky Profession with Many Issues and Problems, Journal of Professional Issues in Engineering Education and Practice, ASCE, 119(2), 201-204, April, 1993.
[5] Grimsey, D., and Lewis, M. K., Evaluating The Risks of Public Private Partnerships for Infrastructure Projects, International Journal of Project Management, Elsevier, 20(2), 107-118, February, 2002.
[6] Khodeir, L. M., and Nabawy, M., Identifying Key Risks in Infrastructure Projects–Case Study of Cairo Festival City Project in Egypt, Ain Shams Engineering Journal, Elsevier, 10(3), 613-621, September, 2019.
[7] Assaf, S. A., Bubshaitr, A. A., and Al-Muwasheer, F., Factors Affecting Affordable Housing Cost in Saudi Arabia, International Journal of Housing Markets and Analysis, Emerald, 3(4), 290-307, October, 2010.
[8] Kaliba, C., Muya, M., and Mumba, K., Cost Escalation and Schedule Delays in Road Construction Projects in Zambia, International Journal of Project Management, Elsevier, 27(5), 522-531. July, 2008.
[9] Kumaraswamy, M. M., and Chan, D. W., Determinants of Construction Duration, Construction Management and Economics, Taylor and Francis, 13(3), 209-217, May, 1995.
[10] Mansfield, N. R., Ugwu, O. O., and Doran, T., Causes of Delay and Cost Overruns in Nigerian Construction Projects, International Journal of Project Management, Elsevier, 12(4), 254-260, November, 1994.
[11] Sartain, N., Mian, J., and Peluso, D. Risk Assessment in Geotechnical Engineering Practice, Geo-Risk 2017: Geotechnical Safety and Reliability, Denver, Colorado. doi: 10.1061/9780784480731.024. June 4-7, 2017.
[12] X. D. CHOWDHURY R.N., Slope system reliability with general slip surfaces, Soils and foundations, vol. 34, 1994, pp. 99-105.
[13] Houssam KHELALFA, Nabile OSMANE, Mohammed BOUATIA. Excavation Stability Study with Inclination of Cut Slopes at 45° and 90°in the long-term (LT) and short-term (ST) States: A Case Study. Indian Journal of Engineering, 2020, 17(48), 470-482
[14] Fellenius W (1936) Calculation of stability of earth dams. In:Transactions second congress on Large Dams, pp 445–465
Griffiths, D & Lane, P (1999) Slope stability analysis by finiteelements. Geotechnique, 49(3), pp 387-403.
[15] Lowe J, Karafaith L (1960) Stability of earth dams upon drawdown. In: Proceedings 1st Pan-Am conference soilmechanics and foundation engineering, Mexico City, pp537–552

[16] Morgenstern NR, Price VE (1965) The Analysis of the stabilityof general slip surfaces. Géotechnique 15:79–93
[17] Bowles JE (2001) Foundation analysis and design, 5th edn.McGraw-Hill International Editions, New York
[18] Zabuski L. (2018) The influence of slope geometry on its stability: Spatial and plane analysis, Archives of Hydro-Engineering and Environmental Mechanics (AHEM), 65 (4),243–254
[19] E. Hoek, 2009, Fundamentals of Slope Design, SlopeStability, Santiago, Chile
[20] Babu GLS, Murthy BRS, Srinivas A (2002) Analysis ofconstruction factors influencing the behaviour of soil-nailed earth retaining walls. Proc Inst Civ Eng-Gr Improvement6(3):137–143
[21] Zabuski L. (2008) Investigation of the mechanism of landslidemovement on the test slope including the influence ofexternal factors and internal properties of the rock mass, IBWPAN, Gdansk (internal report), (in Polish)
[22] DeGroot, D.J. (2001), Laboratory measurement and interpretation of soft clay mechanical behaviour, Soil Behaviour and Soft Ground Construction, ASCE GSP 119: 167-200.
[23] Hight, D.W. and Leroueil, S. (2003). Characterisation of soils for engineering purposes. Characterization & Engineering
[24] Jamiolkowski, M., Ladd, C.C., Germaine, J.T., and Lancellotta, R. (1985). New developments in field and lab testing of soils. Proc. 11th Intl. Conf. Soil Mechanics & Foundation Engineering, Vol. 1, San Francisco: 57-154.
[25] Zabuski L. (2008) Investigation of the mechanism of landslidemovement on the test slope including the influence ofexternal factors and internal properties of the rock mass, IBWPAN, Gdansk (internal report), (in Polish) Oberhollenzer, S, Tschuchnigg, F, & Schweiger, HF (2018)Finite element analyses of slope stability problems usingnon-associated plasticity. Journal of Rock Mechanics andGeotechnical Engineering, 10(6), 1091-1101
[26] Griffiths D. V., Marquez R. M. (2007) Three-dimensional slopestability analysis by elasto-plastic finite elements,Geotechnique, 57 (6), 537–546
[27] Stark T. D., Eid H. T. (1998) Performance of three-dimensional slope stability methods, J. Geotech. Geoenviron.Engng, 124 (11), 1049–1060
[28] Bar, N, Yacoub, T & McQuillan, A 2019, 'Analysis of a largeopen pit mine in Western Australia using finite element andlimit equilibrium methods', Proceedings the 53rd US RockMechanics/Geomechanics Symposium, American RockMechanics Association, Alexandria, paper ARMA 19–A-30
[29] Detournay Ch., Hart R. (eds.) (1999) FLAC and NumericalModeling in Geomechanics, Proc. Int. FLAC Symp. onNumerical Modeling in Geomechanics, Minneapolis, Sept.1999, Balkema/Rotterdam/Brookfield
[30] F. Baynes, «Sources of geotechnical risk,» Quarterly Journal of Engineering Geology and Hydrogeology, pp. 321-331, 2010.
[31] H. Brandl, The Civil and Geotechnical Engineer in Society: Ethical and Philosophical Thoughts,Challenges and Recommendations, 2004.
[32] B. Simpson, Reliability in geotechnical design–some fundamentals. In Proceeding of Third international symposium on geotechnical safety and risk, vol. Vol. 1, 2011, pp. 393-399.
[33] Park J, Lee M. A study on the application of BIM(Building information modeling) in the field of non-linear forms architecture. Proceeding of Annual Conference of the Architectural Institute of Korea. 2008 Oct 24-25; Gwangju, Korea. Seoul (Korea): the Architectural Institute of Korea; 2008. p. 209-12.
[34] Ryu, Hanguk, and Kim, Sung-Jin. "Implications Deduction through Analysis of Reverse Engineering Process and Case Study for Prefabrication and Construction of Freeform Envelop Panels." Journal of the Korea Institute of Building Construction 16, no. 6 (December 20, 2016): 579–85. doi:10.5345/JKIBC.2016.16.6.579.
[35] B. V. S. Viswanadham, D. König, and H. L. Jessberger, Discussion: Dimensional analysis for geotechnical engineers, Géotechnique , Volume 51 Issue 1, February 2001, pp. 91-93. https://doi.org/10.1680/geot.2001.51.1.91

[36] R. C. Bachus, Geotechnical Analysis in Karst: The Interaction between Engineers and Hydrogeologists. Conference: 10th Multidisciplinary Conference on Sinkholes and the Engineering and Environmental Impacts of Karst. DOI: 10.1061/40796(177)2
[37] Mali N, Dutt V and Uday KV (2021) Determining the Geotechnical Slope Failure Factors via Ensemble and Individual Machine Learning Techniques: A Case Study in Mandi, India. Front. Earth Sci. 9:701837. doi: 10.3389/feart.2021.701837
[38] S. Van Baars , Causes of Major Geotechnical Disasters . ISGSR 2011 - Vogt, Schuppener, Straub & Bräu (eds) - © 2011 Bundesanstalt für Wasserbau ISBN 978-3-939230-01-4. pp 685 - 692
[39] Sherif Agaiby and Sayed Mohamed Ahmed, Learning from Failures: A Geotechnical Perspective. Proceedings of the International Conference on Forensic Civil Engineering, Nagpur, India 21,22,23 January 2016
[40] S. Djanba, Influence des paramètres : géologiques, géomorphologiques et hydrogéologiques sur le comportement mécanique des sols de la wilaya de Sétif (Algérie), l'Université Mohamed Kheider – Biskra Faculté des Sciences et de la Technologie Département d'Hydraulique et du G. civil, 2015.
[41] Zeroual. F," Etude du comportement d'un mur de soutènement soumis à des sollicitations dynamiques", Mémoire de Magister, Université Batna.
[42] Zheng YR, Zhao SY, Song YK (2005) Advance of study on the strength reduction finite element method [J]. J Logist EngUniv 3:1–6
[43] Wang, L., M. Xie, B. Xu, and T. Esaki. 2015. "A Study on Locating Critical Slip Surface of Slopes." International Journal of Geotechnical Engineering 9 (3): 265–278. https://doi.org/10.1179/1939787914Y.0000000060.
[44] Yang, H., J. Wang, and Y. Liu. 2001. "A new Approach for the Slope Stability Analysis." Mechanics Research Communications 28 (6): 653–669. https://doi.org/10.1016/ S0093-6413(02)00217-3.
[45] Yu, Z., O. O. Eminue, R. Stirling, C. Davie, and S. Glendinning. 2021. "Desiccation Cracking at Field Scale on a Vegetated Infrastructure Embankment." Géotechnique Letters 11 (1): 1–8. https://doi.org/10.1680/jgele.20.00108
[46] Horn J.A. - < Computer analysis of slope stability >. J. ASCEvol.86, SM3, 1960
[47] Little A. L., Price V.E. The use of an electronic computer for slope stability analysis.. Geotechnique vol. B, 1958, p.113-120
[48] Roberto J. Marin & Michael Long (15 Jul 2024): 2D and 3D numerical modelling for preliminary assessment of long-term deterioration in Irish glacial till geotechnical slopes, Georisk: Assessment and Management of Risk for Engineered Systems and Geohazards, DOI: 10.1080/17499518.2024.2379946
[49] F. E. M. Y. Boulon M, Pratique éclairée des éléments finis en Géotechnique », document1, Laboratoire 3S et Terrasol, 2004.
[50] B. W. W. D. Brinkgreve R.B.J., PLAXIS 2D, Finite Element Code for Soil and Rock Analyses, Users Manual. Balkema, Rotterdam, 2006.
[51] Kovarik, J. B. (2000). Qu'est-ce qu'un coefficient de sécurité en génie civil?. Revue française de génie civil, 4(6), 607-651
[52] M. P. A. Alan W. Bishop, The use of the Slip Circle in the Stability Analysis of Slopes, vol. 5, 1955, pp. 7-17.
[53] A. Caquot, méthode exacte pour le calcule de la rupture d'un massife par glissement cylindrique, 1954, pp. 344-355.
[54] Djellit, H. (1987). Évolution tectono-métamorphique du soclekabyle et polarité de mise en place des nappes de flysch enPetite Kabylie occidentale (Algérie) (Doctoral dissertation,Paris 11)

Ecological fuel obtained by recovery the biomass resulting from the pruning of Paulownia trees and plant residues. Determination of calorific value.

Combustibil ecologic obținut prin utilizarea biomasei rezultate din toaletarea arborilor Paulownia și a resturilor vegetale. Determinarea puterii calorifice.

Lukas Ilioni[1], Ricardo Sbera[1], Selena Coandă[1]

[1]University Politehnica Timișoara
Victoriei Square, No. 2, Timisoara, Romania
E-mail: lukas.ilioni@student.upt.ro, ricardo.sbera@student.upt.ro, elena.coanda@student.upt.ro

Coordonatori: Adriana Tokar, Daniel Muntean, Daniel Bisorca, Dănuț Tokar

E-mail: adriana.tokar@upt.ro, daniel-beniamin.muntean@upt.ro, daniel.bisorca@upt.ro, danut.tokar@upt.ro

DOI: 10.37789/rjce.2025.16.1.6

Abstract. *In the current climate context regarding the reduction of net greenhouse gas emissions, the article proposes the creation of an ecological fuel obtained from the trimming of Paulownia trees and plant residues (stems and leaves of Sunflower and corn), residues that are not used in other purposes. For the proposed blends (66.66% Paulownia, 16.67% Sunflower and 16.67% Corn) the calorific value was determined and compared to a sample with 100% Paulownia. The results show that for the mixtures obtained, a decrease in calorific value of 37.32% and 29.74% respectively (depending on the humidity of the mixture) was found compared to the Paulownia standard sample (20,000 J/g), but which is close or even higher than that of other commercial mixtures (sample S4-beech+oak-9,482 J/g). right.*

Key words: ecological fuel, biomass residues, recovery, calorific value

1. Introduction

The objective of achieving climate neutrality in the European Union by 2050 and reducing net greenhouse gas emissions by at least 55% by 2030 compared to 1990 levels requires an energy transition in which renewable energy (wind, solar, hydropower, ocean energy, geothermal energy, biomass and biofuels) play a fundamental role as the

The article was received on 31.03.2024, accepted on 15.01.2025 and published on 14.03.2025

energy sector currently contributes more than 75% of Europe's total greenhouse gas emissions [1], [2].

The new climate target introduced by the 'Fit for 55' package increased the integration of renewables (RES) for Europe from 32% to 45% by 2030 [3].

As regards biomass, the Directive promoting energy from renewable sources stresses the need to apply biomass cascading principles that reduce the risk of rampant deforestation [4].

Biomass consists of two main components: one consists of biodegradable materials from products, waste and residues of biological origin from vegetal and animal substances and various sectors such as agriculture, forestry, fisheries and aquaculture, together with adjacent industries, and the other is the biodegradable part of industrial and municipal waste of biological origin.

The principles of cascading use of biomass refer to [5]:

- *Sustainability* – storage of CO2 through afforestation [3], return of material to biomass stock, reintegration of woody biomass into forests after use (reuse of wood biomass ash (rich in basic minerals, potassium and phosphorus) as forest fertiliser));

- *Resource efficiency* – efficient use of main (timber or veneer) and secondary flows (wood of thin parts of the trunk, sawdust, cutting debris, bark, tops and branches - used for wood-based panels, pulp, wood packaging and bioenergy) of woody biomass, but also of the reuse of agricultural by-products and agroforestry residues (thermal insulation boards, acoustics and anti-vibration, as well as lining material for containers and pots for transplanting plants and trees as an alternative to plastics);

- *Circularity in every stream and every step* – efficient design of the entire life cycle, encouraging collection, recycling and reuse;

- *New products and new markets* - new technologies to transform by-product and waste streams into new products;

- *Subsidiarity* - allocation of biomass at local and regional level for different uses as material and/or energy source, assessment of qualitative and quantitative biomass availability;

In this context, it was analyzed which are the main sources contributing to the supply of biomass for energy in the EU (Fig.1) [6].

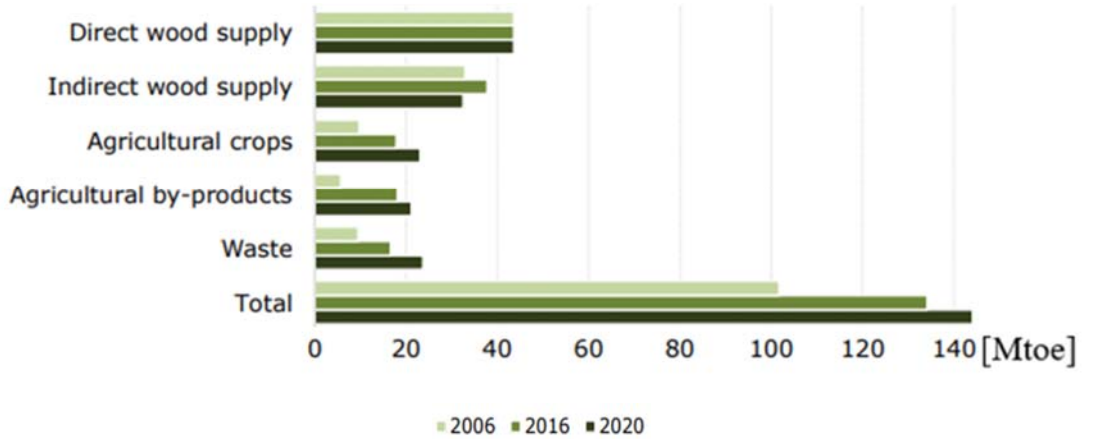

Fig.1. EU internal primary energy supply [6]

Figure 1 shows that forestry is the source that contributes most to the supply of biomass (directly and indirectly) for energy with a percentage of over 60%, followed by agriculture (about 30%), and the remaining about 10% comes from waste (municipal, industrial, etc.). As the new EU targets set by the "Fit for 55" package set more ambitious targets for carbon removals, i.e. 85 million tonnes higher by CO_2 equivalent (Fig. 2), binding targets are set for each country aimed at increasing net removals of greenhouse gases [3].

These targets are addressed in two phases: Phase I – by 2025 – introducing mandatory balance between emissions and removals and Phase II – 2026-2030 – net removals of 310 Mt.

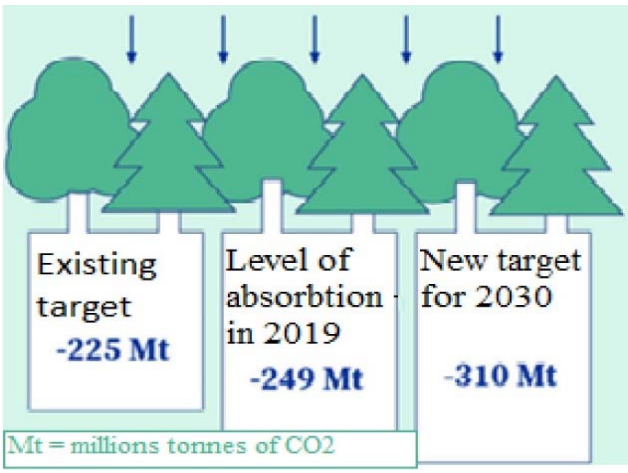

Fig. 2. Targets for carbon removal by 2030 [3]

In the current energy context, the paper proposes an analysis of the sustainable use of biomass resulting from waste from agriculture and forestry. Ignoring the use of energy plants for energy generation, we propose the production of solid biofuel from plant residues (stems, leaves and branches) from crops for food purposes (sunflower, corn) and from Paulownia crops.

The analysed crop plants have the advantage of absorbing satisfactory amounts of CO_2 from the atmosphere and generating calorific values high enough to be used as biofuel. We also propose an analysis of the carbon neutrality of the resulting material. This analysis is based on literature guidelines stating that using biomass for combustion can be carbon neutral [7] and reducing methane emissions into the atmosphere [8].

2. Current state of research

This chapter describes the plants from which solid biofuel will be made, these being:

- Princess Tree (Paulownia Tomentosa) - Paulownia has a high carbon assimilation coefficient, the rapid growth of biomass requires large amounts of CO_2 absorbing around 12.5 t / ha / year [9]. A tree absorbs about 22kg of CO_2 and exhales 6kg O_2 over the course of a year, resulting in a purification of thousands of cubic meters of air. [10] For wood production, between 550-750 trees/ha are planted [11]. The density of Paulownia wood, with a moisture content of 12%, varies from 220 to 350m-3 kg, but most often oscillates around 270 kg $^{m-3}$. [12,13,14] The calorific value of Paulownia biomass is close to that of coal, with a value of 20 MJ/kg [15].
- Sunflower (Helianthus annuus) – According to some general estimates, it is estimated that a sunflower crop can absorb about 1.5 to 2 tons of CO_2 per hectare during the growing period [16],[17]. Research shows that this agro-industrial waste has a calorific value of 17.8 MJ/kg [18]; similar to other solid biofuels currently in use. Freshly harvested sunflower plants may have a higher initial moisture content, which can generally range between 8% and 12% [19].
- Maize (Zea Mays) - Global corn production reaches 1661.25 million tons/year, which constitutes about 27.2% of total agricultural waste. The components of the corn plant consist mainly of about 34.5% stems, 32.3% leaves, 14.3% husks, 12.3% cobs and 6.6% flowers. Maize scraps, among the most abundant agricultural waste in the world, are ubiquitously found after grain harvesting, accounting for about 47-50% of the dry mass of total grain production [20]. Maize residues have a calorific value of 17 MJ/kg [21] and a moisture content below 15% [22], [23], [24], [25].

3. Methods

3.1. Preparation of samples

- Obtaining basic materials.

The raw material for the study was obtained by grinding using a Hecht 6208 shredder. The basic materials come from vegetable waste - stems and leaves from sunflower (S2), corn (S3) and plant residues resulting from pruning Paulownia Tomentosa trees (S1), materials that are shown in Fig. 2. The materials were obtained from local farmers who grow corn and sunflowers (plant residues are abandoned in the

fields), and from boat and musical instrument producers who own Paulownia Tomentosa (sawdust and grooming) crops.

Fig. 1. Basic materials

Tests were also carried out for the comparative study on a mixture of beech and oak (S4) obtained from a local briquette producer. The material for analysis was represented by different types of pellets (diameter 6 mm, length 25 - 35 mm) produced in the Laboratory for fuel analysis, ecological investigations and dispersion of pollutants at the Polytechnic University of Timisoara.

- Measurement of moisture content of obtained materials (before drying).

With the help of the wood humidometer FHM 20, the humidity of the materials used was measured (Fig. 2). The measurements were made at 4 points, considering for the humidity of the samples, the arithmetic mean of the 4 readings (Table 1).

Fig 2. Humidity measurement of materials S1, S2, S3, S4.

Tabel 1

The average humidity of materials S1, S2, S3, S4.

Material	Humidity readings [%]				Medium humidity [%]
	1	2	3	4	
S1	26,9	29,8	27,4	27,3	27,8
S2	10,3	13,3	12,9	14,7	12,8
S3	12,9	13	14,8	14,4	13,7
S4	7,7	8	7	8,2	7,7

Since moisture contents below 15% (recommended by the briquette manufacturer) were obtained for samples S2, S3 and S4, only sample S1 was dried and an average moisture content of 27.8% was measured.

- Establishment of recipes for clean fuels proposed for analysis

Recipes S5 and S6 were made according to Table 2 data by mixing basic materials with proportions of 66.66% Paulownia, 16.67% Sunflower and 16.67% Maize, with different humidity of Paulownia residue.

Tabel 2

New recepies

Sample	Paulownia		Sunflower		Corn	
	Weight [g]	Humidity [%]	Weight [g]	Humidity [%]	Weight [g]	Humidity [%]
S5	4	27,8	1	12	1	13,7
S6	4	6,275	1	12	1	13,7

It can be seen that between the preparation period of the basic materials and the period of preparation of the samples, for the shredding of sample S2 the moisture content decreased and for sample S3 the humidity was kept constant.

3.2. Making samples for experimental trials

Making a biofuel with superior combustion properties requires a low moisture content. Since for samples S2, S3 and S4 humidity below 15% (value recommended by the briquette manufacturer) was obtained at both stages of work, only the material was dried for sample S1 for which an average humidity of 27.8% was measured.

To lower the humidity of Paulownia Tomentosa mince, the drying oven was used (Fig. 3) for 90 minutes, heating the base material to a temperature of 100 ºC.

After preparing the raw materials, a pelletizing press was used (Fig. 4) and 2 types of samples with different composition (S5, S6) were made (Fig. 5).

Fig. 3. Drying oven

Fig. 4. Pelletizing press

Fig 5. Pellet making process

3.3. Measurement of calorific value

Calorific value is expressed as energy released in the form of heat when a compound or material is completely burned in the presence of oxygen. A higher calorific value indicates a higher fuel energy density, meaning it would release more energy per unit of fuel burned. Therefore, in order to obtain the same amount of energy, the amount of fuel needed to be burned is lower in the case of a higher calorific fuel [26].

The calorific value measurement was carried out for samples S1, S4, S5 and S6.

The pellets obtained from pressing were weighed and then fixed with nickel-chromium wire in the calorimetric bomb (Fig. 6).

Fig. 6. Preparation of samples for testing

A calorimetric bomb (Fig. 7) is a device that measures the amount of heat generated by a chemical reaction or complete combustion of a sample of the substance. The principle of operation is based on isolating the sample of the substance in an airtight container and placing it in a container with water. The substance is then incinerated and the heat generated is transferred to the water in the outer container [27].

Fig 7. Preparation of the commissioning of the calorimetic bomb

The water system around the sample absorbs heat and heats up, allowing the amount of heat released by the combustion process to be determined. The temperature variation of the water in the outer container is measured with great precision and is used to calculate the heat energy generated by the reaction. This heat energy is expressed in units of heat, such as kilocalories or joules. Thus, the calorimetric bomb provides an accurate and sensitive method for determining the caloric content of various organic substances (Fig. 8).

Fig. 8. The process of determining calorific value.

4. Results and discussions

In addition to the samples made, a sample of Paulownia Tomentosa was again dried at 100ºC to lower the moisture content. Following the application of the second stage of drying, a humidity of 4% was obtained.

Test results are centralised in Table 3.

Table 3

Measurement results

Environmentally friendly fuel	Calorific value [J/g]		Humidity [%]		CO_2 absorption [t/ha/an]
	From the literature	Measured	Measured before drying	Measured after drying	From the literature
Paulownia [12]	20,000	20,000	24	15 (after first drying)	12
		20,090	24	6,275 (after second drying)	
Sunflower [16]	17,8	-	12	-	1,8
Corn [19]	17,2	-	13,7	-	-
S5 (Paulownia-sunflower-corn mixture)	-	12,536	-	13,18	-
S6 (Paulownia-sunflower-corn mixture)		14,052	-	10	-

From the analysis of Table 3 it can be seen that the highest calorific value is obtained for Paulownia Tomentosa, a value that is confirmed by the specialized literature. In addition, better results can be obtained as the base material has a lower moisture content, but for briquettes or pellets, the humidity cannot be lowered towards zero.

For the proposed mixtures, satisfactory values for calorific value have been obtained. Again, it is noted that for the same proportions of the base materials from which the mixture was made, lowering the humidity increases the calorific value.

5. Conclusions

The comparison of the calorific value obtained for the proposed mixtures (66.66% Paulownia, 16.67% Sunflower and 16.67% Corn-samples S5 and S6) with a sample with 100% Paulownia Tomentosa with humidity of 15% and 6.275% respectively indicates a decrease of 37.32% and 29.74% respectively (depending on the humidity of the mixture), but higher than that of the beech and oak mixture (commercialized briquettes – sample S4) by 32.21% (for S5) and 48.20% (for S6), respectively.

In conclusion, the newly proposed fuels (mixture of 66.66% Paulownia, 16.67% Sunflower and 16.67% Maize), even if they have lower calorific values than mixtures known in the specialized literature (Paulownia - 20MJ / kg), the fact that waste that is not recovered is integrated gives them an advantage in terms of protecting the environment by reducing deforestation.

6. Future directions

In the next stages of research, we aim to identify new unrecovered waste, which has a good energy content and which, in mixtures with biomass with high calorific value, can be recovered as fuel.

References

[1] Parlamentul European, Energia din surse regenerabile, Fișe descriptive despre Uniunea Europeană, disponibil la adresa: https://www.europarl.europa.eu/factsheets/ro/sheet/70/energia-din-surse-regenerabile, accesat: 15.03.2024.

[2] Parlamentul European și Consiliul Uniunii Europene, Directiva (UE) 2023/2413 a Parlamentului European și a Consiliului din 18 octombrie 2023 de modificare a Directivei (UE) 2018/2001, a Regulamentului (UE) 2018/1999 și a Directivei 98/70/CE în ceea ce privește promovarea energiei din surse regenerabile și de abrogare a Directivei (UE) 2015/652 a Consiliului, Seria L, 31.10.2023, disponibil la adresa: https://eur-lex.europa.eu/legal-content/RO/TXT/PDF/?uri=OJ:L_202302413, accesat: 15.03.2024.

[3] Parlamentul European, Fit for 55, https://www.europarl.europa.eu/factsheets/ro/sheet/70/energia-din-surse-regenerabile, accesat: 15.03.2024.

[4] Parlamentul European și Consiliul Uniunii Europene, Directiva (UE) 2023/2413 a Parlamentului European și a Consiliului din 18 octombrie 2023 de modificare a Directivei (UE) 2018/2001, a Regulamentului (UE) 2018/1999 și a Directivei 98/70/CE în ceea ce privește promovarea energiei

din surse regenerabile și de abrogare a Directivei (UE) 2015/652 a Consiliului, Seria L, 31.10.2023, disponibil la adresa: https://eur-lex.europa.eu/legal-content/RO/TXT/PDF/?uri=OJ:L_202302413, accesat: 15.03.2024.

[5] Comisia Europeana, Ghid privind utilizarea în cascadă a biomasei, cu o selecție de exemple de bune practici în materie de biomasă lemnoasă, Oficiul pentru Publicații al Uniunii Europene, 2019.

[6] European Commission, The European Commission`s Knowledge Centre for Bioeconomy, Oficiul pentru Publicații al Uniunii Europene, 2019.

[7] R. Effendi, Bangsawan, I.; Maryani, R.; Justianto, A. Development of wood pellets processing industry for renewable energy. IOP Conf. Ser. Earth Environ. Sci. 2020, 487, 012014

[8] J. Bogner, Abdelrafie Ahmed, M.; Diaz, C.; Faaij, A.; Gao, Q.; Hashimoto, S.; Mareckova, K.; Pipatti, R.; Zhang, T. Waste Management, in Climate Change 2007: Mitigation. Contribution of Working Group III to the Fourth Assessment Report of the Intergovernmental Panel on Climate Change; Cambridge University Press: Cambridge, UK; New York, NY, USA, 20

[9] Bikfalvi Martin "The intelligent tree" Paulownia GreenE Romania 2013.

[10] Angelov Boyan "Paulownia the tree of future" 2010 Velboy Ltd. Bulgaria.

[11] L.B. Magar, Khadka, S.; Joshi, J.R.R.; Pokharel, U.; Rana, N.; Thapa, P.; Sharma, K.R.S.R.; Khadka, U.; Marasini, B.P.; Parajuli, N. Total Biomass Carbon Sequestration Ability under the Changing Climatic Condition by Paulownia tomentosa Steud. Int. J. Appl. Sci. Biotechnol. 2018, 6, 220–226.

[12] P. Icka, Damo, R.; Icka, E. Paulownia tomentosa, a Fast Growing Timber. Ann. Valahia Univ. Targoviste Agric. 2016, 10, 14–19

[13] Akyildiz, M.H.; Kol Sahin, H. Some Technological Properties and Uses of Paulownia (Paulownia tomentosa Steud.) Wood. J. Environ. Biol. 2010, 31, 351–355.

[14] Joshi, N.R.; Karki, S.; Adhikari, M.D.; Udas, E.; Sherpa, S.; Karki, B.S.; Chettri, N.; Kotru, R.; Ning, W. Development of Allometric Equations for Paulownia tomentosa (Thunb) to Estimate Biomass and Carbon Stocks: An Assessment from the ICIMOD Knowledge Park, Godavari, Nepal; International Centre for Integrated Mountain Development: Kathmandu, Nepal, 2015.

[15] Pirro ICKA, Robert DAMO, Engjëllushe ICKA. PAULOWNIA TOMENTOSA, A FAST GROWING TIMBER.

[16] Madan Pal, Ashish K. Chaturvedi, Sunil K. Pandey, Rajiv N. Bahuguna, Sangeeta Khetarpal & Anjali Anand. Rising atmospheric CO2 may affect oil quality and seed yield of sunflower (Helianthus annus L.). Original Paper, 20 September 2014, Volume 36

[17] Zohreh Emami Bistgani, S.A. Siadat, M. Torabi, A. Bakhshande. Influence of plant density on light absorption and light extinction coefficient in sunflower cultivars. April 2012. Research on Crops 13(1):174-179.

[18] Miguel-Angel Perea-Moreno, .Francisco Manzano-Agugliaro, Alberto-Jesus Perea-Moreno. Sustainable Energy Based on Sunflower Seed Husk Boiler for Residential Buildings

[19] Mohammad reza Seifi, R. Alimardani. Moisture-Dependent Physical Properties of Sunflower (SHF8190).

[20] Hossain Zabed, Suely Akter, Junhua Yun, Guoyan Zhang, Mei Zhao, M. Mofijur, Mukesh Kumar Awasthi, M.A. Kalam, Xianghui Qi.Towards the sustainable conversion of corn stover into bioenergy and bioproducts through biochemical route: Technical, economic and strategic perspectives.

[21] Pierre-Luc Lizotte 1; Philippe Savoie; Alain De Champlain Ash Content and Calorific Energy of Corn Stover Components in Eastern Canada, Energies 2015, 8, 4827-4838;

[22] Hoffman, P.C. Ash Content of Forages; University of Wisconsin-Extension: Marshfield, WI, USA, 2005.

[23] Wright, C.L. Effect of harvest method on the nutrient composition of baled cornstalks. In 2005 South Dakota Beef Report; South Dakota State University: Brookings, SD, USA, 2005; pp. 46–47.

[24] Lizotte, P.-L.; Savoie, P. Spring harvest of corn stover. Appl. Eng. Agric. 2011, 27, 697–703.

[25] Lizotte, P.-L.; Savoie, P. Spring harvest of corn stover for animal bedding with a self-loading wagon. Appl. Eng. Agric. 2013, 29, 25–31.
[26] M. Mancini, Å. Rinnan, A. Pizzi, G. Toscano, Prediction of gross calorific value and ash content of woodchip samples by means of FT-NIR spectroscopy, Fuel Process. Technol. 169 (2018) 77–83, https://doi.org/10.1016/j.fuproc.2017.09.021.
[27] Determinarea puterii calorifice a combustibililor solizi si lichizi grei. Bomba calorimetrica. Laboratorul Politehinca Timisoara. Laboratorul de analize de combustibili, investigatii ecologice si dispersia noxelor. http://www.mediu.ro/index.php?pagina=masuratori_termotehnice1, accesat: 28.03.24.

A look at the large capacity shallow geothermal systems with heat pumps units in terms of optimal control

O privire asupra sistemelor geotermale de mică adâncime și de mare capacitate cu pompe de căldură, din punct de vedere al controlului optim

Răzvan –Silviu ȘTEFAN[1], Daniel CORNEA[1]
[1]Technical University of Civil Engineering of Bucharest, Romania
Lacul Tei Blvd, No 124

Email: razvan.stefan@eli-np.ro, danielcornea@hidraulica.utcb.ro

DOI: 10.37789/rjce.2025.16.1.7

ABSTRACT: Today, the best option - and only one that is feasible - for obtaining sustainable solutions for the responsible use of resources is to approach the energy efficiency of an HVAC system by recognizing and seizing the opportunities offered by automation and optimization seen as a whole, in close connection.

Key-words: geothermal system, heat pumps, sustainability

CONTEXT

The construction and commissioning of the ELI-NP's geothermal HVAC System provides a unique opportunity to study the possibilities to optimize of the high-capacity geothermal HVAC Systems by acquiring and capitalizing on the data available as a result of the operational monitoring and to perform mathematical modeling for high-capacity geothermal HVAC Systems.

The case study "Geothermal HVAC System installed at ELI-NP", through monitoring in time and in operation, will provide new information related to the behavior and performance of high-capacity geothermal HVAC systems, which can be exploited and can practically confirm the conclusions / results of the studies achieved so far.

The geothermal HVAC System with heat pumps units serving the ELI-NP research infrastructure is a complex, large-scale system, the largest in Europe, with an

The article was received on 05.06.2024, accepted on 24.02.2025 and published on 04.03.2025

The geothermal HVAC System with heat pumps units serving the ELI-NP research infrastructure is a complex, large-scale system, the largest in Europe, with an installed capacity of 6.2 MW (heating and cooling). Thus, it allows 1) the modeling of many processes, the creation of impact models that can be verified practically, and which will lead to familiarization with the response of high-capacity geothermal HVAC Systems, but also 2) the creation of studies and models for optimization / optimal control which contribute to energy efficiency.

Strictly for the ELI-NP case, the modeling will aim, in the end, to achieve an optimal distribution scheme of the heat transfer fluid and to get predictions in the medium and long term regarding efficiency, benefits and operating costs, impact on the environment.

The impact of automated control on optimized operation

In recent decades, many efforts have been made for the proper design and optimal sizing of geothermal HVAC Systems. At the same time, intensive research activities of HVAC systems have been carried out for several years, aiming at their operation and control with minimum energy consumption, but satisfying the quality and comfort conditions of the environment inside the buildings.

Control strategies can be classified into two categories, local control and optimal control respectively.

The areas addressed by the studies related to HVAC Systems are presented in the diagram in Fig. 1. It can be seen from the diagram that the share of studies associated with optimal control is still small compared to the research carried out in relation to the local control of the systems. This fact is due to the easier implementation of local control strategies and the inconveniences related to the difficulty of collecting a large amount of data needed in the case of optimal control strategies.

These efforts have led to the development of optimal control strategies to make operation more efficient while satisfying indoor thermal comfort requirements, to mitigate soil thermal imbalance (beneficial action for long-term operation) that equally pays attention to both control as well as optimization.

The optimal control of the HVAC systems aims to determine the optimal solution (mode of operation and reference values, also called "set-points") that minimizes the energy demand of the system (implicitly also the cost of operation), under the conditions that are respected indoor comfort parameters and taking into account the inherent and continuous change in indoor environmental requirements and outdoor conditions and in some cases even the characteristics of the HVAC System.

Efficiency is defined as minimizing energy usage while keeping the operational parameters at the required levels. Such an approach is currently known as intelligent building operation and control.

In the last two decades, efforts to develop optimal monitoring and control strategies for HVAC Systems in buildings have intensified, given that modern buildings are now equipped with complete automation systems that allow this. These efforts have materialized in numerous studies and researches added to the specialized literature, which anticipate and even demonstrate that significant reductions in the energy consumption of HVAC Systems can be achieved, even with small increases in operating efficiency.

However, many of the optimal control strategies developed so far have not been implemented due to certain impediments, such as the need to use a complex mathematical apparatus, the reduced possibilities of generalization caused by the constraints imposed by the particularities of each practical application, etc. In practice, the proper, high-energy-efficiency operation of HVAC Systems is a difficult engineering task, both for designers and in their operation.

The following are specified as effects of the automated control:

- Reducing energy costs

Automation and optimization make it possible to operate mechanical systems at maximum efficiency.

- Equipment can be programmed to operate only when required and will therefore generate only the required load at any time.
- The level of control for the construction itself and for all related systems is high.
- Provides automatic detection of the HVAC System failure.
- Provides control over occupant actions.
- Facilitates reporting of equipment performance and problems encountered during operation.
- Creates the possibility of readjusting the parameters with the change of working conditions.
- Ensures knowledge of the long-term operation pattern of the installation, under different operating conditions
- Sophisticated graphic interfaces of the automatic control applications allow the creation, preservation, ranking of the construction documentation of the building with the possibility of easy access to the data of interest.
- Plants require less maintenance, resulting in lower maintenance costs.

- Makes it possible to reduce labor costs through remote monitoring and troubleshooting.
- Modern automated control systems (especially digital ones) are programmable; if a building's needs change, the system can be reprogrammed to meet the new requirements.

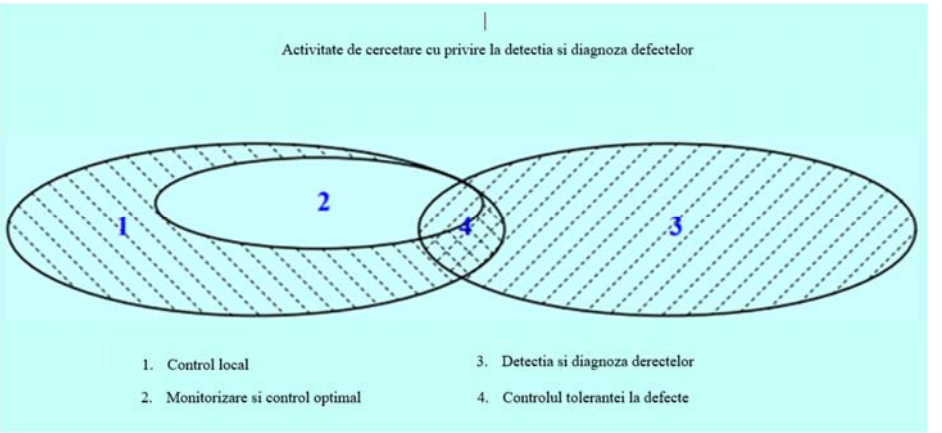

Fig. 1. Studies and research related to the field of control of HVAC systems

The DDC control System at ELI-NP

The Shallow GSHP System at ELI-NP is unique due to its size and technical requirements.

The constraints considered in the design and implementation of the GSHP System at ELI-NP are reviewed here:

- the precise humidity control requirements in many of the laboratories, low temperature and relative humidity being required
- the high air change rates requirements
- multiple operating conditions
- the pressurization requirements
- the limited options to use the energy recovery strategies, in order to avoid the cross-contamination
- the difficulty to anticipate the equipment thermal loads and exhaust requirements
- the high energy consumption of the process and of the research equipment

The system, as described below, is designed to ensure the required air change rates at the optimum energy consumption.

The installation of the Shallow GSHP System at ELI-NP was an important step towards responsible use of the environment. The optimization labels the step taken to rational use of resources.

Optimizing the operation of large consumers brings significant energy savings. Identifying and implementing efficient and inexpensive optimization techniques can bring great benefits to the society, especially in the long run.

Testing integrated optimization techniques for large Shallow GSHP systems is an innovation in itself, and it adds value to the existing ELI-NP Shallow GSHP System. Furthermore, the future results could contribute to the development of optimization criteria for Large Shallow Geothermal Systems.

The geothermal HVAC system installed at ELI-NP is monitored and controlled through the Digital Direct Control (DDC) automation system. Thus, temperature and humidity are continuously monitored, recorded and adjusted, with the information being transmitted in real time to the Building Management System (BMS), which monitors all building systems.

The parameters that should be maintained in research laboratories at ELI-NP are as follows:

- temperature in the Laser room 22 +/- 0.5 ^{o}C
- the temperature in some Laboratories 20 +/- 0.5 ^{o} C
- relative humidity in the Laser room and Laboratories 35-50%, without condensation
- overpressure in the Laser room and Laboratories 40 Pa
- cleanliness class in the Laser room ISO7
- cleanliness class in Laboratories ISO6, ISO7
- and negative pressure of 14 Pa in some laboratories

Preserving the stability of the parameters is the first priority considered in operation of the HVAC System installed at ELI-NP. The energy efficiency is of major importance, considering the high energy consumption involved in the research activity carried out in the ELI-NP research infrastructure.

The two high-power lasers operate in an ISO 7 clean room with an area of approximately 2,500 m^2.

The high hourly air rate change, the overpressure conditions and the requirements of strict control of temperature and relative humidity, as well as the limited options of using energy recovery strategies, lead to a very high energy requirement.

The monitoring and control system of the HVAC System installed at ELI-NP infrastructure monitors all buildings, is similar to a SCADA system and performs the following functions:

- collects all parameter values from the geothermal HVAC System controllers
- allows displaying the values of the parameters read by the sensors installed in the system
- records all parameter values on the server dedicated to data acquisition, in order to create and visualize their time variation graphs

The proposed DDC system is structured according to a system logic of data acquisition, processing and distributed control, based on application programs resident in the controllers' memory, with the possibility of transmission and communication with a central DDC server connected to the intranet network of the BMS system or remotely using TCP/IP communication over the Internet.

The DDC system allows:

- real-time recording of the parameters of interest (temperature and relative humidity of the air introduced), through the sensors located in the piping
- adjusting the values of these parameters to the reference values required by the process
- data storage and development curves for different periods

In the LASER room real-time temperature and relative humidity are recorded inside the duct as well as in the vicinity of the research equipment, at various points of interest.

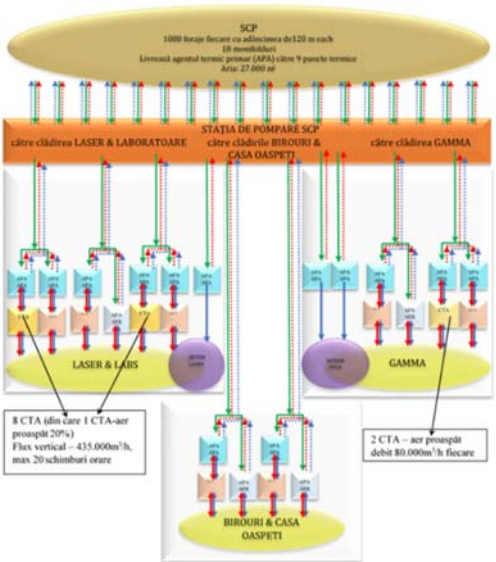

Fig. 2. The Shallow geothermal System in operation at ELI-NP

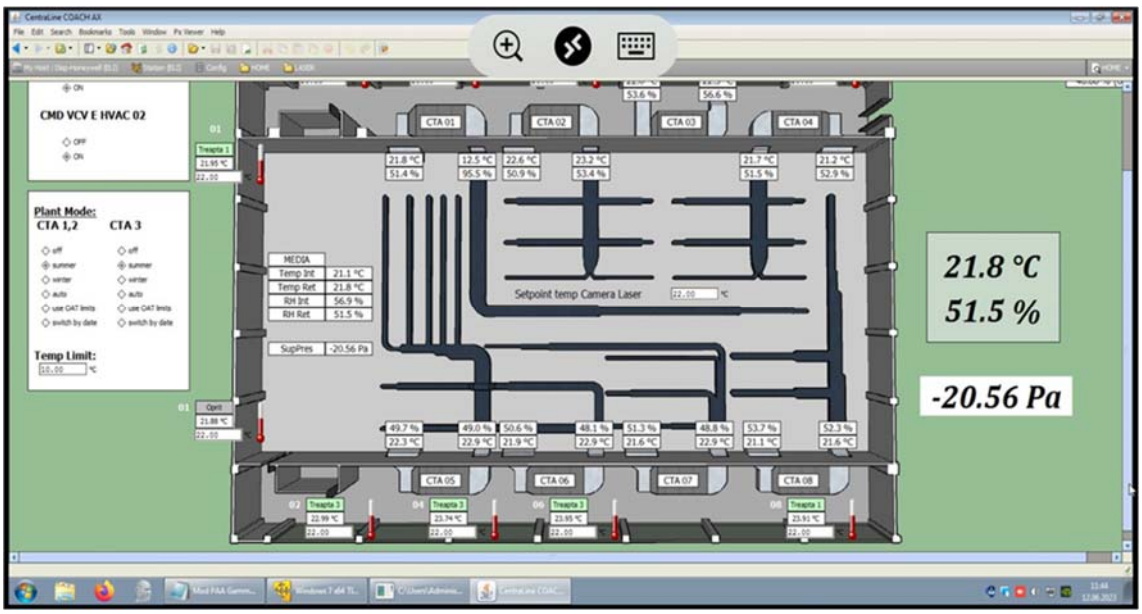

Fig. 3. DDC Screen

Aspects of optimal control and operation of large scale shallow geothermal HVAC Systems

Optimization makes sense in conjunction with the system automation. These, viewed as a whole, in close connection, represent today the best option for obtaining sustainable solutions for the responsible use of resources.

The effects of the operation and automatic control of buildings lead to the reduction of the impact on the environment as well as the reduction of the carbon footprint for buildings in the industrial area considered to be the main vector of impact on the environment.

By capitalizing on the data obtained from the monitoring and exploitation of the high-capacity geothermal HVAC system with heat pumps installed at ELI-NP, together with the related automatic DDC system, the sustainability of geothermal energy as an alternative for high energy efficiency can be practically tested. Compared to similar infrastructures, the ELI-NP research infrastructure has a high energy efficiency, the calculated HVAC system performance coefficients are currently low, but an improvement is expected following the completion and implementation of the ongoing optimization strategy.

Given that there is a worldwide concern to study the energy consumption of infrastructures and research laboratories, the ELI-NP case study can provide information on the reduction of energy consumption due to the use of the HVAC geothermal system with heat pumps.

Together with the multitude of tools / software applications currently in existence, the ELI-NP system allows the creation of several models that can bring new data on the behavior and impact of geothermal heat pump systems. The aim is to evaluate the future performance and optimization of the geothermal system from ELI-NP, itself, but also to use the models for the realization of other similar systems.

From the point of view of the optimization of systems that use closed-loop heat pumps, the main aspects to be followed are those related to the energy efficiency of the pumping stations, also the hydraulic balancing of the system both on the primary circuit and on the secondary circuit.

Studies have been performed to follow these aspects from the perspective of the user of systems. There are similarities with the geothermal system in operation at ELI-NP (i.e. similar usage graphs) but also differences from the current operating situation of the ELI-NP infrastructure in that the thermal parameters of the respective facilities do not require such restrictive operating conditions as in the case of ELI-NP. As a result, the entire operating schedule of the ELI-NP infrastructure will have to be adapted according to operational requirements that take precedence over energy saving requirements.

Having as a starting point the continuous operation of the hydraulic circuits of the primary loop, any operation strategy should consider the reduction of energy consumption by modulating the two control parameters of such a system: flow rate of the heat transfer fluid, respectively the temperature on the primary loop.

The positive effects of the modulation of the flow rate of the heat transfer fluid through the use of variable speed pumping systems, without touching the subject of the conjugate modulation of both the heat transfer fluid flow and the loop temperature. A future research direction involves the simultaneous use as reference parameters of the coolant flow rate and the temperature on the primary loop by using mixing valves mounted on such closed systems. Also, within the ELI-NP infrastructure, out of the desire to increase the system's performance coefficient, a landmark area is used for which the mixing of the heat transfer fluid from the primary loop with the secondary related to the technological cooling circuits was adopted.

So far, the outcomes have been impacted by the primary loop control circuits' ability to detect the parasitic injection of certain flows incident to the primary loop without allowing the system to redefine a control structure to take that combination into account. A second line of research follows from this, involving the installation of field equipment that would be able to give the system simultaneous control capability in terms of both quantitative (heat transfer fluid flow) and qualitative (control temperature on each individual loop).

The control strategy performed was validated by the results obtained during the seven years of operation of the system installed at ELI-NP, generating an insignificant impact on the groundwater temperature. This result leads to the premise that the operation of this system will be possible in nominal load conditions over a period of more than 20 years as thermal response tests in the design phase indicated.

To save energy, any intervention in the operation strategy must be carried out taking into account the fact that the energy source in this case involves an instability factor generated by the geothermal potential, unlike the stability of conventional energy sources (boiler and chiller).

Bibliography

1] *Răzvan Silviu-Ștefan; Contributions to the improvement of the energy efficiency of heating fluid supply circuits in a shallow geothermal system with large capacity, Doctoral thesis, UTCB, Bucharest, 2024*

2] *Z. Ma, „Online Supervisory and Optimal Control of Complex Building Central Chilling Systems. A thesis submitted in partial fulfillment of the requirements for the Degree of Doctor of Philosophy," The Hong Kong Polytechnic University, April, 2008*

Waste heat energy recovery from an electrostatic painting line

Recuperarea energiei termice reziduale de la o linie de vopsire în câmp electrostatic

Diana-Patricia Ţucu[1], Florian-Tamás Negruţ[1]

[1] University Politehnica Timisoara
Victoriei Square, no. 2, Timisoara, Romania
E-mail: diana.tucu@student.upt.ro, florian.tamas@student.upt.ro

Coordinator: Daniel Bisorca

E-mail: daniel.bisorca@upt.ro

DOI: 10.37789/rjce.2025.16.1.8

Abstract. *The paper presents a case study regarding the feasibility of implementing a waste heat recovery system from combustion gases emitted by an electrostatic painting line. Our proposed recovery system aims to bring two main benefits: from an economical point of view, we want to decrease the costs of gas consumption for heating domestic hot water; from a climate and air pollution standpoint, we aim to considerably reduce the amount of combustion gases dumped into the environment, thereby diminishing the greenhouse effect.*

Key words: waste heat recovery, combustion gas, domestic water heating

1. Introduction

The 2413/2023 European Directive established the objective of climate neutrality in the Union by 2050 and an intermediate target of a reduction of net greenhouse gas emissions by at least 55 % compared to 1990 levels by 2030.[1] Nowadays, a lot of industrial waste heat is generated daily in different industrial processes without being put in practical use, causing two main disadvantages: rising concern regarding global warming (by producing greenhouse gas emissions) and wasting energy that could be harnessed rather than dumped into the environment. Therefore, we propose to study how the energy potential from the waste gases emitted into the atmosphere from the components of the electrostatic field painting line can be exploited for energy purposes

[1] Directive (EU) 2023/2413 of the European Parliament and of the Council,18 October 2023

The article was received on 30.03.2024, accepted on 11.02.2025 and published on 14.03.2025

using heat exchangers on the hot exhaust circuit. The recuperated heat will be used for heating cold water, in order to have an adequate supply for the factory`s showers.
Our feasibility study concerns the assembly of painting booths of a local company, situated in the city of Timisoara. S.C. AMBASADOR PLUS S.R.L. is a Romanian, privately owned company, established in 1994, whose main activity is the production and marketing under the brand "ELTIM" of a wide range of heating systems. These include different types of boilers, furnaces, heat exchangers, heat recovery systems and hydrophores, that are being produced since 1957.[2] Since 2021, the company is using an electrostatic painting line, composed of: degreasing cabin, washing booth, drying booth, powder spraying booth, polymerization oven and distiller.

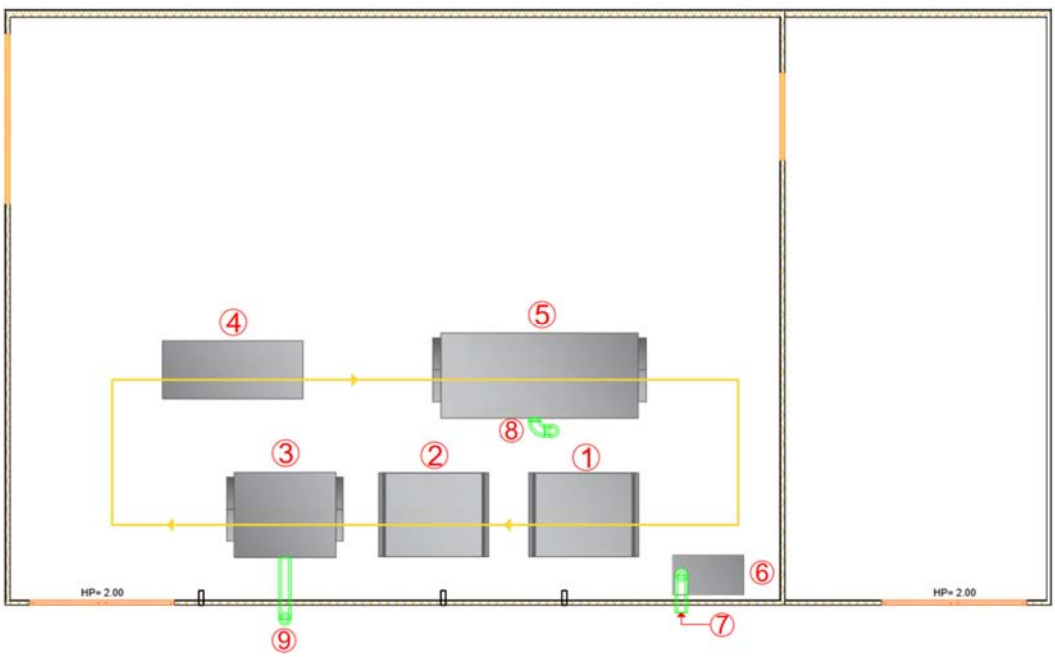

Fig.1. Position of the equipment in the painting hall
1-degreasing cabin; 2-washing booth; 3-drying booth; 4-powder spraying booth; 5-polymerization oven; 6-distiller; 7-chimney for evacuating combustion gases from the distiller; 8- chimney for evacuating combustion gases from the polymerization oven; 9- chimney for evacuating combustion gases from the drying booth, D=150

The technological units of the painting line are working simultaneously, in the following order: The painting process starts in the degreasing cabin (1), where the components are degreased from oils and greases. Further on, they are transported on the conveyor belt (yellow), located above the technological units, to the washing booth (2). After that, the pre-treated components are dried in the drying booth (3) before being painted. Inside the booth the operating temperature is 150 degrees Celsius and the

[2] https://www.eltim.ro/info/25/Eltim---cazane-de-baie-cazane-de-incalzire-centrala-boilere-electrice-boilere-termice.html

intense air movement required for drying is provided by 2 circulating fans. After drying, the components are transported to the powder spraying booth (4) and further to the polymerization oven (5), where the painted objects are dried at a temperature of 190°C. The distiller (7) has the role of ensuring evaporation of wastewater generated during the process, condensation and reuse of vapours during heating and selection of the generated sludge.

In the first phase, we aim to recover the heat from the combustion gases present in the chimneys of the drying booth and distiller. Both the drying booth and the distiller are equipped with chimneys with a diameter of 150 mm for evacuating the hot combustion gases formed as a result of the processes carried out in the equipment.
For designing and dimensioning our heat recovery solution we determined the heat recovery potential, starting with an energy audit. Since the factory has only one general gas metre, with no individual metres for the painting equipment, we had to analyse the company's gas bills and interpret the values, bearing in mind that the gas is used for the painting line, central heating and also for warm water, thus the gas consumption increases significantly in the colder months. With this in mind, we estimated an average warm season consumption of 300 m^3 /month (From May to October).

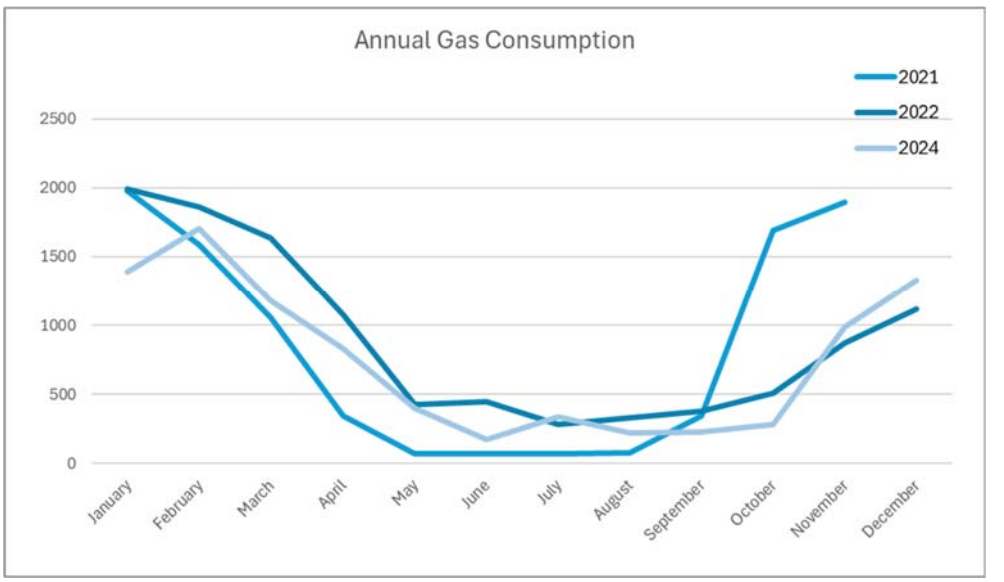

Fig. 2. The annual gas consumption of the company

According to the technical files of the products, the burners' maximum flow rate is 4.5 m^3 /h. By analysing and filtering the information, we have reached the following estimation: Out of the average summer consumption, 50 m^3 are used for heating the water and the rest is used by the 3 painting equipments (84 m^3/ equipment is used to assure the painting process).

2.The proposed heat recovery system

For the first phase of the recovery system, we plan to put the heat exchangers on the 2 machines that have the exhaust chimney (1) on the same wall: the drying booth and the distiller. To assure safe and uninterrupted exploitation of the machines, we decided on 3 in series heat exchangers (3), controlled with valves (2), with the following functional scenarios:

1. Normal heat recovery

In this scenario, the valve status is the following:

- V1.1, V1.3, V2.1 and V2.3 are open
- V1.2, V2.2, V3.1 and V3.2 are closed

Each chimney has its own tubular heat exchanger for improved thermal energy recovery. Valves V3.1 and V3.2 are meant to separate the two exhaust chimneys, so that they do not influence each other's flow. The water from the accumulation tank (5) is being circulated through the exchangers, entering at the top cold and exiting at the bottom warm, returning to the hot water accumulation tank.

2. Overheating protection / Malfunctioning mode

This mode assures continuity and safe operation of the painting line. In case of overheating or malfunctions detected at one of the heat exchangers, the appropriate valves will isolate the malfunctioning heat exchanger(s). For example, if the water in the first heat exchanger were to overheat, valve V1.3 would close and valve V3.1 would open, ensuring the continuation of energy recovery. If the water accumulated in the tank reaches the set maximum temperature, then valves V1.1 and V2.1 will close and valves V1.2 and V2.2 will open.

3. Service mode

This mode can isolate the individual heat exchangers for maintenance purposes or by-pass completely the recovery system, by opening and closing the right combination valves.

The recovery of thermal energy starts with circulating the cold water from the accumulation tank (5) with the help of a circulation pump (4). The cold water enters at the top part of each heat exchanger and exits at the bottom, with an increased temperature. We chose a heat exchanger with countercurrent flow for improved energy transfer between the 2 fluids. The hot water resulted after the recovery process will be stored in an accumulation tank, at a high temperature (70-75°C). From here it will be used as the primary agent in one of the coils of a 2coil boiler for domestic hot water. The other coil, placed at the upper end of the boiler, will be reserved for a backup system, such as a gas water heater (CT).

With the described waste heat recovery system we aim to design the heat exchangers so that we can value around 50% of the useful energy of the exhaust gases. Preliminary calculations have shown that the 2 painting equipments can assure the necessary heat for the showers that take place daily in the factory. By also recovering the waste heat from the polymerization oven we can help reduce the load on the central heating system in the cold months.

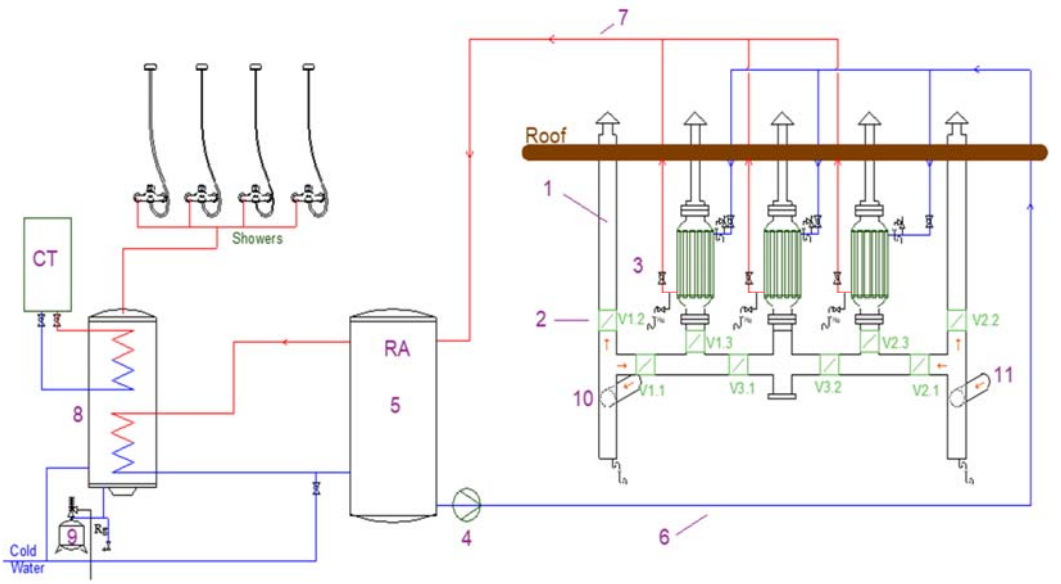

Fig 3. The functional scheme of the proposed heat recovery system
1-exhaust chimney, 2-control valves, 3-heat exchanger, 4-water pump, 5-thermal energy accumulation tank, 6-cold water, 7-hot water, 8-2 coil boiler, 9-expansion tank, 10-polymerization oven exhaust pipe, 11-distiller exhaust pipe, CT- gas water heater

3. Cost-benefit analysis

At the end of each workday, around 10 workers in the factory take showers. Estimating a consumption of 35 litres/person of warm water, we can deduce a 400 litres per day consumption (including warm water use during the day for activities like hand washing).

To prepare the hot water needed for the showers the factory uses 18.4 kW per day from burning natural gas. Bearing in mind this consumption and the efficiency of the gas water heater, the annual energy consumption for heating water is 4700 kW; this equals, at the beginning of 2024, when the gas prices are still being capped by the government, to about 4150 RON (835 EUR).

In Table 1 there are presented the results of investment calculation for our proposed heat recovery system, resulting in a total cost of 8000 Euros.

Taking into consideration the approximate value of the investment and the yearly savings made by the system we can observe that the company will recover its investment after less than 10 years. Furthermore, the company will reduce its carbon footprint by just consuming less natural gas.

Table 1

Calculation of the investment

Product	Qty	Unit	Price/Unit [EUR]	Total [EUR]
Flue gas valve 150mm	9	pcs	12	108
Heat recovery system (only cost of materials)	3	pcs	70	210
Accumulation Tank 2mc	1	pcs	300	300

Calculation of the investment

Water pumps	2	pcs	150	300
2 Coil Boiler (only cost of materials)	1	pcs	260	260
Water circulation pipes	35	m	8	280
Flue gas channel	8	m	70	560
Expansion Tank (only cost of materials)	1	pcs	30	30
Drain valve	4	pcs	6	24
Isolating valve	11	pcs	6	66
Safety valve	9	pcs	10	90
T Section with access panel	1	pcs	65	65
Condensate drain trap	2	pcs	40	80
Technical room 8m^2 (modular container)	1	pcs	1500	1500
Energy Meter	2	pcs	55	110
Thermal Energy Meter	2	pcs	155	310
Electrical Installation	[-]	[-]	1100	1100
Pipe Insulation	35	m	6	210
Connections to the water supply network	[-]	[-]	500	500
Automation system	[-]	[-]	600	600
Engineering Cost	[-]	[-]	500	500
Total cost				7203
TOTAL (including unpredictable costs)				8000

4.Conclusions

The paper shows how to increase the energy efficiency of a company by using the waste energy potential of the facility. The paper presents both the conceptual solution for the implementation of the waste energy recovery installation and its use to cover the domestic hot water needs as well as the synthetic way to carry out a cost-benefit analysis to help the beneficiary in making a decision to promote the investment. The implementation of the work will contribute to the reduction of CO2 emissions into the atmosphere and implicitly to the EU objective of reducing greenhouse gas emissions by 55% by 2030.

References

[1] ***, Directive (EU) 2023/2413 of the European Parliament and of the Council,18 October 2023.
[2] ***, Eltim - cazane de baie, cazane de incalzire centrala, boilere electrice, boilere termice, Available: https://www.eltim.ro/info/25/Eltim---cazane-de-baie-cazane-de-incalzire-centrala-boilere-electrice-boilere-termice.html, Accessed at: March 2024.
[3] I. Ionel, C. Ungureanu, D. Bisorca, “Termoenergetica si mediul”-Editie revizuită, Editura Politehnica Timisoara, 2006.

Air conditioning system with ice-slurry: theory, simulation and validation

Sistem de aer condiționat cu gheață-slurry: teorie, simulare și validare

Emil Iakabos[1], Florea Chiriac[1], Anica Ilie[1], Alina Girip[1] and Madalina Teodora Nichita[1]

[1] Department of Thermodynamic Sciences, Faculty of Building Services,
Technical University of Civil Engineering Bucharest,
66 Pache Protopopescu Blvd., 020396 Bucharest, Romania

e-mail: *office@eebc.ro, florin_chiriac2001@yahoo.com, ilie.anica@utcb.ro, alina.girip@utcb.ro, madalina.nichita@utcb.ro*

DOI: 10.37789/rjce.2025.16.1.9

Abstract: The acceleration of global climate change, along with its adverse effects on the sustainability of the built environment, is closely linked to rising greenhouse gas emissions and energy consumption. The construction sector, as one of the largest energy consumers, accounts for nearly 40% of total energy usage and carbon dioxide emissions, with heating, ventilation, and air conditioning (HVAC) systems contributing a significant share. Consequently, the development of sustainable materials to enhance the energy efficiency of HVAC systems is critical.

Ice cooling, though ancient in origin-dating back 5,000 years to the use of ice blocks for food preservation-offers modern opportunities for sustainable cooling solutions. With dwindling natural resources and a growing emphasis on environmentally friendly technologies, there is renewed interest in cooling methods that maximize performance while minimizing ecological impact.

This paper presents a detailed analysis of water-ice air conditioning systems, discussing their theoretical principles, mathematical models for heat transfer, numerical simulations applied to a hypothetical case, and validation through experimental and theoretical data. Simulations and calculations for a water-ice mixture air conditioning system demonstrate its capability to effectively cool large areas for extended periods, significantly reducing energy consumption. The validation of results confirms that this system is well-founded and represents a viable solution for commercial and industrial buildings requiring efficient and environmentally friendly climate control.

Key-words: climate, greenhouse, HVAC

1. Introduction

The increasing demand for environmentally friendly and energy-efficient solutions in the field of refrigeration and air conditioning has led to the development of

The article was received on 03.02.2025, accepted on 24.02.2025 and published on 14.03.2025

innovative technologies [1]. Among them, water-ice air conditioning systems have gained attention due to their excellent heat transfer properties and efficiency compared to conventional systems using classic refrigerants[2]. Water-ice is a mixture of fine ice particles suspended in a liquid solution (generally water or water with glycol), capable of transporting a significant amount of cold through the latent heat of melting of the ice.

Recent studies underscore the cost-effectiveness of water-ice combinations, attracting the interest of prominent producers in comfort, commercial, and technology cooling systems. Yau [3] used the Transient Systems Simulation Program to assess air conditions and energy consumption in a typical library situated in a tropical region, both with and without an ice slurry-cooling coil. He suggested incorporating ice slurry-cooling coils into HVAC systems in such settings to improve energy efficiency and dehumidification. Kalaiselvam [4].performed numerical analysis on the thermal transfer and pressure drop characteristics of a tube-fin heat exchanger inside an ice slurry HVAC system. The research, which examined a slurry including 14% ice fraction, 16% ethylene glycol, and 70% water by volume, determined that the system achieved a 7.4% enhanced temperature decrease relative to traditional chilled water systems, attributable to the latent heat absorption of the ice slurry during melting. Padang [5] examined drag reduction by circulating ice slurry via a spiral tube, altering the ice percentage from 3% to 21%. The findings indicated a significant decrease in drag (32% at 6% ice percentage), resulting in enhanced flow velocities inside the spiral pipes.

This paper presents a detailed analysis of water-ice air conditioning systems, discussing the theoretical principles, mathematical models for heat transfer, a numerical simulation applied to a hypothetical case, and a validation by experimental and theoretical data.

2. The operating principle of the ice water mixture air conditioning system

2.1 Ice-slurry system description

The ice-slurry air conditioning system is composed of several essential parts, each playing a role in the cooling process:

- Water-ice mixture generator: Produces suspension of finely divided ice particles in liquid. This can be a solution of water and glycol, to prevent complete freezing at low temperatures.
- Storage tank: Stores the ice-water mixture suspension until distribution to points of use is required
- Distribution system: The pipes and pumps that transport the water-ice mixture suspension to different areas of the building or industrial equipment for cooling.
- Heat exchangers: Transfer heat from the space to be cooled to the water-ice mixture suspension, partially melting the ice particles and ensuring efficient cooling.

The block diagram below shows the general flow of operations of a water-ice air conditioning system:

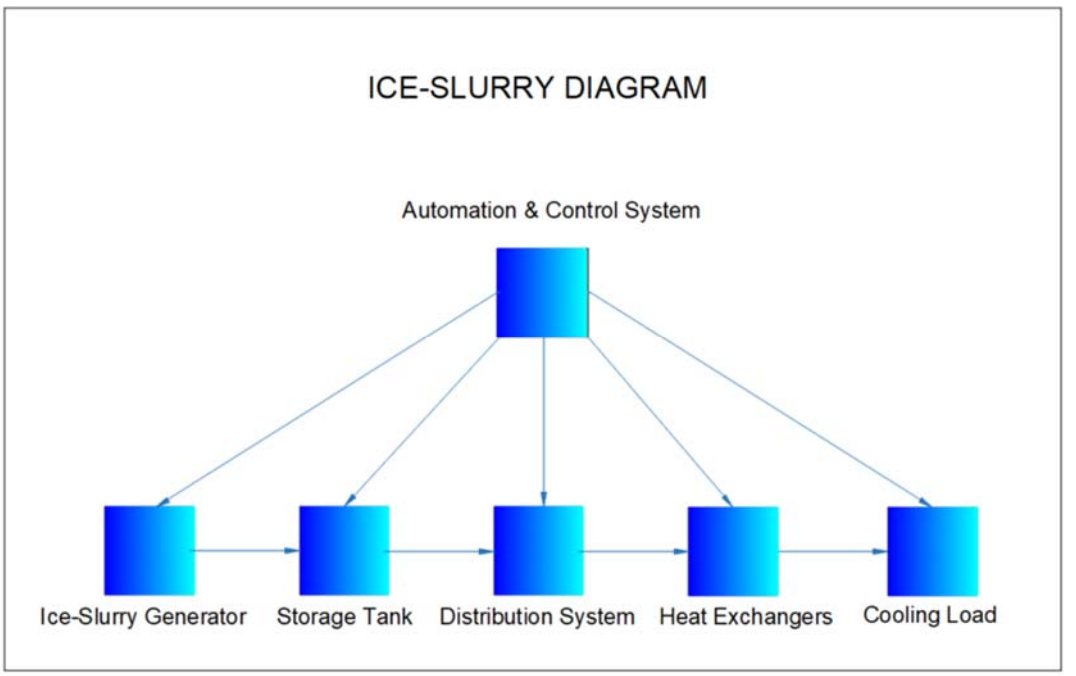

2.2 Cooling process

The air conditioning system works by taking heat from the cooled environment and transferring it to the water-ice mixture suspension. The main property that makes the water-ice mixture efficient is the use of the latent heat of melting of the ice particles. Thus, even when the ice particles begin to melt, the temperature of the suspension remains constant, ensuring a constant and efficient heat transfer.

The basic formula for calculating the energy absorbed by the ice-water mixture during the cooling process is:

$$Q_{latent}=m_{ice}\cdot L_f$$

Where:

- m_{ice} - is the ice weight (kg),
- L_f - is the latent heat of melting of ice (334 kJ/kg).

Also, the energy absorbed by the liquid in the suspension is described by the formula::

$$Q_{sensitive}=m_{liq}\cdot cp\cdot \Delta T$$

Where:

- m_{liq} - is the liquid weight (kg),
- c_p - is the specific heat capacity of the solution (4.18 kJ/kg·°C for water),
- ΔT - is the temperature difference between inlet and outlet (°C).

3. Mathematical models and thermodynamic equations

3.1 Heat transfer in the water-ice mixture system

Heat transfer through the heat exchangers in air conditioning system using ice-water is achieved by both convection and phase change as the ice particles melt. To

maximize the efficiency of the system, the ice mass and the proportion of ice in suspension are adjusted according to the cooling needs.

The total heat flux Q transferred through the heat exchanger can be expressed by the equation:

$$Q=U\cdot A\cdot \Delta Tm$$

Where:

- U - is the global heat transfer coefficient ($W/m^2\cdot °C$),
- A - is the area of the heat exchanger (m^2),
- ΔTm - is the logarithmic average temperature difference between the fluid and the cooled environment (°C).

3.2 Calculation of the mass of the water-ice mixture

For a commercial space with a cooling requirement of 100 kW and an operating time of 10 hours, we can calculate the mass of water-ice mixture required using the following relationship:

Q_{total} = Cooling power ×operating time

Qtotal=100 kW×10 hours=100 kW×36000 s=3.6×106 kJ

Q_{total}=100kW×10hours=100kW×36000s=3.6×106kJ

Assuming that the fraction of melted ice is 50%, and that ΔT is 10°C, the formula for the required mass of water-ice mixture becomes:

$m_{ice}=Q_{total}(cp\cdot \Delta T+Lf\cdot 0.5)$

Substituting values:

$m_{ice}=3.6\times 106(4.18\cdot 10+334\cdot 0.5) \Longrightarrow m_{ice}=3.6*106*208.8\approx 17{,}240$ kg

Thus, to cool the space during the 10 hours, approximately 17,240 kg of water-ice mixture are required.

4. Numerical simulation

4.1 The simulated scenario

The numerical simulation was performed for a 1000 m^2 commercial space, with a cooling requirement of 100 kW and an operating time of 10 hours. The simulated parameters included:

• Inlet water-ice mixture: 0°C, with 30% ice and 70% water/glycol solution.

• Initial space temperature: 28°C.

• Desired final temperature: 22°C.

• Flow rate of water-ice mixture: 1.5 kg/s.

4.2 Simulation results

After running the numerical simulation, the following results were obtained:

• Maximum cooling power: 105 kW.

• Total cooling time: 7.5 hours to reach the target temperature of 22°C.

• Energy consumption: The system consumed approximately 1667 kWh to cool the space over a period of 10 hours, which represents a 40% higher energy efficiency compared to traditional systems.

4.3 Temperature vs. time graph

The graph obtained from the simulation shows (Fig. 1) a uniform decrease in temperature over the 7.5 hours, confirming the efficiency of heat transfer through the water-ice mixture and the system's ability to maintain a constant temperature by using the latent heat of fusion.

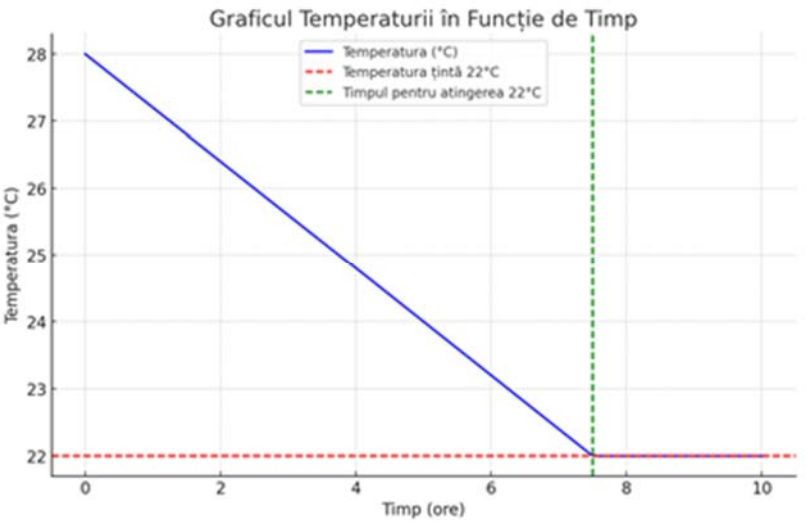

Fig. 1 graph obtained from the simulation

5. Validation of results

5.1 Validation through experimental data

To validate the simulation results, a study by Xie et al. [6] was used, which investigated the performance of a water-ice air conditioning system in a commercial environment. The study showed that a 120 kW system with a 25% ice water-ice suspension exhibited similar cooling capacity to that obtained in our simulation.

5.2 Theoretical validation

The analytical solution for the calculation of the mass of the water-ice mixture and the heat flux was compared with the simulation results. The basic formula for the required mass of the water-ice mixture was confirmed by theoretical solutions, with a deviation of 5%, which is acceptable in the context of thermodynamic calculations.

6. Advantages and limitations of the system

Advantages

• High energy efficiency: Water-ice mixing systems utilize latent heat of fusion, reducing energy consumption.

• Low environmental impact: Does not require traditional refrigerants, reducing the carbon footprint.

• Cold storage capacity: The system can store cold during periods of low demand.

Limitations

• Technical complexity: Production and maintenance of water-ice mixing plants can be expensive.

• Need for optimization: Systems must be well sized to avoid oversizing pipes and heat exchangers.

7. Conclusions

Simulations and calculations for a water-ice air conditioning system show that it can effectively cool large spaces over long periods, significantly reducing energy consumption. Validation of the results demonstrates that this system is well-founded and represents a viable solution for commercial and industrial buildings that require efficient and environmentally friendly air conditioning..

References

1. Arenas-Larrañaga, M., et al., *Performance of solar-ice slurry systems for residential buildings in European climates.* Energy and Buildings, 2024. **307**: p. 113965.
2. Dumitrescu, R., A. Ilie, and F. Chiriac, *Experimental comparative research on ice-slurry vs. cooled water in comfort air-conditionig systems* 2009.
3. Yau, Y.H. and S.K. Lee, *Feasibility study of an ice slurry-cooling coil for HVAC and R systems in a tropical building.* Applied Energy, 2010. **87**(8): p. 2699-2711.
4. Kalaiselvam, S., P. Karthik, and S. Ranjit Prakash, *Numerical investigation of heat transfer and pressure drop characteristics of tube-fin heat exchangers in ice slurry HVAC system.* Applied Thermal Engineering, 2009. **29**(8-9): p. 1831-1839.
5. Padang, M.U. *Experimental investigation of ice slurry rheology on spiral pipes with glycol for HVAC in fish vessel.* in *AIP Conference Proceedings*. 2020.
6. Liang, Y., et al. *Experimental investigation on the energy and economic performance of an ice-slurry-based dynamic ice storage system.* in *Healthy Buildings 2023: Asia and Pacific Rim*. 2023.

Heating systems using heat pump thermal adjustment

Sisteme de încălzire care utilizează reglajul termic al pompei de căldură

Florin IORDACHE[1], Mugurel TALPIGA[1]

[1] Technical University of Cvil Engineering Bucharest
Bd. Lacul Tei nr. 122 - 124, cod 020396, Sector 2, Bucharest, Romania

E-mail: fliord@yahoo.com, talpiga.mugurel@gmail.com

DOI: 10.37789/rjce.2024.16.1.10

Abstract: The objective of the work is an analysis of the adjustment performed on the electric power absorbed by the heat pump to ensure the thermal regulation of the central heating installation. The situation in which the heat pump is the only source that supplies the heating system was considered. The heat pump must therefore be sized to have the capacity to cover the consumer's calculated heating needs. It is presented in the work the importance of the dimensioning principle of the heating system: high temperature, medium temperature, and low temperature heating systems. The importance of the climatic zone on the capacity of the heat pump is also required.

Cuvinte cheie: pompă de căldură, reglaj termic

Rezumat: Lucrarea are ca obiectiv o analiza asupra reglajului efectuat asupra puterii electrice absorbite de pompa de caldura pentru asigurarea reglajului termic al instalatiei de incalzire centrala. S-a considerat situatia in care pompa de caldura este singura sursa care alimenteaza instalatia de incalzire. Pompa de caldura, se impune in consecinta sa fie dimensionata a avea capacitatea de a acoperii necesarul de incalzire de calcul al consumatorului. Se prezinta in cadrul lucrarii Importanta pincipiului de dimensionare al instalatiei de incalzire : instalatie de temperatura ridicata, temperatura medie si temperatura joasa. Se remerca si importanta zonei climatice asupra capacitatii pompei de caldura.

Key-words: heat pump, thermal adjustment

Introduction

The heat pump can be a source of thermal energy for a central heating system or/and for a domestic hot water preparation system. If it is the only source of energy for the building's central heating system, then its dimensioning must be done accordingly. An important problem, however, is the provision of thermal power regulation of the

The article was received on 03.03.2024, accepted on 24.02.2025 and published on 14.03.2025

system, regulation that must be ensured by the heat pump through the regulation of electric power absorbed from the national system. Both the capacity of the heat pump and its power regulation are dependent on a series of parameters that intervene both in the definition of the heat pump but equally in the definition of the central heating system.

Methodology

The paper will insist on the importance of the parameters related to the building and the central heating system in determining the dimensioning and regulation of the heat pump. We refer to the thermal transfer capacity of the building envelope, Hinc (W/K), the climatic zone in which the building is located by the calculated external temperature, te0 (oC), and the dimensioning hypothesis of the central heating system: high temperature system (tT0/tR0 = 90/70 oC), medium temperature system (tT0/tR0 = 70/50 oC), and low temperature system (tT0/tR0 = 50/30 oC). It is known that between the 3 types of systems mentioned, an important difference is the size of the heating surface, which is large in the case of the low temperature system, medium in the case of the medium temperature system and small in the case of the high temperature system. We do not propose however, within this work, let's also analyze the correlation between the heating system sizing principle and the size of the heating surface.

Regarding the heat pump, the considered parameters are the isentropic efficiency of the compressor η_{iz} and the efficiency of the electric motor, η_{el}. The nominal electric power is the one that is determined based on the calculated heat requirement of the building as will be presented below. The relationships used were also presented in previous works [1], [2] and [3]. Thus, considering the expression of the temperature of the thermal agent according to compliance with the qualitative thermal regulation, it results:

$$\Delta\theta = \theta_{CD} - \theta_{VP} = t_T - t_e = \left(1 + \frac{t_{T0} - t_{i0}}{t_{i0} - t_{e0}} \cdot \frac{1 - E_0}{1 - E}\right) \cdot \left(t_{i0} - t_e\right)$$

with simplified form $\left(E = E_0\right)$:

$$\Delta\theta = \theta_{CD} - \theta_{VP} = t_T - t_e = \left(1 + \frac{t_{T0} - t_{i0}}{t_{i0} - t_{e0}}\right) \cdot \left(t_{i0} - t_e\right) \quad (1)$$

The simplified form refers to the consideration of a constant value of the global thermal transfer coefficient, k, of the heating surface. Regarding the expressions of the energy efficiency of the machine as a heat pump and as a refrigeration machine, these are respectively:

$$\begin{aligned} COP &= \eta_{EL} \cdot \left(1 + \eta_{iz} \cdot \left(M \cdot 86.864 \cdot \Delta\theta^{-0.759} - N\right)\right) \\ EER &= \eta_{EL} \cdot \eta_{iz} \cdot \left(M \cdot 86.864 \cdot \Delta\theta^{-0.759} - N\right) \end{aligned} : \quad (2)$$

Thermal and electrical powers can be written as bellow:

$$\begin{aligned} P_{CD} &= COP \cdot P_{EL} \\ P_{VP} &= EER \cdot P_{EL} \\ P_{CD} &= P_{VP} + \eta_{EL} \cdot P_{EL} \\ P_{INC} &= H_{INC} \cdot \left(t_{i0} - t_e\right) \end{aligned} \quad (3)$$

Referring to the simplified form for a more synthetic exposition, when sizing (choosing) the heat pump, the maximum power given by the condenser must be equal to the calculated heat requirement:

$$\begin{aligned} P_{CD0} &= P_{INC0} \\ COP_0 \cdot P_{EL0} &= H_{INC} \cdot \left(t_{i0} - t_{e0}\right) \end{aligned} \quad (4)$$

Where:

$$\begin{aligned} COP_0 &= \eta_{EL} \cdot \left(1 + \eta_{iz} \cdot \left(M \cdot 86.864 \cdot \Delta\theta_0^{-0.759} - N\right)\right) \\ &with: \\ \Delta\theta_0 &= \theta_{CD} - \theta_{VP} = t_{T0} - t_{e0} = \left(1 + \frac{t_{T0} - t_{i0}}{t_{i0} - t_{e0}}\right) \cdot \left(t_{i0} - t_{e0}\right) \end{aligned} \quad (5)$$

Then:

$$P_{EL0} = \frac{H_{INC} \cdot \left(t_{i0} - t_{e0}\right)}{COP_0} \quad (6)$$

Next, the current thermal power in operation is determined based on the required thermal power of the consumer and the COP associated with the current operating situation according to relation (2). In the current operating situation, the power absorbed by the vaporizer and supplied to the condenser results quite easily according to the relations presented. In current operation, the temperature of the thermal agent at the entrance to the heating installation is given by the well-known qualitative thermal regulation relationship and consequently we have the relationships (1).

For thermal and electrical powers we obtain:

$$P_{EL} = \frac{H_{INC} \cdot (t_{i0} - t_e)}{COP}; \quad \frac{P_{EL}}{P_{INC}} = \frac{1}{COP}$$

$$P_{VP} = EER \cdot P_{EL}; \quad \frac{P_{VP}}{P_{INC}} = \frac{EER}{COP} \tag{7}$$

$$P_{CD} = COP \cdot P_{EL};$$

Simulation

The set of temperatures of the thermal agent (t_{T0}/t_{R0}) chosen for the sizing of the central heating system, was identified as an important parameter on the energy results. The following figures show these results regarding the energy efficiencies, the thermal and electrical powers involved and the ratios between them.

In fig. 1 the energy efficiency of the heat pump increases as the outside temperature is higher. The considered heat pump is of the air-water type and the result obtained is natural. It can also be seen from fig.1 that the adoption of a lower temperature level of the thermal agent in the heating system leads to an increase in the energy performance of the heat pump.

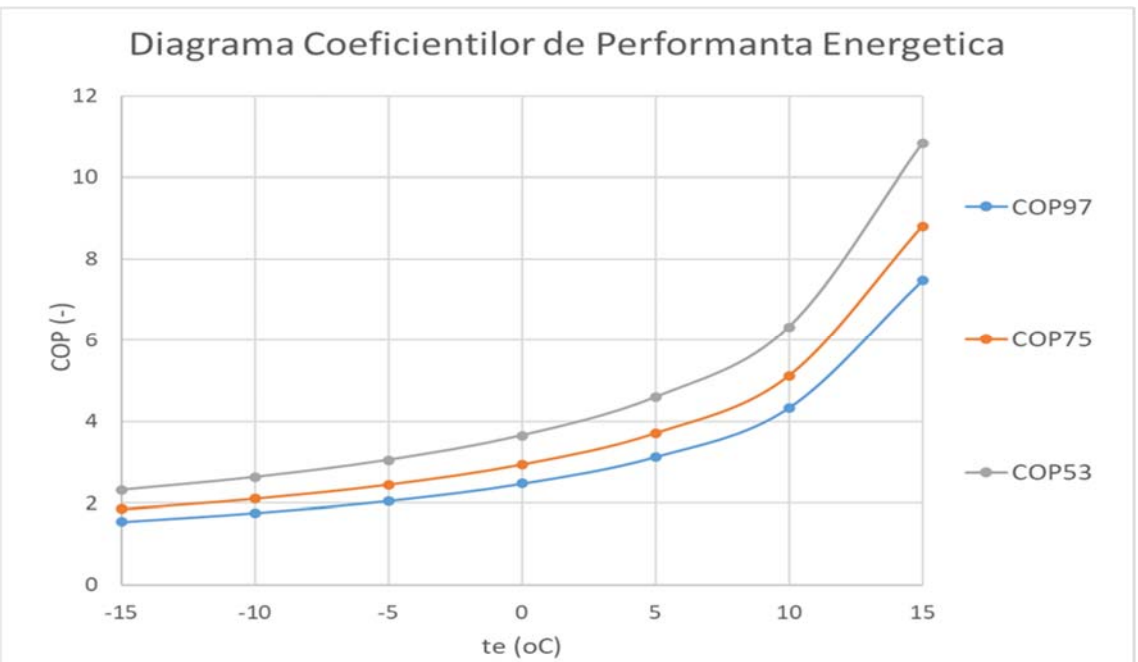

Fig. 1

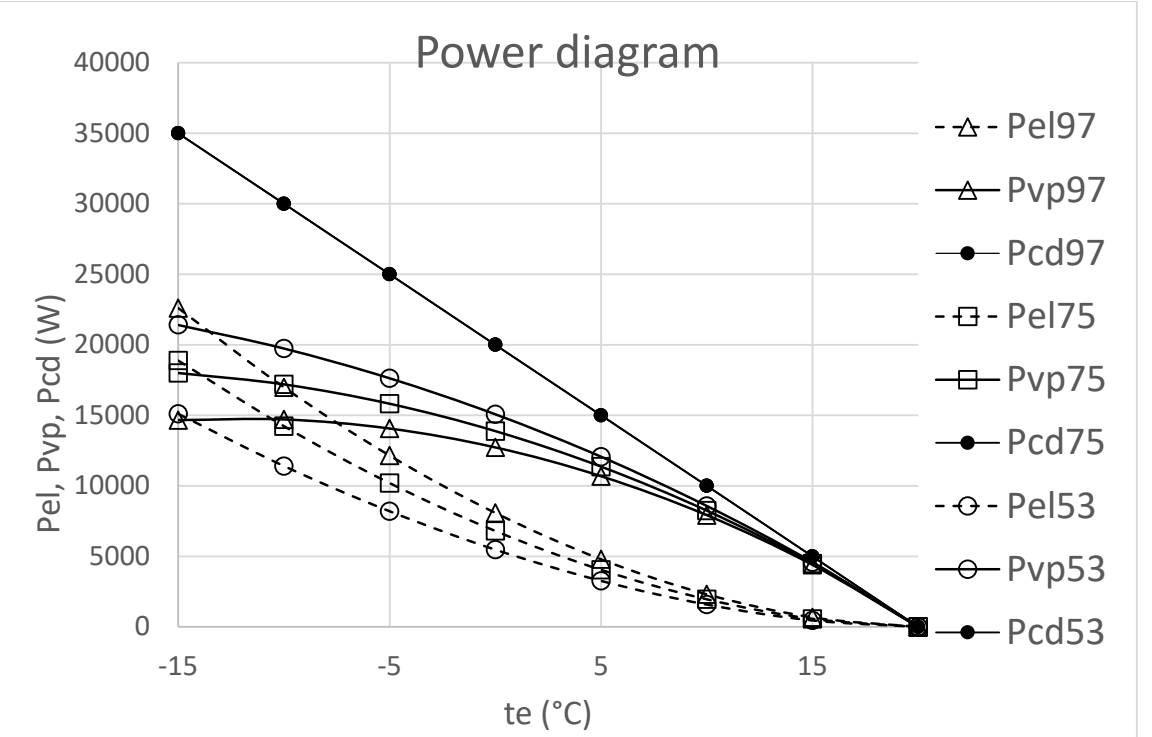

Fig. 2

Fig. 2 shows a diagram of the actual values of the thermal powers obtained in the case of a consumer characterized by a heat transfer capacity of the building in the amount of Hinc = 1000 W/K. It is observed that if the dimensioning of the heating system was made according to a lower level of the temperatures of the heating agent (respectively (tT0/tR0 = 50/30 oC)) the result is a lower electrical power absorbed from the national system associated with a lower thermal power higher absorbed at the level of the heat pump evaporator.

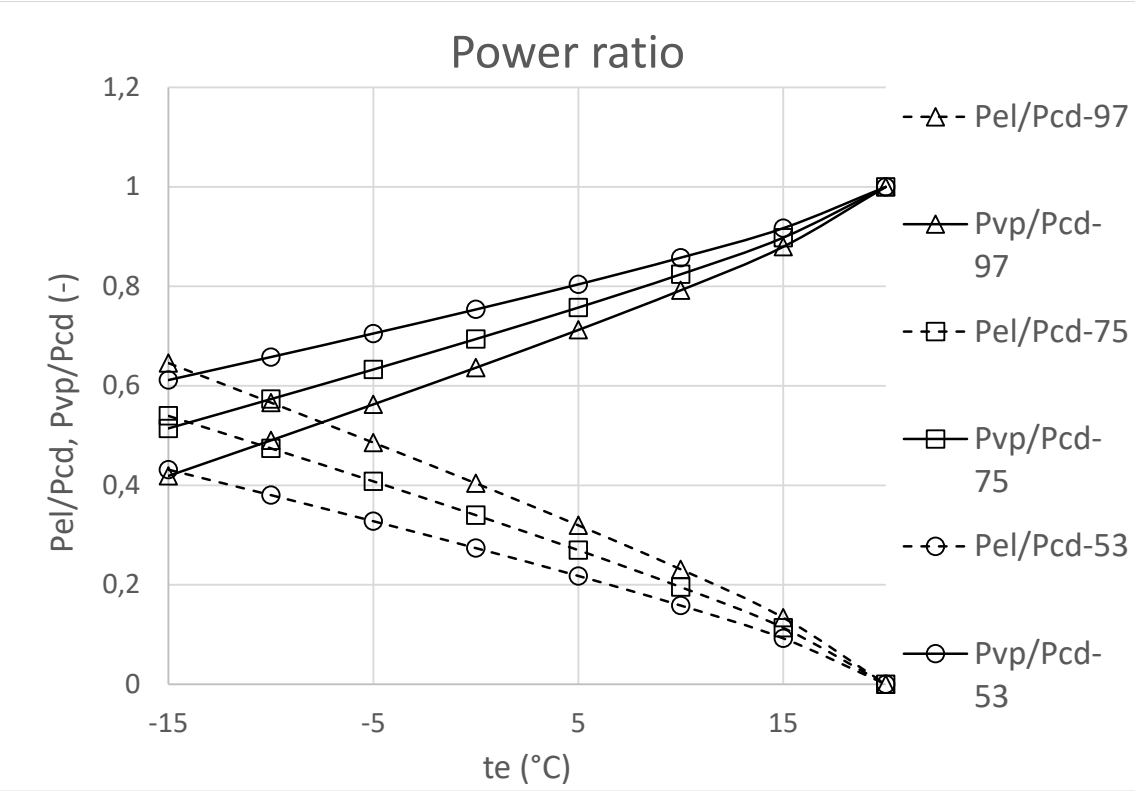

Fig.3

Fig.3 shows the ratio diagram between the absorbed electric power and the required power of the consumer and between the thermal power absorbed at the heat pump evaporator and the required power of the consumer. And these reports presented in fig. 3 express the same conclusion from the previous figures, that the sizing of heating installations at lower temperature levels is beneficial for the adoption of the heat pump as an energy source.

Discussions

From an energetic point of view, adopting a heat pump as an energy source for a heating system is superior to using a thermal plant. Its performance is all the greater as the heating system is characterized by a larger surface resulting from the adoption of a lower temperature level of the heating agent. Based on the presented relationships, it is easy to carry out an economic analysis in which to consider the additional investments and the reductions in operating costs due to a lower level of temperatures of the thermal agent in the central heating system.

Abbreviations

t_{i0} – design internal temperature, ^oC;
t_{e0} – design external temperature, ^oC;

t_e – external temperature, ^oC;
t_{T0} – worst case scenario design heating system fluid exit temperature, ^oC;
t_{R0} – worst case scenario design heating system fluid input temperature, ^oC;
t_T – design building heating fluid input temperature, ^oC;
θ_{CD} – condenser temperature, ^oC;
θ_{VP} – evaporator temperature, ^oC
$\Delta\theta$ – condenser and evaporator temperature difference, ^oC;
H_{INC} – building heating capacity, W/K;
P_{EL} – heat pump electrical power consumption, W;
P_{EL0} – worst case scenario heat pump electrical power consumption, W;
P_{CD} – condensing thermal power, W;
P_{CD0} – worst case scenario condensing power, W;
P_{VP} – evaporator power, W;
P_{INC} – building heating demand, W;
COP_0 – worst case scenario Coeficient of Performance, -;
COP – Coefficient of Performance, -;
EER – energy efficiency ratio, -;
E – building heating facility thermal module; -
η_{EL} – electrical compressor efficiency, -;
η_{iz} – izentropic efficiency, -;
M=0.958, N=1.5321 – working parameters in the correlation between isentropic efficiency and Carnot efficiency $\varepsilon_{iz} = M \cdot \varepsilon_C - N$ and: $\varepsilon_C = 86.864 \cdot \Delta\theta^{-0.759}$ - Carnot efficiency, -;
COP97, COP75, COP53 – COP of 3 cases t_{T0}/t_{R0} = 90/70 ^oC, 70/50 ^oC, respectively 50/30 ^oC;
Pel97, Pvp97, Pcd97 – electrical power, evaporator respectively condenser por for the case t_{T0}/t_{R0} = 90/70 ^oC;
Pel75, Pvp75, Pcd75 – electrical power, evaporator respectively condenser por for the case t_{T0}/t_{R0} = 70/50 ^oC;
Pel53, Pvp53, Pcd53 – electrical power, evaporator respectively condenser por for the case t_{T0}/t_{R0} = 50/30 ^oC;

References:

[1] - Procedura de evaluare a indicatorilor de performanta pentru masini frigorifice sau pompe de caldura – Florin Iordache, Alexandru Draghici – Revista Romana de Inginerie Civila, Volumul 10 (2019) nr. 4 – Matrix Rom, Bucuresti;

[2] – Procedura simplificata de evaluare a performantei energetice a pompelor de caldura. Analiza energetica si economica – Florin Iordache, Mugurel Talpiga - Revista Romana de Inginerie Civila, Volumul 13 (2022) nr. 4 – Matrix Rom, Bucuresti;

[3] – Modelarea functionarii echipamentelor si sistemelor termice aferente cladirilor – Florin Iordache – editura Matrix Rom, 2021, Bucuresti;

Architectural integration of photovoltaic panels on the facades of existing buildings. Case Study

Integrarea arhitecturala a panourilor fotovoltaice pe fatadele cladirilor existente. Studiu de caz

Natalia Bărgăoanu[1], Andreea Zuba[1]

[1]Politehnica University Timișoara
Victoriei Square, No.2, Timisoara, Romania
E-mail: natalia.bargaoanu@student.upt.ro, andreea.zuba@student.upt.ro

Coordinators: Adriana Tokar, Daniel Muntean

E-mail: adriana.tokar@upt.ro, daniel.muntean@upt.ro

DOI: 10.37789/rjce.2025.16.1.11

Abstract. *Photovoltaic energy represents an outstanding solution for combating climate change and promoting sustainable development, offering benefits such as extensibility and clean energy source. Its integration into buildings as a vital component in modern architecture and sustainable construction has multiple advantages, from saving materials to generating sustainable energy and reducing dependence on fossil fuels. However, the high initial cost and dependence on sunlight are important disadvantages, but using innovative technologies and creative approaches, photovoltaic energy can play an essential role in ensuring a sustainable future and providing functional, aesthetic and sustainable building facades. The case study proposes the modernization of an existing building by installing photovoltaic panels on the western facade and on the roof, thus resulting in an annual electricity production of 16.73 MWh.*

***Key words*:** *photovoltaic panels, architecture, solar energy, energetic efficiency*

1. Introduction

Photovoltaic energy is a remarkable discovery that can play a significant role in addressing climate change issues and promoting sustainable development [1]. Converting solar energy into electricity is one of the cleanest and most sustainable methods of energy production.

It is impressive to see the progress made towards zero energy buildings, and the targets set by the European Union for reducing energy consumption in buildings are an important step in the right direction. The implementation of these buildings and other

The article was received on 30.03.2024, accepted on 14.02.2025 and published on 14.03.2025

renewable energy technologies can help reduce dependence on fossil fuels and lower greenhouse gas emissions [1,2].

It is also impressive to note how efficient a single photovoltaic cell can be, capable of producing between 1 and 2 W [1]. This underlines the enormous potential of this technology, especially when implemented on a large scale.

Therefore, the continuation of research and the implementation of photovoltaic technology is essential for ensuring a sustainable future and for combating climate change.

The benefits of photovoltaic energy are multiple [1]:

- Extensibility - the capacity of the solar panels can be easily adjusted according to the needs of the users.
- Clean and sustainable energy source - photovoltaic (PV) panels use sunlight, an inexhaustible and non-polluting source of energy, protecting the environment.
- Durability and reliability - photovoltaic systems can operate efficiently for a long time without major problems after installation, having a small number of moving parts and requiring little maintenance. This feature gives them resistance to weather conditions such as humidity, wind, snow and lightning.

However, there are also some disadvantages [1]:

- High initial cost - The initial installation of a PV system can be expensive.
- Dependence on sunlight - Electricity generation is only possible during the day, depending on the availability of sunlight, which requires adequate energy storage systems for later use.
- Reduced efficiency due to pollution - The surface of solar panels can be affected by pollution, leading to a drop in efficiency. Studies show that dirt can reduce the efficiency of panels by up to 3.5%, requiring periodic cleaning.

2. Photovoltaic panels on the building envelope

The integration of photovoltaic technology into building architecture represented a significant change in the field of sustainable construction. Buildings with extensive areas offer the opportunity to generate energy by integrating photovoltaic systems. These systems can be incorporated into building facades, roofs or can be used as shading elements to regulate natural light. Integrating these systems into the structure of buildings brings benefits in terms of saving materials, reducing electricity costs, reducing dependence on fossil fuels and adding an aesthetic dimension to the building's architecture.

Despite these advantages, photovoltaic integration in building facades plays a crucial role in shaping the urban landscape, through unaesthetics due to the visibility of the panels. Large building facades can be covered with photovoltaic panels to achieve optimal efficiency. The use of PV in facades can provide protection against excessive solar radiation and replace traditional materials, while providing an aesthetic appearance and additional protection [1].

Although the vertical orientation of facades can reduce the efficiency of photovoltaic systems, the modules can be mounted at an angle to improve the efficiency of power generation [1].

In the past, electricity generation was limited to rooftops or large open spaces, but now it can be innovatively and multifunctionally integrated into the structure of buildings, becoming an essential component of architectural projects. By emphasizing the fusion between aesthetics, functionality and energy sustainability, current models encourage a creative and non-conformist approach to traditional architecture [3].

Apart from traditional integration (Building Integrated Photovoltaics), modern integrated facade solutions also include elements such as fireproof and insulating materials, cladding elements and electrical components. Building facade PV integration technology has the advantage of the design freedom offered by custom solar panels that are not limited to standard shapes or sizes, ranging from 360mm to 3600mm wide, easily adapting to any architectural structure.

These solutions can adopt various typologies:

- Rain screen - recognized as one of the most effective ways to increase durability and reduce maintenance costs, this facade protects the building structure from weather phenomena such as rain and wind. In addition, the ventilation layer helps to reduce the thermal load of the building, while generating sustainable and free electricity. The ventilated solar facade allows for quick and easy installation, inspection and reuse in both new and renovated buildings.
- Curtain wall - in this scenario, solar panel systems are fully integrated into the building envelope and replace traditional support elements or glazed panels. The durable toughened glass surface, which is an integral part of the building's water- and air-tight structure, provides low-maintenance cladding and a minimal environmental footprint, while still generating electricity.
- Blinds - also known as brise soleil, are architectural elements that combine solar protection and energy production by mounting fins on the building facade, either horizontally or vertically. They thus become key components of architectural design.
- Blind systems - offer a wide variety of finishes with exclusive high-performance photovoltaic panels and discreetly and efficiently integrated. They are designed to fit perfectly into the design of the building, while respecting the specific regulations and local requirements of urban architecture.

When designing facades, a number of factors influence their design, from compositional and geographical elements to environmental considerations. Facades are an essential interface between the environment and the interior of the building, shaping its envelope and serving as a link between the exterior and interior life [4].

In this context, contemporary architecture seeks to enrich the role of facades, exploiting their potential through technological innovation. Today, technology is integrated to create more textured and expressive facades, exploring various materials and promoting circular and low-carbon architecture.

Understanding facades as the envelope of buildings and realizing the growing global demand for efficient use of resources in the built environment, there is a need to capitalize on the sunlight incident on building facades. In this sense, PV integration has become increasingly relevant in creating a new aesthetic for facades and minimizing environmental impact. These systems, with their technical capabilities and aesthetic qualities, lead to the creation of attractive, durable and resistant solar facades. They generate a positive impact on the built environment through the efficient incorporation of PV on the one hand, but also on the environment through the production of free and sustainable energy for buildings.

Solar energy can be used effectively in every season if sunlight is available. The strategic placement of solar panels on facades, instead of just being installed on roofs, allows energy to be obtained even in regions with cold climates and low solar incidence, albeit with low efficiency. This strategy extends the efficiency of solar energy use by adapting to variable climate conditions, ensuring consistent performance throughout the year.

Apart from the aesthetic advantages, the solar panels integrated on the facade are also notable for their durability and resistance to various weather conditions. Considering the need for a facade to withstand climatic conditions while maintaining structural integrity, these systems are designed to withstand difficult weather conditions, adapt to the local environment and are built from durable materials, giving them resistance to extreme temperatures (wind pressure and snow accumulation). Durability and environmental responsibility make them a practical and cost-effective solution for a wide variety of building types, whether for new construction or retrofit projects. By prototyping and developing modern models (colors that mimic a metallic or ceramic look, finishes, texture, dimensions and shape), alternatives can be explored to meet the individual needs of each project and meet specific additional standards. These designs offer an alternative to traditional cladding with strong and durable solutions without compromising quality, architectural integrity or aesthetics.

3. Case Study

The building for which the case study was carried out is located in Timișoara on Calea Șagului street (Fig. 1), 9m high, being developed on 3 levels, ground floor, respectively 1st and 2nd floor, incorporating on the ground floor of the building a commercial space intended for the sale of car parts and car accessories, and the 2 floors include block spaces. It is a building made of concrete, with the main facade facing West (Fig. 2).

Fig. 1. Location of the analyzed building

Fig. 2. The facade of the analyzed building (ProMotor from Timișoara).

This building was chosen due to its advantageous position and because it has red PVC tiles integrated on the main facade, this color being representative of the economic agent that carries out its activity in office spaces. The photovoltaic panels will be placed only on the west-facing facade because the east-facing facade includes balconies that shade the facade (Fig. 3).

We chose to replace the PVC boards with red photovoltaic panels (Fig. 3) in order to achieve an energy efficiency of the building, at the same time to offer a pleasant appearance without dissolving the original appearance imposed by the building (Fig. 4).

Fig. 3. Red photovoltaic panel

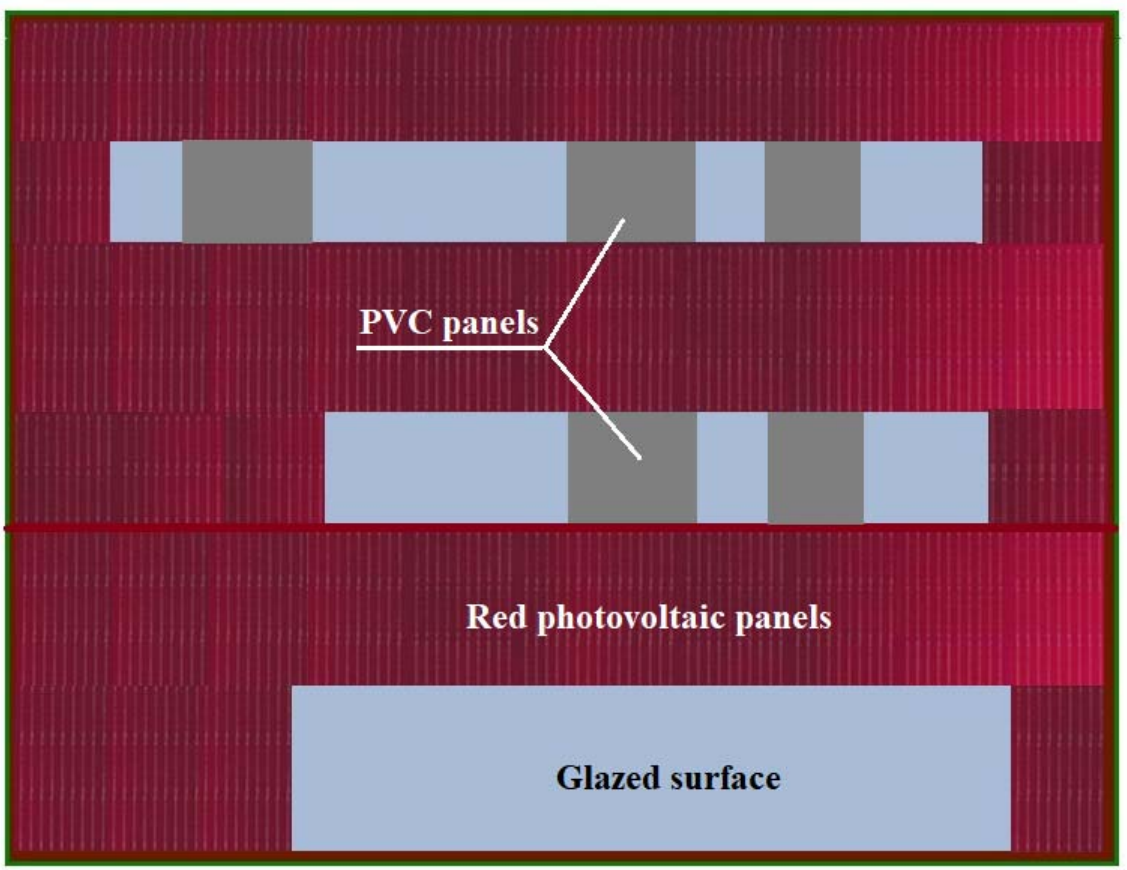

Fig. 4. the placement of photovoltaic panels on the facade of the building

The Polysun SPTX Constructor calculation program [5] was used to simulate the photovoltaic system. In order to use the existing surface potential, we proposed the placement of photovoltaic panels on the roof of the building, which is made of sheet

metal. EvoCells 400 MIB type panels with a maximum production power of 400 W were placed on the roof (Fig. 4).

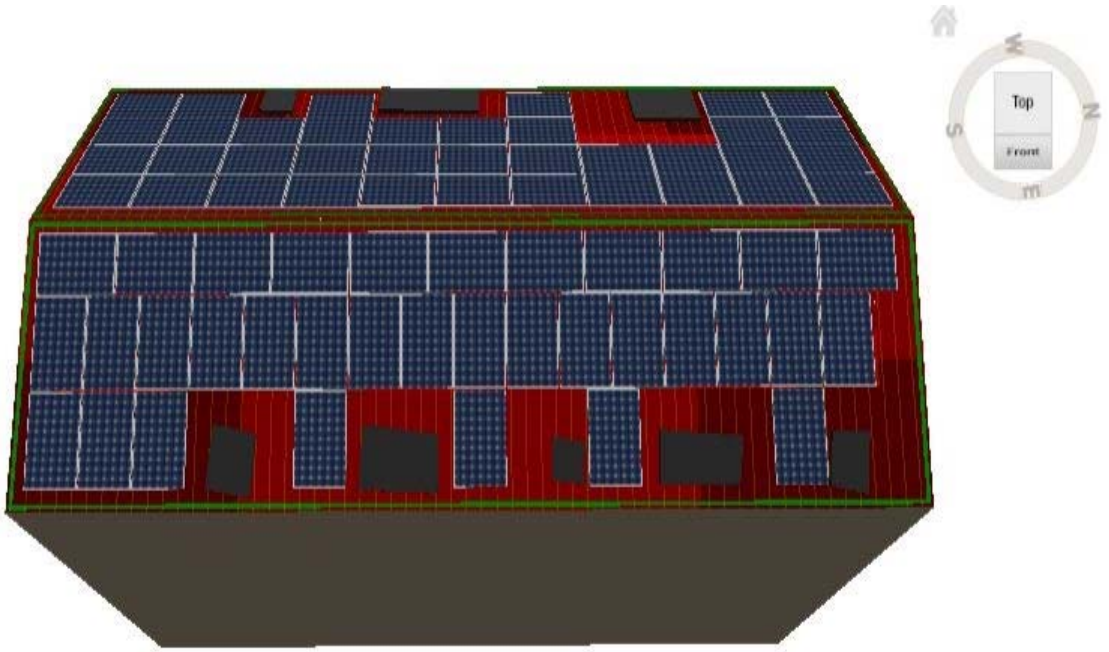

Fig. 5. Placement of photovoltaic panels on the roof of the building

The installed power of the photovoltaic system is 49.96 kW. Following the simulation, the annual production of the photovoltaic system was 16.73 MWh. The monthly electricity production can be seen in the graph in Fig. 6.

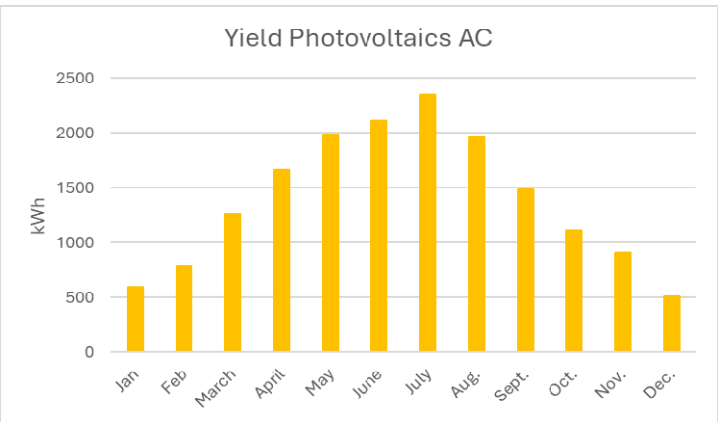

Fig. 6. Monthly electricity production

In addition to the benefit brought by the production of electricity, the use of photovoltaic panels also has the great advantage of reducing the amount of CO2 compared to the production of electricity using classic fuels. In Fig. 7 shows the amount of CO2 saved using this method of electricity production.

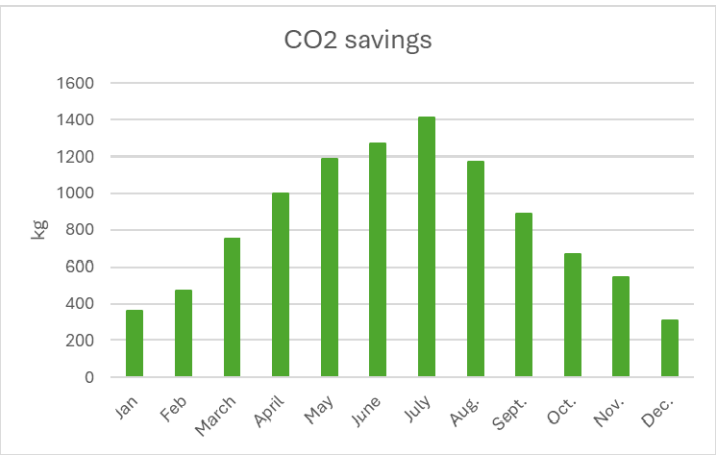

Fig. 7. CO2 savings

It should also be emphasized that the production of electricity is significant during the summer months, when the amount of energy produced is greater than the amount consumed in the internal electrical installation, so that the surplus energy produced can be delivered to the SEN. In Fig. 8 presents the annual energy flow.

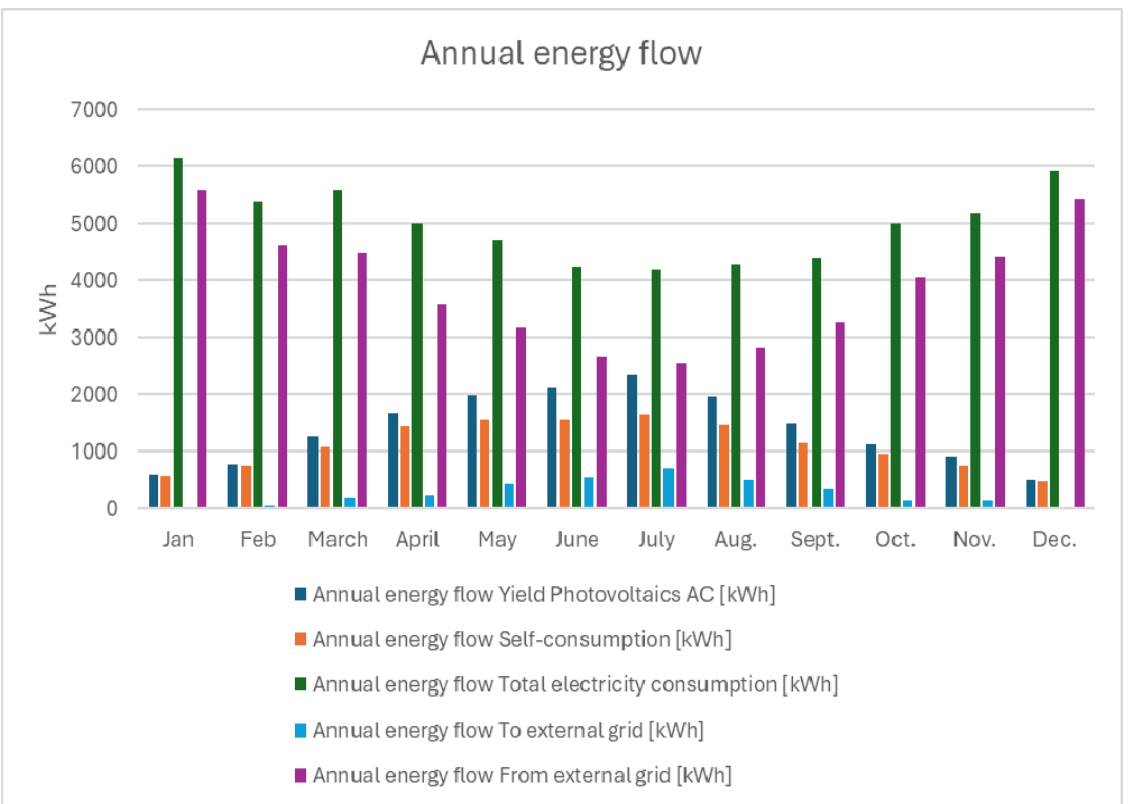

Fig. 8. Annual energy flow

6. Conclusions

In conclusion, photovoltaic energy represents a viable and promising solution for combating climate change and promoting sustainable development in the construction sector. Its integration into building facades presents significant advantages, including the generation of clean and sustainable energy, saving resources and reducing dependence on traditional energy sources. However, it is essential to further address the challenges of cost and reliance on sunlight in order to maximize the benefits of PV technology in creating a sustainable and aesthetically pleasing built environment, thereby helping to build a greener and more sustainable future.

Referinţe

[1] S.S. Shehu, Z.A. Halil, „Integration of Photovoltaics in Modern Building Facade: A Comparison of Photovoltaic Integrated Façade", in International Journal of Recent Research in Civil and Mechanical Engineering (IJRRCME), vol. 2, Issue 2, Month: October 2015 – March 2016, pp. 66-80.

[2] M. Cinca, Non-conventional energy sources – Course support, University Politehnica Timisoara, 2024.

[3] E. Souza, „Flexibility and Innovation: Customized Solar Panels for Facade Integration" in Archdaily, disponibil online la adresa , https://www.archdaily.com/1010399/flexibility-and-innovation-customized-solar-panels-for-facade-integration?ad_source=search&ad_medium=projects_tab&ad_source=search&ad_medium=search_result_all, Accessed: 18.03.2024.

[4] E. Tovar, „Durable and Resilient Solar Facades: 5 Essential Architectural Principles" in Archdaily, disponibil online la adresa: https://www.archdaily.com/1013143/durable-and-resilient-solar-facades-5-essential-architectural-principles?ad_source=search&ad_medium=projects_tab&ad_source=search&ad_medium=search_result_all, Accessed: 20.03.2024.

[5] ***, Polysun SPTX Constructor software from Vela Solaris.

Assessing the Impact of Air Conditioning Systems on Aerosol Dispersion within Intensive Care Units

Evaluarea impactului sistemelor de aer condiționat asupra dispersiei aerosolilor în cadrul Unităților de Terapie Intensivă

Cătălin-George Popovici[1], Emilian-Florin Țurcanu[1], Vasilică Ciocan[1], Nelu-Cristian Chereches[1], Sebastian-Valeriu Hudișteanu[1], Ana Diana Ancaș[1], Marina Verdeș[1], Marius-Vasile Atanasiu[2], Larisa Anghel[3,4]

[1] Technical University "Ghe. Asachi" of Iasi, Faculty of Civil Engineering and Building Services, Department Building Services, D. Mangeron 67 str., 700050, Romania;
[2] Technical University "Ghe. Asachi" of Iasi, Faculty of Mechanical Engineering, Department of Mechanical Engineering and Road Automotive Engineering, D. Mangeron 67 str., 700050, Romania;
[3] University of Medicine and Pharmacy "Grigore T. Popa", MD Institute of Cardiovascular Diseases "Prof. Dr. George I.M.Georgescu" Iasi, Romania
[4] MD, Institute of Cardiovascular Diseases "Prof. Dr. George I.M.Georgescu" Iasi, Romania;

E-mail: florin-emilian.turcanu@academic.tuiasi.ro

DOI: 10.37789/rjce.2025.16.1.12

Abstract. *This comprehensive study investigates the influence of air conditioning (AC) systems on aerosol dispersion within Intensive Care Units (ICUs), emphasizing the critical context of patient cough events. This research uses advanced Computational Fluid Dynamics (CFD) simulations to analyze airflow patterns, aerosol behavior, and potential exposure risks within ICU settings, offering valuable insights for healthcare facility design and infection control protocols.*

Keywords: Aerosol Dispersion, ICU Airflow Patterns, CFD Simulation.

1. Introduction

The propagation of aerosols within healthcare settings, especially Intensive Care Units (ICUs), is a critical concern for infection control and patient safety. In these environments, the minute particles suspended in the air can travel considerable distances, carrying potentially infectious agents. The management of aerosol dispersion is thus integral to reducing the risk of nosocomial infections [1].

Aerosols in ICUs originate from various sources, including medical procedures, equipment, and, significantly, the respiratory activities of patients, such as coughing or

The article was received on 04.04.2024, accepted on 12.02.2025 and published on 14.03.2025

sneezing. When a patient coughs, a complex mixture of particles of varying sizes is expelled, creating a potential pathway for transmitting pathogens like viruses and bacteria. The behavior and fate of these particles in the ICU atmosphere depend on several interrelated factors influenced by the air conditioning (AC) systems:

Air Velocity and Flow Patterns: AC systems dictate air movement within a room, influencing how aerosols travel and settle. High air velocity can carry particles over longer distances. Still, strategic airflow design can enhance the removal of these particles by directing them toward filtration systems or out of the room [1].

Temperature: The temperature affects air buoyancy, creating convection currents that can influence aerosol movement. Warmer air rises, potentially carrying aerosols upward, while cooler air descends. By controlling room temperature, AC systems can impact these currents and thus the vertical distribution of aerosols.

Humidity: Humidity levels can alter aerosol dynamics by affecting particle evaporation and size. Higher humidity can slow the evaporation of the moisture in aerosols, maintaining their size or causing them to grow by coalescence, which might impact their deposition rate and transport distance. AC systems that control humidity can thus influence these dynamics [2].

Room Geometry and Air Distribution: The physical layout of an ICU, including the placement of beds, equipment, and the location of air supply and exhaust points, interacts with the AC system to create unique airflow patterns. These patterns can either contribute to the effective dispersion and removal of aerosols or lead to areas of stagnant air where particles accumulate.

Given these complexities, the role of AC systems in modulating aerosol dispersion is pivotal. Effective AC system design and operation in ICUs should aim to achieve optimal air exchange rates, remove contaminants efficiently, and maintain comfortable and safe environmental conditions for patients and healthcare workers. This necessitates a multidisciplinary approach, incorporating insights from engineering, infection control, and healthcare operations to design AC systems that can respond to the dynamic conditions of ICU environments and minimize airborne transmission risks.

2. Material and method

Room Configuration and Simulation Setup.

To accurately assess the impact of air conditioning systems on aerosol dispersion, a detailed and realistic representation of the ICU room is essential. The room configuration setup in the simulation model would include:

Dimensions: The exact length, width, and height of the ICU room need to be specified. These dimensions are crucial as they influence air movement and particle distribution patterns within the space (Fig. 1) [5].

Bed Placement: The location of patient beds affects the source points of aerosol generation and determines the critical areas where air quality needs to be meticulously controlled. The placement should reflect typical ICU layouts to ensure the simulation's

relevance to real-world settings.

Air Inlets and Outlets: The positions of vents, air returns, and any other openings that facilitate air exchange are mapped out in detail. The effectiveness of aerosol removal is significantly influenced by how air circulates, which is dictated by the location of these inlets and outlets (Fig.1).

Specifications of the AC System: Critical parameters include:

Air Change Rates: This is the rate at which the air within the ICU is replaced with fresh or filtered air, typically measured in changes per hour (ACH). Higher ACH values are associated with more effective dilution of airborne contaminants.

Filtration Efficiency: The quality of air filters within the AC system, often quantified by the Minimum Efficiency Reporting Value (MERV) or High-Efficiency Particulate Air (HEPA) standards, which indicate their ability to trap particles of specific sizes.

Airflow Patterns: The direction and speed of air being circulated by the AC system, which should ideally promote the dispersal of clean air and the evacuation of potentially contaminated air.

CFD Simulation Approach

The CFD simulation translates the physical scenario into a computational model, allowing for the analysis of airflow and aerosol dynamics under various conditions:

Boundary Conditions: These are the set conditions at the simulation's edges, such as walls, windows, and doors, which could affect airflow. For instance, walls are typically treated as no-slip boundaries, meaning the air velocity at the wall is zero, reflecting the physical reality (Fig. 1) [3].

Mesh Generation: This step involves dividing the room into discrete, small volumes or cells, which the simulation uses to solve the governing equations of fluid flow. A finer mesh can provide more detailed results but requires more computational power. Key areas, like around the patient's bed or near air inlets and outlets, might be assigned finer meshes for enhanced accuracy (Fig. 1) [3].

Solver Settings: These settings determine how the simulation calculates the flow field and particle trajectories. They include time step size, convergence criteria, and the choice of turbulence and particle dispersion models.

Aerosol Generation Modeling: This component simulates the generation of aerosols due to a patient coughing. It includes:

Droplet Sizes: Aerosols are modeled in a range of sizes to reflect the diversity generated by coughing. Smaller aerosols (<5 microns) can remain airborne for extended periods, while larger droplets settle more rapidly [4].

Emission Rates: The rate at which particles are introduced into the air, which can be based on empirical data from studies of cough aerosols [3].

By carefully setting up the room configuration and the CFD simulation parameters, researchers can create a sophisticated model that provides valuable insights into how AC systems influence aerosol dispersion in ICUs, informing strategies to minimize infection risks.

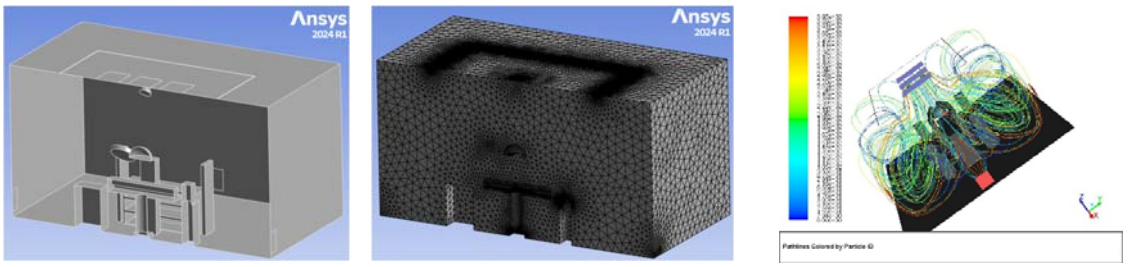

a) b) c)

Fig. 1. a) Geometry; b), c) Mesh and air lines dispersion

3. Results

3.1 Airflow Patterns

Visualization and Analysis: Utilizing CFD simulation outputs, airflow within the ICU can be visualized through vector fields or streamlines, which illustrate the direction and speed of air movement. This visualization helps identify how air travels around the room, interacts with obstacles like furniture or medical equipment, and impacts aerosol transport (Fig. 2) [3].

Zones of High and Low Air Exchange: Through the analysis, specific areas within the ICU can be pinpointed where air exchange is either particularly efficient or insufficient. High air exchange zones are typically near air inlets or in the direct path of strong airflow, whereas low exchange zones are often in corners or behind obstructions where air movement is minimal [3].

Impact of AC Settings: The configuration of the AC system—including fan speeds, vent locations, and directional controls—plays a significant role in shaping these airflow patterns. By adjusting these settings, the distribution of air can be altered to reduce the occurrence of stagnant air pockets or recirculation zones that might harbor higher concentrations of aerosols.

3.2 Aerosol Dispersion and Concentration

Trajectories and Dispersion Patterns: The CFD simulations can track aerosol particles of various sizes as they are emitted in a coughing event, showing how they disperse throughout the room. These trajectories reveal the influence of airflow patterns on particle movement and highlight potential paths of exposure. [Fig. 2]

Concentration Distributions: Over time, the simulations can aggregate aerosol concentrations across the room, illustrating how particles accumulate or diminish in different areas. These concentration maps can pinpoint high-risk zones where aerosols linger, posing greater risks to patients and healthcare workers.

3.3 Impact of AC System Variations

Comparative Analysis: By simulating various AC configurations, the study can evaluate how changes in system design or settings influence aerosol dispersion. For example, increasing the air change rate may show a significant reduction in aerosol concentrations, or altering vent positions might disperse concentrations more evenly [3].

Mitigating Aerosol Accumulation: The effectiveness of each AC configuration in reducing aerosol accumulation provides critical insights. For instance, configurations that enhance vertical airflow may prove effective in removing aerosols from the breathing zone, while others might better prevent aerosol spread between adjacent beds.

Optimization Recommendations: Based on the comparative analysis, specific recommendations can be formulated for AC system settings that optimize particle dilution and removal. These may include guidelines on ideal air change rates, filter specifications, and airflow patterns that should be targeted in ICU design and operation to enhance air quality and minimize infection transmission risks.

By comprehensively analyzing these factors, healthcare facilities can develop informed strategies to leverage AC systems as proactive tools in infection control, ultimately enhancing patient and staff safety within ICUs.

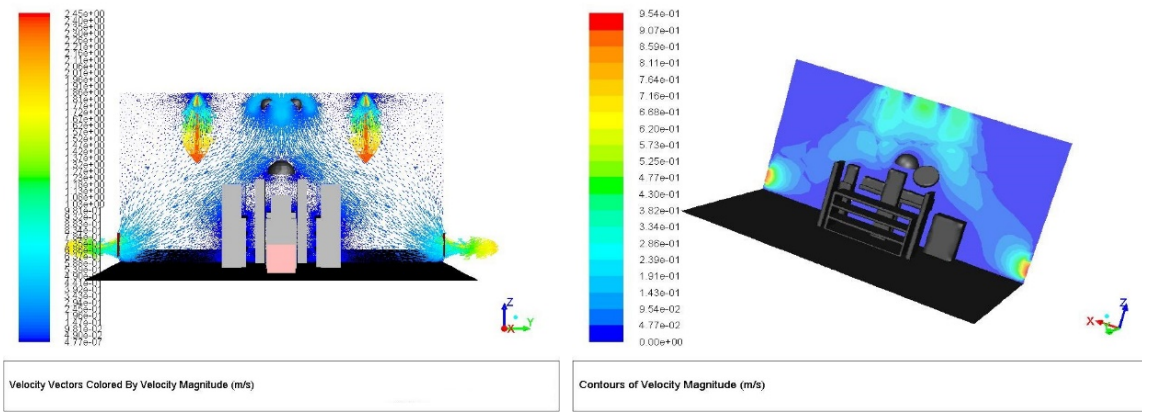

a) b)

Fig. 2. a), b) Contours of Velocity

4 Discussion

Interpretation of CFD results in the context of infection control, emphasizing the importance of strategic AC system design and operation.

Consideration of practical implications for ICU management, including potential adjustments to AC settings during outbreaks.

Limitations of the study, such as assumptions in aerosol generation and behavior, and suggestions for future research.

5 Conclusion

This study underscores the critical role of AC systems in influencing aerosol dispersion within ICUs, highlighting the necessity for evidence-based HVAC design and operation approaches to enhance patient and staff safety. The research provides actionable insights into optimizing air circulation and aerosol mitigation strategies in critical care settings through detailed CFD analysis.

References

[1] M. Ahmadzadeh, E. Farokhi, M. Shams, "Investigating the effect of air conditioning on the distribution and transmission of COVID-19 virus particles", in Journal of Cleaner Production, https://doi.org/10.1016/j.jclepro.2021.128147, September 1, 2021.

[2] L. Borro, L. Mazzei, M. Raponi, P. Piscitelli, A. Miani, A. Secinaro, "The role of air conditioning in the diffusion of Sars-CoV-2 in indoor environments: A first computational fluid dynamic model, based on investigations performed at the Vatican State Children's hospital", Environmental Research, https://doi.org/10.1016/j.envres.2020.110343, New York, N.Y. Print, February 1, 2021.

[3] M. Basak, S. Mitra, "Pathways to community transmission of COVID–19 due to rapid evaporation of respiratory virulets", in Journal of Colloid and Interface Science, https://doi.org/10.1016/j.jcis.2022.03.098, August 1, 2022.

[4] J. Kurnitski, M. Kiil, P. Wargocki, A. Boerstra, O. Seppänen, B. W Olesen, L. Morawska, "*Respiratory infection risk-based ventilation design method"*. Building and Environment. https://doi.org/10.1016/j.buildenv.2021.108387, December 1, 2021.

[5] Z. Liu, D. Yin, Y. Niu, G. Cao, H. Liu,& L. Wang. "*Effect of human thermal plume and ventilation interaction on bacteria-carrying particles diffusion in operating room microenvironment"* in Energy and Buildings. https://doi.org/10.1016/j.enbuild.2021.111573, January 1, 2022.

Geopolymer concrete based on fly ash and slag using recycled aggregate from building demolition

Beton geopolimeric pe bază de cenușă zburătoare și zgură utilizând agregat reciclat din demolarea clădirilor

Lucian Paunescu[1], Enikö Volceanov[2,3], Bogdan Valentin Paunescu[4]

[1]Daily Sourcing & Research SRL
95-97 Calea Grivitei street, sector 1, Bucharest 010705, Romania
E-mail: lucianpaunescu16@gmail.com

[2]University „Politehnica" of Bucharest, Faculty of Science and Materials Engineering,
313 Independence Splai, sector 6, Bucharest 060042, Romania
E-mail: evolceabov@yahoo.com

[3]Metallurgical Research Institute SA
39 Mehadia street, sector 6, Bucharest 060042, Romania
E-mail: evolceanov@yahoo.com

[4]Consitrans SA
56 Polona street, sector 1, Bucharest 010504, Romania
E-mail: pnscbogdan@yahoo.com

DOI: 10.37789/rjce.2025.16.1.13

Abstract. *A new version of the geopolymer concrete composition including recycled aggregate from the demolition of buildings as fine aggregate was tested in this experiment. Different weight proportions were tried together with the natural aggregate (river sand) and determinations of mechanical and physical characteristics of the geopolymer were carried out. Given that the main effect of the recycled aggregate addition was increasing compressive and flexural strengths, while the other characteristics decreased, the solution adopted was corresponding correlation of characteristic values to obtain a product with optimal properties (version 3): 2105 kg·m^{-3}-density, 4.3 %-water-absorbing, 54.9 MPa-compressive strength, 9.2 MPa-flexural strength, and 22.9 GPa-elasticity modulus.*

Key words: *geopolymer concrete, recycled aggregate, building demolition, granulated blast furnace slag, compressive strength.*

Rezumat. *O nouă variantă a compoziției betonului geopolimeric incluzând agregat reciclat din demolarea clădirilor a fost testată în acest experiment. Au fost încercate diferite proporții masice împreună cu agregatul natural (nisip de râu) și au fost efectuate determinări ale caracteristicilor mecanice și fizice ale geopolimerului. În condițiile în*

The article was received on 18.12.2023, accepted on 14.02.2025 and published on 14.03.2025

care principalul efect al adăugării agregatului reciclat a fost creșterea rezistențelor la compresiune și încovoiere, în timp ce celelalte caracteristici au scăzut, soluția adoptată a fost corelația corespunzătoare a valorilor caracteristicilor pentru a obține un produs cu proprietăți optime (varianta 3): 2105 kg·m^{-3}-densitatea, 4,3 %-absorbția apei, 54,9 MPa-rezistența la compresiune, 9,2 MPa-rezistența la încovoiere, și 22,9 GPa-modulul de elasticitate.

Cuvinte cheie: beton geopolimeric, agregat reciclat, demolarea clădirii, zgură granulată de furnal, rezistența la compresiune.

1. Introduction

The new concept regarding the economical and environmentally friendly material type patented and developed by the French inventor J. Davidovits in the last decade of the 20th century has aroused the interest of manufacturers and users in the field of construction materials]1]. The new material called geopolymer is an amorphous semi-crystalline material formed by the geopolymerization reaction between alumino-silicate materials and an alkaline activator. The geopolymer precursors require to be rich in alumina and silica, playing a major role in the hardening process of the geopolymer as well as in formation of the N-A-S-H gel together with other elements ensuring the strength feature of the material [2]. The geopolymer formed in this way has the ability to replace the traditionally binder used in the manufacture of concrete (ordinary Portland cement) due to its pozzolanic properties as well as mechanical and durability ones. The processing of materials that make up the geopolymer requires low energy consumption and almost negligible emissions of greenhouse gases (carbon dioxide) [3].

According to the literature [4], coal fly ash is the main geopolymeric material, as a by-product of the energy industry, used as a substitute binder for cement in the construction concrete manufacturing process. Silicon and aluminum oxides from fly ash composition with low calcium content have the ability to react with the alkaline activator solution forming the geopolymer paste that binds together the fine and coarse aggregate as well as other un-reacted materials constituting the geopolymer concrete. Recent experiments using ground granulated blast furnace slag [5] have shown that geopolymers made with metallurgical slag exhibit good early-age mechanical resistance properties, especially compressive strength. However, some disadvantages of using the slag have been identified such as high shrinkage and low hardness. These disadvantages were overcome by the combined use of slag together with metakaolin or fly ash as well as the use of metakaolin together with fly ash and silica fume. Kim et al. [6] observed that adding silica fume as a precursor together with slag could improve the reactivity of blast furnace slag through the filling effect, leading to increasing the compressive strength.

An economic solution was recently tested in the process of manufacturing geopolymer concrete using concrete waste recycled from the demolition of buildings in the form of coarse aggregates [7, 8] due to their higher weight proportion in the

concrete composition. The European Commission considers that construction and demolition waste represent 25-30 % of the total waste [9]. According to the data provided by Tam et al. [10], currently EU countries produce around 200 million tons of recycled aggregates, of which about 80 % are used for building construction and about 20 % for road construction. The decrease of mechanical features as a result of recycled aggregates application was improved by the addition of superplasticizers. The paper [11] aimed at the application of these recycled wastes in the form of fine aggregates replacing natural sand. The similar effect of decreasing the mechanical strength of concrete was counteracted by the use of superplasticizers.

Geng and Sun [12] have identified the particle surface of fine recycled concrete aggregate as being rough, with many pores, and microcracks, that differentiate this aggregate type from fine natural aggregate. According to [13], average values of recycled aggregate density are between 2.18-2.56 $g \cdot cm^{-3}$ and water-absorbing for 24 hours has average values of 9.9 vol. %. Water-absorbing ability is increasing in the case of lower sizes of the aggregate. Thus, the concrete made with fine recycled aggregate requires more mixing water compared to usual concrete, increasing the water/cement ratio. As a result, mechanical strength and durability decrease and shrinkage increases.

According to Pereira et al. [14], lower water/cement ratio improves compactness and mechanical features of concrete and an effective method is the use of superplasticizers. However, few works on concrete durability made with fine recycled concrete aggregate and superplasticizer are known. The concrete durability is characterized by carbonation and penetration of chloride ions.

The replacement in proportions of 30-100 % of fine natural aggregate with fine recycled aggregate in a reference concrete of 60 MPa as well as the use of a carboxylate-based superplasticizer and a water/cement ratio between 0.41-0.48 led to decreasing the compressive strength after 28 days by 3.7-7.6 % corresponding to the replacement proportions mentioned above and the increase of water-absorbing by immersion by 16.8-46 %. The carbonation depth and the chloride penetration coefficient increased by 40-110 % with the increase of the proportion of aggregate replacement [15, 16].

The experiment carried out by Cartuxo et al. [11] by replacing fine natural aggregate with fine recycled aggregate reached acceptable results by using a high-performance superplasticizer (SikaPlast 898) based on the combination of modified polycarboxylates in aqueous solution that works by electrostatic and respectively, by steric repulsions. The use of superplasticizer SikaPlast 898 decreased the following characteristics of cement-based concrete: water/cement ratio (up to 25 %), water absorption by immersion (up to 43 %), capillary water absorption (up to 66 %), carbonation depth at 91 days (up to 80 %), and the chloride migration coefficient (up to 46 %).

The work [17] is a review recently carried out by Thomas et al. in the field of using aggregates recycled from the construction demolition in the composition of geopolymer concrete. According to the conclusions of this study, the workability of geopolymer concrete is improved by increasing the quantity of recycled aggregates.

The compressive strength has higher values compared to cement-based concrete and is improved by increasing the addition of blast furnace slag. The curing process of the geopolymer concrete with embedded recycled aggregate having slag in the binder composition is advantageous if the process temperature is ambient, while in the case of the binder containing fly ash a higher temperature (below 100 °C) is appropriate, leading to increasing mechanical properties. The tendency to decrease the compressive strength was observed in the case of geopolymer concrete with coarse recycled aggregate due to the higher water absorption compared to coarse natural aggregate, but also due to the inferior properties of the recycled aggregate. The microstructural characteristics are superior to those of the reference concrete. The abrasion resistance of the geopolymer made by mixing fly ash with 5-15 % Portland cement and metakaolin is higher. Water absorption and sorptivity of geopolymer concrete are increased by increasing the proportion of recycled aggregate. The resistance of concrete to the attack of sulfuric acid is very high. Regarding the penetration of chlorides through the geopolymer concrete containing recycled aggregates, the resistance level is acceptable within certain limits. From the point of view of authors, the replacing problem of traditional natural aggregates with aggregates recovered from the building demolition is at a stage where scientific research should continue to improve knowledge in order to industrially apply the optimal technical solution.

Tan et al. [18] presented in their work an effective method of increasing the mechanical strength of geopolymer concrete by introducing into its composition the ground mixture of recycled aggregate from demolition and metallurgical slag. Both the compressive strength and the flexural strength of the geopolymer concrete have increased. According to the reported results, the compressive strength could reach 70 MPa after 7 days.

The authors' team of the current paper has recently made several experimental versions of geopolymer concrete [19-22] using different alumino-silicate wastes as a substitute for Portland cement, but until now they have not tried use recycled residual concrete from building demolitions as a substitute for fine natural aggregate. In the work presented below, fly ash and ground granulated blast furnace slag were chosen as alumino-silicate industrial by-products for the complete replacement of ordinary Portland cement. Recycled construction concrete from the building demolition was recovered to be used as fine aggregate of the geopolymer concrete after its mechanical processing in order to obtain by crushing-grinding the particle size range below 3 mm. Under the conditions of dwindling sand reserves worldwide [23], the approach to other sources, such as the case of residual concrete from demolitions, is justified. To compensate for the increased water-absorbing capacity of the recycled aggregate compared to the natural one, a suitable additive (polycarboxylate ether) was used.

2. Methods and materials

The adopted method is based on the complete replacement of the traditional concrete binder (Portland cement) with alumino-silicate industrial by-products: coal fly ash and granulated furnace slag having adequate cementitious properties to replace

cement as a binder. The purpose of adopting these materials rich in alumina and silica, existing in significant quantities in the world industry, is the significant reduction of fossil fuel consumption and implicitly, of greenhouse gas emissions into the atmosphere compared to the cement manufacturing process.

The method of transforming alumino-silicate materials into geopolymers is based on the geopolymerization reaction, which is the essence of Davidovits' invention. The reaction, activated in an alkaline environment, leads to the formation of three-dimensional structure of the polymer chain and the ring formed by Si-O-Al-O bonds. Although the reaction mechanism has not yet been accepted by all specialists, in principle it could include the following stages: the dissolution of silicon and aluminum atoms under the action of hydroxide ions from the alkaline solution, the transport and condensation of precursor ions into monomers, and the polymerization of monomers into polymer structures [24].

The fresh geopolymer concrete preparation involves several stages. First, the alkaline activator containing sodium silicate (Na_2SiO_3) solution and sodium hydroxide (NaOH) in the form of solid pellets dissolved in water is separately prepared. The mixture of the liquid solution is then poured over the mixture of solid materials (fly ash and ground granulated blast furnace slag), the two components being mixed for 3 min until the paste is formed. The fine aggregate obtained by grinding the recycled concrete from the demolition, coarse aggregate consisting of natural gravel with dimensions below 18 mm, the additive (polycarboxylate ether) as a fine powder, and supplementary water were added over the paste. After a new mixing for about 5 min, the fresh geopolymer concrete was poured into metal molds and introduced into a sealed room for the curing treatment with hot air at 80 °C for 24 hours. After the completion of the mentioned treatment, the hardened specimens were removed from molds and stored for 7 and 28 days before testing their physical-mechanical features.

The materials used in this experiment were: coal fly ash and granulated blast furnace slag as binder completely replacing Portland cement, solution of Na_2SiO_3 and NaOH in the form of pellets soluble in water composing the alkaline activator, ground recycled concrete from demolition and natural sand as fine aggregate (below 2.7 mm), natural gravel (below 18 mm) as coarse aggregate, and polycarboxylate ether as a water-reducing additive.

Class F-fly ash was the type of ash purchased over 7 years ago and stored at Daily Sourcing & Research Bucharest, from Paroseni-Thermal power plant (Romania). The ash captured in electro filters of the plant after the fine purification of waste gases resulting from anthracite burning had grain size below 200 μm and required additional mechanical processing (grinding) to reduce the size below 40 μm. The chemical composition of fly ash with low CaO content (3.5 %) suitable for the production of geopolymer is shown in Table 1.

Granulated blast furnace slag was purchased from ArcelorMittal Galati (Romania) about 10 years ago and stored at the Metallurgical Research Institute Bucharest. The slag was taken in the form of granules between 2-6 mm and was ground to sizes below 80 μm. Its chemical composition is presented in Table 1.

Table 1

Chemical composition of fly ash and slag (wt. %)

Material	SiO_2	Al_2O_3	TiO_2	Fe_2O_3	CaO	MgO	Na_2O	K_2O	SO_3
Class F fly ash	54.4	26.5	1.5	4.8	3.5	2.5	0.4	0.6	1.7
Granulated blast furnace slag	36.4	11.6	-	0.8	41.8	5.8	0.3	0.4	-

Alkaline activator solution was composed of an aqueous solution of Na_2SiO_3 (38 % concentration) and NaOH pellets dissolved in water (12 M molarity). Alkaline activator components were commercially purchased.

Fine aggregate of geopolymer concrete was represented by natural sand (river sand) and recycled residual building concrete from demolition. River sand had dimensions in the range of 1.2-2.7 mm and his chemical composition mainly contained SiO_2 (97.5 %). Waste building concrete was arbitrarily selected from a demolition site. The chemical composition determining of the selected specimen was carried out in Metallurgical Research Institute on the X-ray fluorescence spectrometer. The main components of the concrete were 49.8 % SiO_2, 16.9 % CaO, 9.8 % Al_2O_3, and 7.6 % Fe_2O_3. The sample was crushed and ground, the particle size selected for the experiment being below 3 mm.

The coarse aggregate of geopolymer concrete was represented by natural gravel with grain size under 18 mm. Its oxide composition included 55.9 % SiO_2, 18.0 % CaO, 4.2 % Al_2O_3, and 3.0 % Fe_2O_3.

Polycarboxylate ether (in form of fine powder) originally from India was chosen as a water-reducing additive.

Four experimental variants were adopted in this experiment for making geopolymer concrete using fine recycled aggregate from building demolition, being presented in Table 2.

Table 2

Composition of geopolymer concrete variants

Composition	Version ($kg \cdot m^{-3}$)			
	No. 1	No. 2	No. 3	No. 4
Class F-fly ash	380	330	290	225
Ground granulated blast furnace slag	70	120	160	225
Na_2SiO_3	214	214	214	214
12 M NaOH	89	89	89	89
Fine aggregate - recycled concrete aggregate (below 3 mm)	-	140	350	550
- natural sand (1.2-2.7 mm)	930	790	580	380

Composition	Version ($kg \cdot m^{-3}$)			
	No. 1	No. 2	No. 3	No. 4
Coarse aggregate (granite gravel) (below 18 mm)	920	920	920	920
Polycarboxylate ether	3.2	3.3	3.5	3.5
Water	132	132	132	132

Table 2 includes different ratios between the binder components of mixture (fly ash and slag). Thus, the ash/slag ratio has values within the limits of 1.00-5.43, the weight proportion of ground granulated blast furnace slag increasing from 15.6 % (version 1) to 50 % (version 4).

The main interest element of this experiment was changing the ratio between the components of the fine aggregate of geopolymer: recycled concrete aggregate and natural sand. Version 1 contained only natural sand (930 $kg \cdot m^{-3}$), while version 4 changed this ratio in favour of recycled aggregate (550 $kg \cdot m^{-3}$) compared to natural sand (380 $kg \cdot m^{-3}$). The coarse aggregate (granite gravel) did not influence this experiment having adopted a constant value of 920 $kg \cdot m^{-3}$. As mentioned above, polycarboxylate ether was added into the geopolymer composition having the role to reduce the water content required by recycled concrete aggregate used as a fine aggregate. The components of the alkaline activator (Na_2SiO_3 and NaOH) were adopted in the ratio 2.40 and the Na_2SiO_3/binder ratio was chosen at 0.48 [25].

The investigation of geopolymer concrete characteristics was carried out in two directions: one regarding the workability parameters of fresh concrete and another regarding the physical, mechanical, and microstructural features of hardened concrete. The workability of fresh concrete was determined using Abram's cone (EN 12350-2: 2006). The density was measured by the Archimedes' method using the water-intrusion method (ASTM D792-20). The water absorption was determined by the method of immersing the sample under water (ASTM D570). Compressive strength was examined using the method contained in EN 12390-3: 2001 and flexural strength was measured applying the three-point bend test on the specimen (SR EN ISO 14125: 2000). Modulus of elasticity was determined in conformity with ASTM C469-02e1. The microstructural peculiarities of geopolymer concrete specimens were analyzed with Biological Microscope model MT5000 with image captured, 1000 x magnification.

3. Results and discussion

Abram's cone test for slump flow indicated a good level of workability of the fresh geopolymer concrete, the slump flow values falling within the limits of 180-215 mm, according to the data in Table 3.

Table 3

Values of Abram's cone test for slump flow

Version	No. 1	No. 2	No. 3	No. 4
Slump flow (mm)	215	206	193	180

Generally, fresh mixes of geopolymer concrete have good viscosity and cohesion properties. By increasing the amount of blast furnace slag in the binder composition, the tendency to reduce these properties values dwindles. The explanation of Thomas et al. [17] for this evolution is the high amount of liquefied calcium ions of the slag and its fast reaction with the alkaline activator forming calcium silicate hydrate, that precipitates. Recycled concrete aggregate, having an inherent mortar content on its surface, absorbs water in larger quantities compared to natural aggregate during mixing, thus reducing the workability of geopolymer concrete.

The following stage of determining the specimen features referred to the mechanical, physical, and microstructural characteristics of geopolymer concrete made after the curing process of fresh concrete poured into molds, followed by the storage of specimens removed from the molds for 7 and 28 days. The density, water absorption ability, compressive strength, flexural strength, modulus of elasticity, and microstructural peculiarities of the four geopolymer concrete specimens have been investigated. Results are presented in Table 4.

Table 4

Mechanical and physical characteristics of geopolymer concrete specimens

Characteristic	Version			
	No. 1	No. 2	No. 3	No. 4
Density ($kg \cdot m^{-3}$)	2320	2216	2105	2030
Water absorption (vol. %)	3.8	4.0	4.3	4.5
Compressive strength (MPa)				
- after 7 days	31.0	34.7	38.9	43.1
- after 28 days	44.5	49.8	54.9	63.2
Flexural strength (MPa)				
- after 7 days	3.5	3.9	4.3	5.9
- after 28 days	7.2	8.5	9.2	11.2
Modulus of elasticity (GPa)	34.8	28.3	22.9	16.8

Analyzing the data in Table 4, it is found that measuring density results of geopolymer concrete samples incorporating recycled concrete waste from demolitions as a fine aggregate indicate significant decreases with increasing this waste proportion in the fine aggregate composition up to 59.1 % (2030 $kg \cdot m^{-3}$) compared to 2320 $kg \cdot m^{-3}$ obtained in the version using only natural fine aggregate.

It was experimentally found that the use of recycled aggregate from demolitions has higher water absorption due to the cracks created during the recycling process, thus affecting the workability of the fresh geopolymer. On the other hand, the partial replacement of fly ash with blast furnace slag has the opposite effect, reducing the water absorption. Table 4 practically shows the combined result of the two opposite effects, observing a slight increase in absorbing water in versions with higher inclusion

of recycled aggregate. Thus, water absorption increased from 3.8 vol. % (version 1) to 4.5 vol. % (version 4).

Compressive strength of geopolymer concrete with embedded recycled aggregate as well as using fly ash and especially, blast furnace slag as complete substitute for cement as a binder proved to increase significantly, reaching very high values after 28 days (up to 63.2 MPa) and also after 7 days (up to 43.1 MPa).

In principle, flexural strength is negatively influenced by embedding recycled aggregate in fine aggregate composition. However, the addition of more than 30 % blast furnace slag in the binder mixture contributed to the significant improvement of the strength under the conditions of high proportions of recycled aggregate of at least 50 %. According to Table 4, the maximum flexural strength values reached 11.2 MPa after 28 days and respectively, 5.9 MPa after 7 days in version 4 (with 59.1 % recycled aggregate and 50 % blast furnace slag).

Determining the modulus of elasticity of geopolymer concrete with embedded recycled aggregate highlighted a sharp decrease of its value with the increase of recycled aggregate weight proportion up to 59.1 %. Thus, the modulus of elasticity decreased from 34.8 GPa (version 1) up to 16.8 GPa (version 4).

Images of geopolymer concrete specimens with embedded recycled aggregate made in this experiment are shown in Fig. 1.

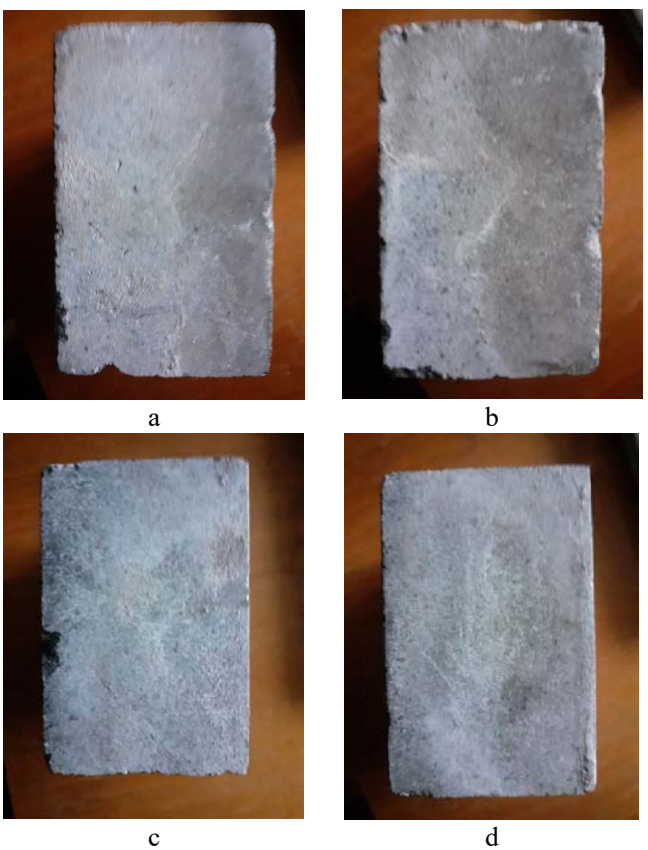

Fig. 1. Geopolymer concrete specimens with embedded recycled aggregate
a – version 1; b – version 2; c – version 3; d – version 4.

All four specimens shown in Fig. 1 have compact and homogeneous surfaces, typical for construction materials with high mechanical strength.

Pictures representing microstructural peculiarities of geopolymer concrete specimens with embedded recycled aggregate are shown in Fig. 2.

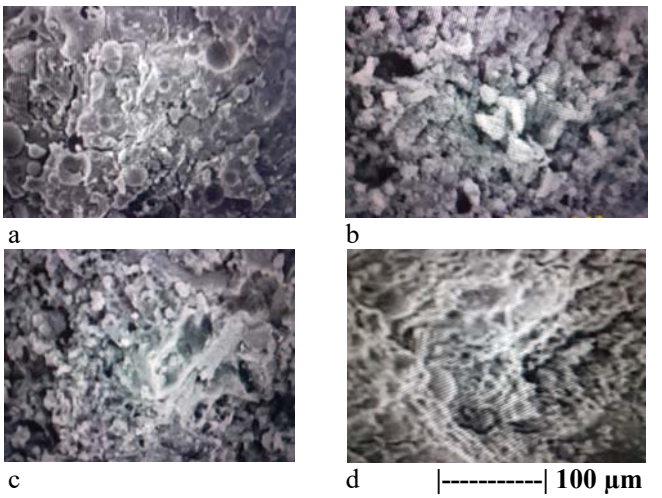

Fig. 2. Microstructural peculiarities of geopolymer concrete specimens with embedded recycled aggregate
a – version 1; b – version 2; c – version 3; d – version 4.

The spherical shape of the fly ash granules is visible in the first two pictures (a and b) of Fig. 2, then it fades in (c), so that picture (d) shows a predominantly typical structure containing metallurgical slag [26].

The comparative analysis of the geopolymer concrete specimens incorporating recycled aggregate made in this experiment requires the investigation of the limits of their characteristics influenced by the proportions of the recycled aggregate compared to the natural one in the geopolymer concrete composition. The testing of the mechanical and physical properties of specimens incorporating between 0-59.1 % recycled aggregate in the fine aggregate composition identified the decrease in the geopolymer density, the slight increase in water absorption, the significant increase in the compressive strength, the increase in flexural strength, especially at proportions above 50 %, and the sharp decrease of modulus of elasticity. Also, the slump flow test showed a slight tendency to decrease the geopolymer workability.

Choosing the optimal experimental variant by correlating the appropriate characteristics as a whole led to the determination of version 3 as the best of the four made versions. Features of this version include the density of 2105 $kg \cdot m^{-3}$, water absorption of 4.3 vol. %, compressive strength of 38.9 MPa after 7 days and 54.9 MPa after 28 days, flexural strength of 4.3 MPa after 7 days and 9.2 MPa after 28 days as well as modulus of elasticity of 22.9 GPa.

4. Conclusions

The paper aimed at the manufacture of geopolymer concrete based on fly ash and ground granulated blast furnace slag using different additions of recycled concrete waste from the demolition of buildings in the form of aggregate together with natural fine aggregate (sand). The interest of researchers for the valorization of waste resulting from the demolition of buildings as recycled aggregate under the conditions of its application in the geopolymer concrete is relatively recent, as long as the geopolymer itself is a recent invention. Until now, the world research in this field has not reached optimal results that are unanimously recognized. The research team of the current work has recently carried out several researches on making geopolymer concretes having original contributions on the binder mixture from different alumino-silicate wastes, but the combination of binder solutions with those of geopolymer fine aggregate is made for the first time. The originality of the work consists in the correlation of the excellent features obtained for compressive strength (maximum 63.2 MPa) and flexural strength (maximum 11.2 MPa) with other decreasing properties such as density, water-absorbing, and modulus of elasticity, so that the overall performance of geopolymer to be valuable.

Referinţe

[1] J. Davidovits, M. Davidovits, N. Davidovits, „Process for Obtaining a Geopolymeric Alumino-Silicate and Products thus Obtained", US Patent no. 5342595, 1994.

[2] H. Castillo, H. Collado, T. Droguett, M. Vesely, P. Garrido, S. Palma, „State of the Art of Geopolymers: A Review", e-Polymers, De Gruyter ed., 2022. https://doi.org/10.1515/epoly-2022-0015

[3] F. N. Okoye, „Geopolymer Binder: A Veritable Alternative to Portland Cement", Materials Today: Proceedings, vol. 4, no. 4, Part E, 2017, pp. 5599-5604. https://doi.org/10.1016/j.matpr.2017.06.017

[4] B. V. Rangan, „Low-Calcium Fly Ash-Based Geopolymer Concrete", in Concrete Construction Engineering Handbook (chapter 26), E. G. Nawy (ed.), Second Edition, CRC Press, New York, the United States, 2008.

[5] G. Liang, W. Yao, Y. Wei, „A Green Ultra-High Performance Geopolymer Concrete Containing Recycled Fine Aggregate: Mechanical Properties, Freeze-Thaw Resistance and Microstructure", Science of The Total Environment, Elsevier, vol. 895, 2023. https://doi.org/10.1016/j.scitotenv.2023.165090

[6] G. W. Kim, T. Oh, S. K. Lee, N. Banthia, „Development of Ca-Rich Slag-Based Ultra-High-Performance Fiber-Reinforced Geopolymer Concrete (UHP-FRGC): Effect of Sand-to-Binder Ratio", Construction and Building Materials, Elsevier, vol. 370, 2023. https://doi.org/10.1016/j.conbuildmat.2023.130630

[7] Miren Etxeberria, E. Vázquez, A. Marí, Marilda Barra-Bizinotto, „Influence of Amount of Recycled Coarse Aggregates and Production Process on Properties of Recycled Aggregate Concrete", Cement and Concrete Research, vol. 37, 2007, pp. 735-742.

[8] K. Rahal, „Mechanical Properties of Concrete with Recycled Coarse Aggregate", Building and Environment, vol. 42, 2007, pp. 407-415.

[9] Beata Sadowska, J. R. Jimenez, J. M. Fernández-Rodriguez, F. Moreno-Perez, J. R. Cañas, Y. A. Rivas-Sanchez, „Modern Building Materials", in Buildings 2020+: Constructions, Materials and

Installations, Printing House of Bialystok University of Technology (Dorota Anna Krawczyk, ed.), pp. 53-105, Bialystok-Cordova-Vilnius, 2019. ISBN 978-83-65596-70-3.

[10] V. W. Y. Tam, M. Soomro, A. C. J. Evangelista, „A review of Recycled Aggregate in Concrete Applications (2000-2017)", Construction and Building Materials, Elsevier, vol. 172, 2018, pp. 272-292. https://doi.org/10.1016/j.conbuildmat.2018.03.240

[11] F. Cartuxo, J. de Brito, L. Evangelista, J. R. Jiménez, E. F. Ledesma, „Increased Durability of Concrete Made with Fine Recycled Concrete Aggregates Using Superplasticizers", Materials MDPI Basel, Switzerland, (Sarker, P.K. academic ed.), vol. 9, no. 2, 2016. https://doi.org/10.3390/ma9020098

[12] J. Geng, J. Sun, „Characteristics of the Carbonation Resistance of Recycled Fine Aggregate Concrete", Construction and Building Materials, vol. 49, 2013, pp. 814-820.

[13] L. Evangelista, J. de Brito, „Concrete with Fine Recycled Aggregates: A Review". European Journal of Environmental and Civil Engineering. vol. 18, 2014, pp. 129-172.

[14] P. Pereira, L. Evangelista, J. de Brito, „The Effect of Superplasticizers on the Mechanical Performance of Concrete Made with Fine Recycled Concrete Aggregates", Cement and Concrete Composites, vol. 34, 2012, pp. 1044-1052.

[15] L. Evangelista, J. de Brito, „Mechanical Behaviour of Concrete Made with Fine recycled concrete aggregates, Cement and Concrete Composites, vol. 29, 2007, pp. 397-401.

[16] L. Evangelista, J. de Brito, „Durability Performance of Concrete Made with Fine Recycled Concrete Aggregates", Cement and Concrete Composites, vol. 32, 2010, pp. 9-14.

[17] B. S. Thomas, J. Yang, A. Bahurudeen, S. N. Chinnu, J. A. Abdalla, R. A. Hawileh, H. M. Hamada, „Geopolymer Concrete Incorporating Recycled Aggregates: A Comprehensive Review", Cleaner Materials, Elsevier, vol. 3, 2022. https://doi.org/10.1016/j.clema.2022.100056

[18] J. Tan, J. Cai, X. Li, J. Pan, J. Li, „Development of Eco-Friendly Geopolymers with Ground Mixed Recycled Aggregates and Slag", Journal of Cleaner Production, Elsevier, vol. 256, 2020. https://doi.org/10.1016/j.clepro.2020.120369

[19] L. Paunescu, B. V. Paunescu, E. Volceanov, G. Surugiu, „Geopolymer Concrete-A Suitable Alternative Solution for the Global Reduction of CO_2 Emissions in Manufacturing the Concrete", Nonconventional Technologies Review, vol. 26, no. 4, 2022, pp. 25-30.

[20] B. V. Paunescu, L. Paunescu, E. Volceanov, „Microsilica and Steel Dust as Nano- and Micro-Particles Addition for Increasing the Mechanical Strength of Fly Ash and Blast Furnace Slag-Geopolymer Concrete", Romanian Journal of Civil Engineering, vol. 14, no. 2, 2023, pp. 120-129.

[21] L. Paunescu, E. Volceanov, A. Ioana, B. V. Paunescu, „High-Strength-Geopolymer Building Material", Journal of Engineering Studies and Research, vol. 28, no. 4, 2022, pp. 107-115.

[22] L. Paunescu, B. V. Paunescu, E. Volceanov, „High Mechanical Strength-Geopolymer Concrete Based on Coal Fly Ash and Ground Recycled Residual Glass Added in the Fine Aggregate", Bulletin of Polytechnic Institute of Iasi, vol. 69 (73), no. 2, 2023, pp. 81-93.

[23] *** „The Problem with our Dwindling Sand Reserves", UN Environment Programme, February 2023. https://www.unep.org/news-and-stories/story/problem-our-dwindling-sand-reserves

[24] V. C. Nguyen, D. T. Bul, V. T. Dang, „Recent Research Geopolymer Concrete, Proceedings of the 3rd ACF International Conference ACF/VCA, Ho Chi Minh City, Vietnam, November 11-13, 2008, pp. 235-241.

[25] J. Xie, J. Zhao, J. Wang, C. Fang, B. Yuan, Y. Wu, „Impact Behaviour of Fly Ash and Slag-Based Geopolymeric Concrete: The Effects of Recycled Aggregate Content, Water-Binder Ratio and Curing Age", Construction and Building Materials, Elsevier, vol. 331, 2022. https://doi.org/10.1016/j.conbuildmat.2022.127359

[26] Maria Izquierdo, X. Querol, J. Davidovits, D. Antenucci, H. Nugteren, C. Fernández-Pereira, „Coal Fly Ash-Slag-Based Geopolymers: Microstructure and Metal Leaching", Journal of Hazardous Materials, vol. 166, no. 1, 2008, pp. 561-566. https://doi.org/10.1016/j.hazmat.2008.11.063